

Geothermal reservoirs in the Danish area: temperatures, resources and models for long-term energy extraction

Niels Balling, Marton Major, Sven Fuchs, Anders Mathiesen,
Carsten Møller Nielsen, Thomas Mejer Hansen,
Lars Kristensen and Andrea Förster



Scientific report
Department of Geoscience
Aarhus University
December 2019

Geothermal reservoirs in the Danish area: temperatures, resources and models for long-term energy extraction

GEO THERM – Geothermal energy from sedimentary reservoirs
– Removing obstacles for large scale utilization

Innovation Fund Denmark: project 6154-00011B
Final report in WP4

Niels Balling¹, Marton Major¹, Sven Fuchs², Anders Mathiesen³,
Carsten Møller Nielsen³, Thomas Mejer Hansen¹,
Lars Kristensen³ and Andrea Förster²

¹Department of Geoscience, Aarhus University

²German Research Centre for Geosciences, GFZ Potsdam

³Geological Survey of Denmark and Greenland, GEUS

Contents

Preface.....	1
Dansk resumé	2
Summary.....	5
1. Introduction.....	8
2. A new 3D geothermal model	9
2.1 Method and data.....	9
2.2 Model results with temperatures of geothermal reservoirs.....	9
3. Geothermal resources	16
3.1 Method	16
3.2 Reservoir thermal resources maps	17
4. Rock thermal properties.....	21
4.1 Sample preparation and laboratory measurements.....	21
4.2 Measuring results.....	22
4.3 Summary	25
5. Reservoir simulation – conceptual models	26
5.1 Method and theory	26
5.2 Heat extraction by geothermal doublets	27
Model set up, parameters and boundary conditions	27
Modelling results, long-term heat extraction.....	28
Conclusions	35
5.3 Combined heat extraction and heat storage.....	35
ATES basic concept.....	36
Model examples and results.....	37
Discussion and conclusions.....	39
6. Reservoir simulation – geothermal plants.....	42
6.1 The Thisted plant.....	42
The reservoir	44
Model set up and modelling procedure.....	44
Statistical reservoir models	44
Initial and boundary conditions	46
Results and discussion.....	48

Conclusions	52
6.2 The Sønderborg plant	53
The reservoir	53
Model set up and modelling procedure	54
Model parameters and boundary conditions	57
Results and discussion	60
Conclusions	64
6.3 The Margretheholm plant	64
Main results	66
Conclusions	67
6.4 General conclusions	67
References	68

Preface

This report summarizes results from Work Package 4 (WP4) in project GEOTHERM, an Innovation Fund Denmark project. The theme for WP4 was 'Resources assessment and energy extraction'. Three participating institutions, Department of Geoscience, Aarhus University, (AU) (work package lead), Geological Survey of Denmark and Greenland (GEUS) and German Research Center for Geosciences, Potsdam (GFZ) collaborated in carrying out this research, which was completed during the period of March 1, 2017 to December 1, 2019.

Results from previous work-package progress reports, some of which now published, or in print for publication, as well as new results are included. Some research work was initiated during previous research projects, including projects by Innovation Fund Denmark, and completed in this project.

All authors of this report contributed with results.

As input for thermal modeling, Sven Fuchs (GFZ) and Andrea Förster (GFZ) provided new rock thermal laboratory measurements on core samples from Danish deep boreholes.

The new 3D geothermal model for onshore Denmark was developed by Niels Balling (AU), Sven Fuchs (AU/GFZ) and Anders Mathiesen (GEUS), with Sven Fuchs performing model thermal parameter estimation and temperature modelling. GEUS provided detailed structural and geological information, including results from a recent regional reinterpretation of seismic data.

Based on the temperature data from the geothermal model and results from reservoir simulations, Sven Fuchs and Anders Mathiesen calculated the amount geothermal resources in the main geothermal reservoirs.

For the evaluation of important parameters for a robust and resource-sustainable long-term energy extraction, comprehensive reservoir simulation was carried out. Marton Major (AU), as part of his PhD project (funded by Innovation Fund Denmark and Aarhus University), carried out numerical modelling on conceptual reservoir models, including models with combined geothermal production and heat storage. He also carried out reservoir modelling for the geothermal plant in Thisted and Carsten Møller Nielsen (GEUS) performed reservoir simulation for the geothermal plant in Sønderborg. Thomas Mejer Hansen (AU) contributed with geostatistical reservoir models and Lars Kristensen (GEUS) provided reservoir properties from well-log data analysis.

As work package leader, Niels Balling was responsible for compiling project results and for writing this report.

Dansk resumé

Geotermiske reservoirer indeholder store mængder varmeenergi, der under de rette betingelser kan udnyttes til opvarmningsformål eller, i særligt gunstige områder med høj temperatur, til el-produktion. Selv om ressourcen er meget stor, vil der ved langtidsudnyttelse, lokalt for det aktuelle reservoir, ske en udtynding af ressourcen. Produktionskapacitet og samlet energiproduktion for et geotermisk anlæg afhænger af reservoirets temperatur, hydrauliske og termiske egenskaber samt anlæggets produktionsprofil.

Det overordnede mål for arbejdet under GEOTHERM WP4 har været at tilvejebringe grundlæggende information om danske geotermiske reservoirer i form af temperatur og ressourcestørrelse samt om den termiske langtidsudvikling af reservoiret ved udnyttelse i geotermiske anlæg. Der er vurderet hvilke faktorer, der har særlig betydning for produktionstemperaturen og størrelsen af den producerede energi med henblik på en pålidelig og ressourcemæssig bæredygtig udnyttelse.

Detaljeret kendskab til undergrundens termiske egenskaber indgår med stor vægt i den termiske modellering og i forståelsen af årsager til variationer i undergrundens temperatur. Der er i projektets første fase gennemført nye supplerende målinger af bjergartstermiske egenskaber i form af varmeledningsevne, termisk diffusivitet og varmekapacitet på udvalgte kerneprøver af forskellig lithologi fra danske dybe borer. Resultaterne har været brugt i den termiske modellering.

Der er udviklet en ny numerisk 3D geotermisk model med detaljeret information om temperaturfordelingen i undergrunden til stor dybde for hele det danske landområde. Den anvendte strukturelle model, med dybder til de geotermiske reservoirer, er baseret på en ny regional gendolking af seismiske data. Den geotermiske model indeholder termiske egenskaber for lithologiske enheder bestemt fra petrofysiske borehuls-logs og nye estimater for varmestrøm, der, sammen med målte temperaturer i dybe borer, er anvendt som modelbindinger. Modellen er baseret på avanceret invers termisk modellering med optimeret tilpasning af modelparametre, så der sikres fuld overensstemmelse med målte temperaturdata. Geotermiske reservoirer, med temperaturer på omkring 45–80 °C, der er velegnet til opvarmningsformål, findes i store regionale områder.

Den regionale geotermiske ressourceestimering er opdateret. Der indgår temperaturdata fra den nye temperaturmodel og ny information om reservoirtykkelser og porøsitet. Som noget nyt er der, baseret på resultater fra projektets reservoirsimulering (se nedenfor), også medtaget et langsigtet varmebidrag fra lag over og under reservoiret. Der er gennemført beregning af den samlede varmeenergi per enhedsareal ('Heat in Place', angivet i GJ/m²) for de vigtige geotermiske reservoirer samt tilsvarende estimater for størrelsen af ressourcen, der kan udnyttes med udgangspunkt i en geotermisk dublet (anlæg med to borer; produktion og reinjektion).

Der præsenteres regionale temperatur- og ressourcekort for de vigtigste geotermiske reservoirer: Frederikshavn, Haldager Sand, Gassum samt Bunter Sand/Skagerrak. Den beregnede 'udnyttelige energi' for de individuelle reservoirer er generel af størrelsesordenen 3–10 GJ/m² og op til ca. 15 GJ/m² lokalt for Gassum og Bunter Sand/Skagerrak reservoirerne. For en opskallering til større områder bemærkes, at for hver GJ/m² opnås der 10⁶ GJ/km² (= PJ/km²) varmeenergi. Det svarer til

24.000 ton olieækvivalent (toe) for hver kvadratkilometer. Adskillige reservoirenheder har således varmeenergi svarende til omkring 100.000–200.000 toe per kvadratkilometer.

Der er gennemført state-of-the-art numerisk reservoirsimulering for konceptuelle modeller med beregning af langtidsudvikling for temperatur og tryk i reservoir og produktionsboring for en geotermisk dublet. Der er udført tilsvarende simuleringer af langtidsudvikling for de danske geotermiske anlæg i Thisted og Sønderborg, hvor der er taget hensyn til de aktuelle geologiske forhold og øvrige lokale randbetingelser. Der er også medtaget en sammenfatning af resultater fra tilsvarende tidligere modelberegninger for anlægget i København (Margretheholm).

Simuleringerne viser en meget lang termisk levetid for reservoierne. Der ses meget lille temperaturfald i produktionen efter fremkomst af det kolde injektionsvand, typisk omkring 5 °C, eller mindre, for modeltider på op til 100 år og længere. Det gælder for afstande på 1000–1500 m i reservoiret mellem produktion og injektion og med de produktionsrater på omkring 150 m³/time, der ofte anvendes i geotermiske anlæg. Ved markant mindre afstande mellem produktion og injektion (600 m for modeleksempel) modelleres et tidligt og, over tid, væsentligt fald i produktionstemperatur. Afstand mellem borerne i reservoiret har således væsentlig betydning. Til gengæld betyder reservoirtykkelse markant mindre for den termiske udvikling, end man kunne forvente. Små tykkelser på ned til omkring 10-20 m viser også kun lille langtidsreduktion i produktionstemperatur.

Reservoirsimuleringerne viser, at det kolde injektionsvand genererer en meget betydelig strøm af varmeenergi til reservoiret fra lagene over og under reservoiret. Det fremgår også, at der, efter ankomst af det kolde vand, hentes store mængder varmt vand med tilstrømning fra retninger væk fra fronten af det kolde vand. Disse faktorer forklarer langtidsudviklingen med den meget beskedne reduktion i produktionstemperatur.

Når der findes historiske produktionsdata fra geotermiske anlæg (tidsserier for flowrater, temperatur og tryk) kan modelsimuleringer sammenlignes med og tilpasses de aktuelle data. Det kan sikre en god og robust forudsigtelse af fremtidig produktion til hjælp for planlægning og reservoirstyring. Der er gennemført sådanne simuleringer for anlæggene i Thisted og Sønderborg. For Thisted, efter 34 års drift (status i 2018; med driftsstop i sommerperioden), modelleres en påvirkning af det kolde injektionsvand ud til en afstand på kun 500 - 600 m fra injektionsboringen, eller omkring en tredjedel af afstanden mellem injektions- og produktionsboringen.

Med moderne vedvarende energisystemer produceres ofte store mængder energi, der er forskudt i tid i forhold til energibehov, så der er behov for energilagring. Blandt mulighederne er lagring af varme i undergrunden evt. i kombination med geotermisk produktion. Der er gennemført numerisk simulering i konceptuelle modeller med kombineret geotermisk produktion og sæsonbestemt (sommer til vinter) varmelagring i et dybt reservoir. Størrelsen af den genindvundne varme og tilhørende forøgede ydelse er beregnet. I de aktuelle eksempler genindvindes omkring to tredjedele af den lagrede energi.

Sammenfatning af væsentlige generelle resultater fra arbejds pakken:

- Der findes regionalt i landet enorme tilgængelige geotermiske energiresourcer i sedimentære reservoirer inden for de temperatur- og dybdeniveauer, der er anvendelige til opvarmningsformål. Det gælder også ved byer med et betydeligt varmebehov.
- Ved hjælp af moderne modelleringsværktøjer kan langtidsudvikling af temperatur- og trykfordeling i reservoirer simuleres til brug for design af anlæg med en stabil og ressourcemæssig bæredygtig produktion.
- Ved udnyttelse af et geotermisk reservoir er levetiden inden temperaturen sænkes markant ved produktionsbrønden meget lang og væsentligt længere end hidtil antaget.
- Ved udnyttelse over lang tid fås også varmeenergi fra lagene over og under reservoirer, og der hentes fortsat betydelige mængder varmt vand væk fra fronten af det kolde injektionsvand. Det er med til at forklare den lange termiske levetid.
- Det er muligt at kombinere geotermisk produktion og sæsonlagring af varme i undergrunden. En stor andel af den lagrede energi kan genindvindes.

Alle temperatur- og ressourcedata foreligger i digital form og vil indgå i opdatering af GEUS' WebGIS portal for 'Dyb geotermi' (dybgeotermi.geus.dk). Disse data, kombineret med supplerende information om reservoirernes hydrauliske egenskaber, udgør basal information for den geotermiske efterforskning.

Summary

Geothermal reservoirs contain large amounts of thermal energy, which, under the right conditions, can be utilized for heating purposes or, in favourable areas with high temperatures, for electricity generation. Although the resources are very large, the long-term exploitation results in a local reservoir depletion of heat energy. Production capacity and total amount of energy for a geothermal plant depend on the temperature, hydraulic and thermal properties of the reservoir and the production profile of the plant.

The overall goal of GEOTHERM WP4 was to provide basic information on Danish geothermal reservoirs in terms of temperatures, the amount of thermal resources as well as on the long-term thermal evolution of the reservoir by exploitation. Factors that are of importance for the production temperature within a geothermal plant and the amount of energy produced are assessed. It is essential to achieve a reliable and resource-sustainable energy utilization.

Detailed knowledge of the thermal properties of the subsurface is needed for the thermal modelling and for the understanding of variations in subsurface temperature distribution. Thus, new measurements of rock thermal properties were carried out in terms of thermal conductivity, thermal diffusivity and heat capacity of selected core samples of different lithology from Danish deep boreholes. The results were used in the thermal modelling.

A new comprehensive 3D numerical geothermal model with detailed temperature distribution to great depth for the entire Danish land area has been generated. The structural model, with depths to geothermal reservoirs, is based on a new regional reinterpretation of seismic data. The geothermal model contains thermal properties for lithological units determined from petrophysical well logs and new estimates of heat flow, which, together with temperature data from deep boreholes, are used as model constraints. It is based on advanced inverse thermal modelling with parameter optimization to ensure full agreement between measured borehole temperatures and model values. Geothermal reservoirs with temperatures within the approximate range of 45 to 80 °C, suitable for heating purposes, are found to cover large regional areas.

A complete update of the regional geothermal resource estimation has been completed. Temperature data from the new temperature model and new information on reservoir thicknesses and porosity are included. Applying project results from reservoir simulation (see below), a long-term energy contribution from layers above and below reservoirs has been taken into account in addition to the main contribution from the reservoir itself. The calculations include, for each reservoir, the amount of thermal energy ('Heat in Place' per unit area, presented as GJ/m²), as well as an estimate of the amount of heat that can be utilized taking a geothermal doublet as base unit (two wells; production and reinjection).

Regional temperature and resource maps are presented for the main geothermal reservoirs: Frederikshavn, Haldager Sand, Gassum and Bunter Sand/Skagerrak. For individual reservoirs, resources maps show estimates of 'usable energy', generally within the range of 3–10 GJ/m², and up to about 15 GJ/m², locally for some areas of the Gassum and the Bunter Sand/Skagerrak reservoirs. For upscale to larger areas, we note that, for each GJ/m², we obtain 10⁶ GJ/km² (= PJ/km²)

of heat energy, which is 24,000 ton oil equivalent (toe) for each square kilometre. Thus, several reservoir units may provide heat energy corresponding to about 100,000–200,000 toe per square kilometre.

State-of-the-art numerical reservoir simulations are presented for conceptual models with long-term evolution of temperature and pressure in the reservoir and in the production well for a geothermal doublet. Similar simulations of long-term temperature evolution are carried out for the Danish geothermal plants in Thisted and Sønderborg. Here, local geological conditions, as well as other local boundary conditions are taken into account. A summary of results from similar previous model simulations for the geothermal plant in Copenhagen (Margretheholm) are also included.

The reservoir simulations show very small temperature drops in production after arrival of the cold injection water, around 5 °C, or less, for production times of up to around 100 years and more. This applies to distances of 1000–1500 m between production and injection wells and with production rates of 150 m³/h, typically applied in geothermal plants. At small distances (600 m in example), an early, and over time, significant decrease in production temperature is modelled. Thus, spacing between the wells in the reservoir is of great importance. In contrast, reservoir thickness means significantly less than might be expected. Small thicknesses, down to around 10–20 m, show small long-term decreases in production temperature.

Model simulations show that the cold injection water, on long-term production, generates a significant flow of heat to the reservoir from the layers above and below the reservoir, resulting in a marked thermal recharge of the reservoir. It is also seen, how large quantities of warm water is produced from flow directions away from the cold-water front. These factors explain the long-term evolution with small reductions in production temperature.

When historical production data are available (time series for flow rates, temperature and pressure), model simulations can be compared with and adapted to the current data. This will assist in a good and robust prediction of future production and aid in planning and reservoir management. Such simulations have been carried out for the Thisted and Sønderborg plants. In Thisted, after 34 years of operation (status in 2018; no production in summer season), the effect of cold injection water is modelled out to a distance of only 500–600 m from the injection well, or about one-third of the distance between injection and production well.

With modern renewable energy systems, large amounts of energy may be produced that are displaced in time in relation to energy demands. This asks for energy storage for which subsurface heat storage is an option. Such heat storage is simulated in a conceptual model with combined geothermal production and seasonal (summer to winter) heat storage in a deep reservoir. The amount of recovered heat and associated increased production is calculated. In the present examples, about two-thirds of the stored energy are recovered.

Summary of main general results of this work package:

- Regionally across the country, vast amounts of geothermal resources are available in sedimentary reservoirs within temperature and depth levels suitable for heating purposes. This also applies to areas of cities with a significant heating demand.

- By modern modelling tools, long-term development of temperature and pressure distribution in the reservoir can be simulated for use in designing geothermal plants with stable and sustainable production.
- With exploitation of geothermal reservoirs, lifetime, before production temperature is significantly lowered, is very long and substantially longer than previously assumed.
- For long-term exploitation, thermal energy is also extracted from layers above and below the reservoir as well as from areas not significantly affected by the cold injection water. This results in a long thermal life time.
- It is possible to combine geothermal production and subsurface seasonal heat storage. A significant part of the stored energy can be recovered.

All temperature and resource data are available in digital form and will be included in an update of GEUS' WebGIS portal for deep geothermal energy (<http://dybgeotermi.geus.dk/>). These data, combined with supplementary information on the hydraulic properties of the reservoirs, constitute basic information for geothermal exploration.

1. Introduction

Sedimentary reservoirs generally contain vast amounts of geothermal resources. Still, for long-term exploitation, reservoir systems are locally depleted in heat during production. Production capacity and life-cycle energy extraction for a geothermal plant depends on reservoir hydraulic properties and temperature as well as production profile. The main objectives of GEOTHERM WP4 was to assess the geothermal resource base of Danish sedimentary reservoirs and evaluate energy extraction potential to provide basic information for a reliable and resource-sustainable long-term geothermal utilization.

In the first part of the project, for constraining subsurface thermal models, supplementary rock thermal properties were measured on selected core samples from deep wells representing different lithologies.

A new 3D numerical geothermal model for onshore Denmark has been developed with detailed structural input from a newly available regional reinterpretation of seismic data (Vosgerau *et al.*, 2016). This model provides detailed information of temperature distribution of main geothermal reservoirs.

Based on this temperature information and results of numerical reservoir simulation, an updated regional resource assessment was performed. The resource estimates now take into account a long-term contribution of heat from layers above and below the reservoir. Temperature and resource maps are presented for the following main geothermal reservoirs: Frederikshavn, Haldager Sand, Gassum and Bunter/Skagerrak.

Reservoir simulation techniques, known from the oil and gas industry and groundwater modelling, are available as state-of-the-art numerical software systems. With the inclusion of heat flow and temperature, such systems (FEFLOW and Eclipse) were applied to produce long-term evolution of temperature and pressure in the reservoir during production and for the overall geothermal production performance.

Numerical modelling includes results from conceptual models where the importance of thermal recharge by flow of heat from layers above and below reservoirs is evaluated, as well as sensitivity of production profile to thickness of reservoir and distance between production and reinjection wells. These studies are followed by modelling on selected Danish cases, including the existing geothermal plants at Thisted and Sønderborg, with information on local subsurface geology and plant specific boundary conditions.

When historical production data exist, the simulated and observed production data can be matched, ensuring a robust simulation for predicting future production performance and a sustainable reservoir management. Such modelling results are presented for the Thisted and Sønderborg plants.

Modern renewable energy supply systems often produce a surplus of energy in terms of heat that is displaced in time in relation to demand. This asks for long-term seasonal energy storage for which subsurface heat storage is a possibility. Numerical simulations on conceptual models were extended to include examples of combined geothermal production and seasonal heat storage with an evaluation of the amount of heat recovered and increased total performance.

2. A new 3D geothermal model

A new geothermal model for onshore Denmark has been developed. It includes detailed numerical 3D temperature distribution for the deep basins and the upper part of the crystalline crust as well as new heat-flow data for deep boreholes which were applied as model constraints together with measured deep borehole temperatures. For the first time, on a countrywide scale, a comprehensive analysis of well-log data provides well-constrained thermal rock parameter input for a fully parameterized and calibrated numerical subsurface temperature model. This model is now published in Fuchs *et al.* (2020), with a detailed description of methodology and results. Here, a summary is given with emphasis on the modelled temperature distribution of geothermal reservoirs. Figure 2.1 shows the study area, with main structural elements and positions of deep boreholes. For an outline of main potential geothermal reservoirs, with their regional distribution and relations to main tectonic structures, we may refer to Nielsen (2003) and Mathiesen *et al.* (2010).

2.1 Method and data

Early subsurface temperature models for the Danish area (e.g. Balling *et al.*, 1981, 2002) were based on a dense grid of 1D analytical temperature-depth profiles. Now, 3D numerical models have been developed (Balling *et al.*, 2016; Fuchs and Balling, 2016; Poulsen *et al.*, 2017), with emphasis on parameter inverse calibration methodology and its application. Inverse parameter calibration procedures are widely used in groundwater modelling (e.g. Hill and Tiedeman, 2007), but, so far, with little application for subsurface thermal modelling. Such parameter estimation, or optimization procedures, were demonstrated to be of great importance, in particular in applying borehole-temperature data for constraining the thermal rock properties (Fuchs and Balling, 2016; Poulsen *et al.*, 2017) and were applied in the present study.

Our model builds on lab-constrained well-log derived rock thermal parameters (thermal conductivity, specific heat capacity and radiogenic heat production), a procedure by Fuchs *et al.* (2015), new heat-flow determinations for 21 deep-well sites as well as on a new digital structural geological model. This fully updated structural model, based on a reinterpretation of all available reflection seismic lines across the country (Vosgerau *et al.*, 2016), provides information on depth levels and thicknesses of 15 sedimentary units used as 'model input layers' for the sedimentary succession including potential geothermal reservoirs (Fig. 2.2). With a model base at 15 km depth, also the upper parts of the crystalline crust are included.

2.2 Model results with temperatures of geothermal reservoirs

New values of terrestrial surface heat flow range from 65 to 76 mW/m² (mean: 72±3) for the Danish Basin, 77 to 86 mW/m² (mean: 81±5) for the Danish part of the North German Basin and from 61 to 63 mW/m² (mean: 62±1) for the Sorgenfrei-Tornquist-Zone/Skagerrak-Kattegat Platform, respectively. Heat flow from the mantle is estimated within the range of 26–36 mW/m².

Modelled temperatures are validated against independent temperature measurements (137 values from 46 shallow and deep wells) showing very small differences to observations (rms = 1.2 °C, ame = 0.7°C) demonstrating a high prognostic accuracy.

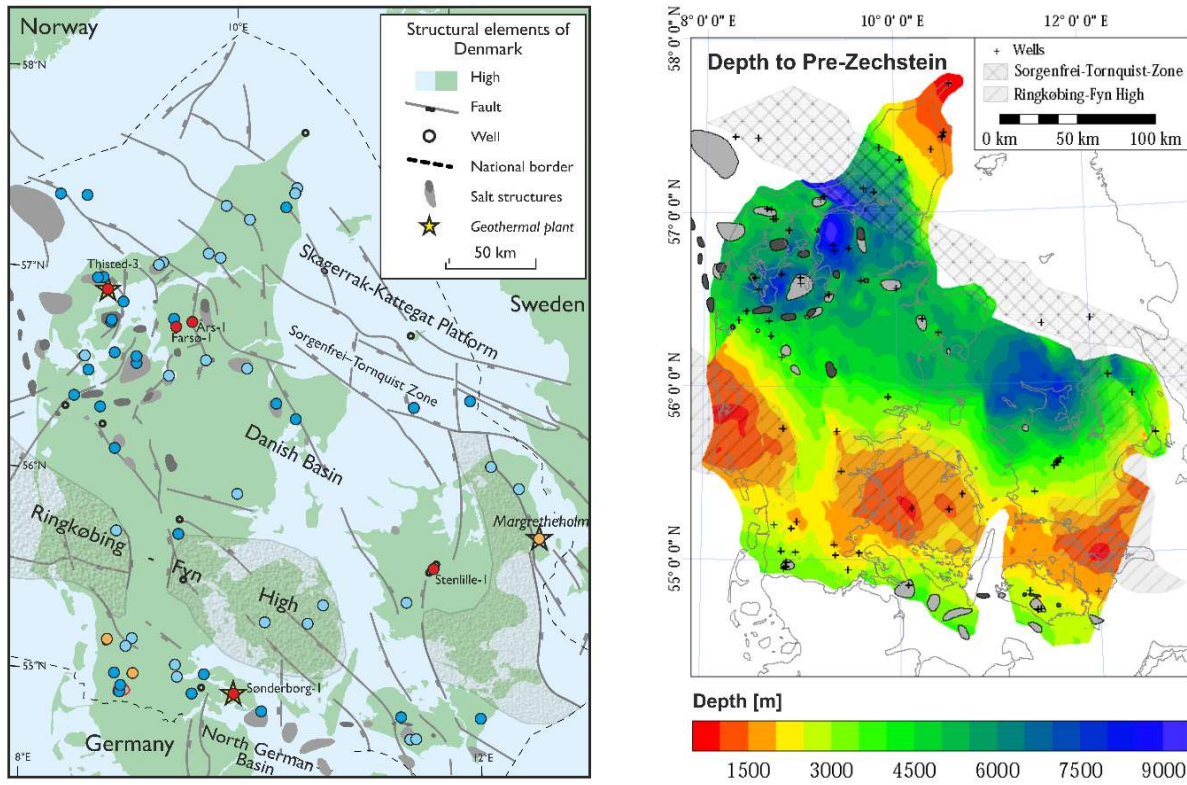


Figure 2.1. Left: Map of the study area with structural elements and deep wells (color code, red disks: with accurate equilibrium temperature logs; orange: with formation test temperatures; dark blue: with corrected bottom-hole temperatures (BHT; equilibrium estimates); light blue: wells with uncorrected BHTs (only minimum temperature estimates); small black circles: with no temperature information). Right: Depth to top Pre-Zechstein emphasizing deep basins and other structural elements shown in the structural map. (Areas around Langeland, south-eastern part shown in white, are not included due to complex subsurface).

Model temperature results in terms of selected key figures are shown below. This applies to temperature maps for the constant depths of 1000, 2000, 3000 and 5000 m (Fig. 2.3) and maps for the main geothermal reservoir formations: Frederikshavn Fm, Haldager Sand Fm, Gassum Fm and Bunter/Skagerrak Fm (Fig. 2.4).

The modelled temperature field reveals significant lateral variability. At 1000 m depth temperatures are generally within the range of 30–40 °C with the lowest temperatures at around 25 °C and the highest values of up to 45–50 °C found mainly in the southernmost part of Denmark (south of the Ringkøbing-Fyn High) and locally in the central parts of the Danish Basin. For 2000 m depth, temperatures are within the range of 50–80 °C with 60–70 °C for most areas and the highest values in parts of the Danish Basin in central and northern Jutland. At 3000 m depth, temperatures cover a board range of 75–110 °C where, more than 100 °C are found in the central and deeper parts of the Danish Basin.

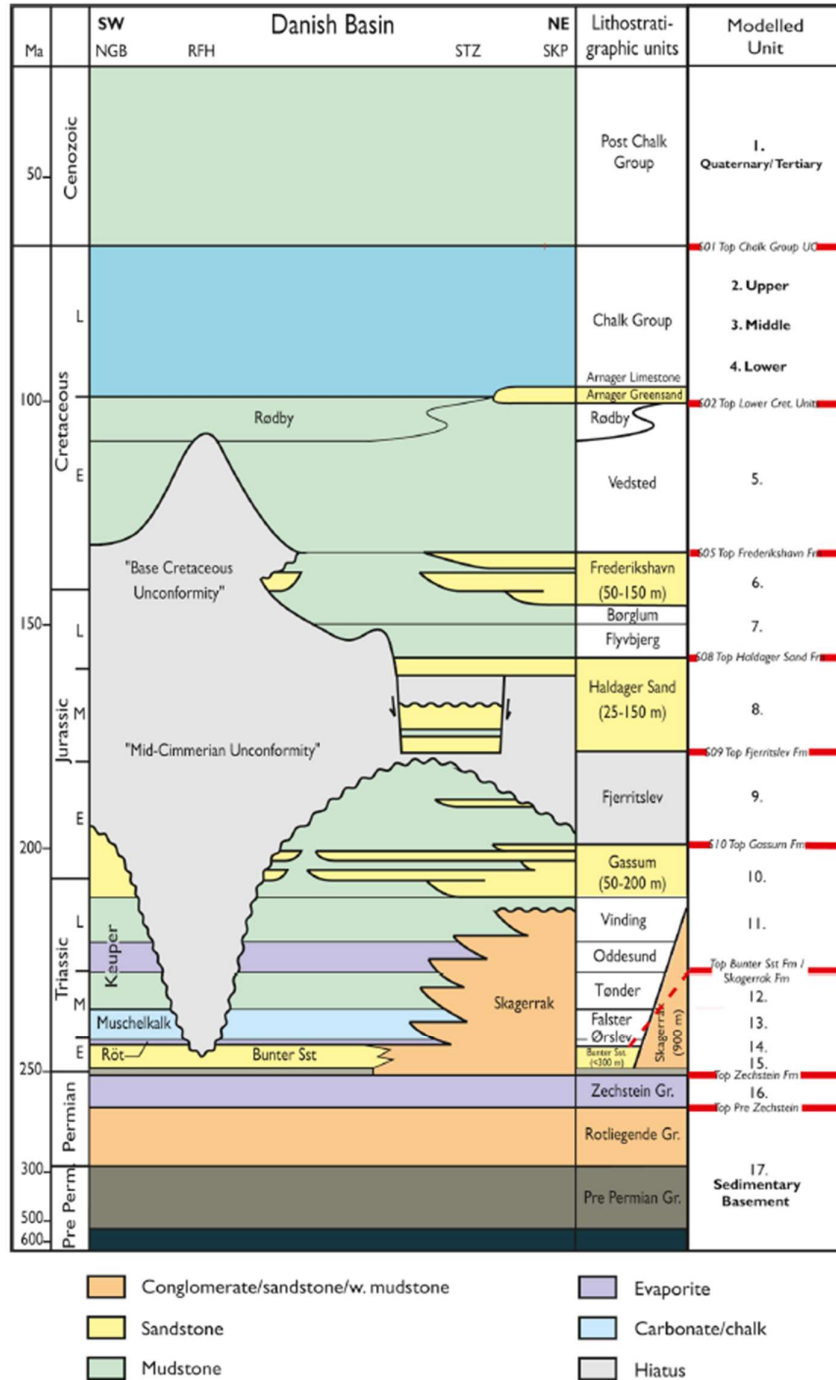


Figure 2.2. Schematic time stratigraphic cross section displaying lithostratigraphic units across main structural elements from south/southwest to north/northeast (North German Basin, NGB; Ringkøbing-Fyn High, RFH; Danish Basin; Sorgenfrei-Tornquist Zone, STZ; Skagerrak-Kattegat Platform, SKP, see also Fig. 2.1). The main potential geothermal reservoirs are shown in yellow and orange. Total thickness ranges are indicated in brackets in the lithostratigraphic-units column. The Gassum and the Bunter Sandstone/Skagerrak reservoirs have a large regional distribution, whereas the remaining reservoirs have a more limited distribution. Lithological units, implemented into the numerical geothermal model are indicated with their associated numbers (right column).

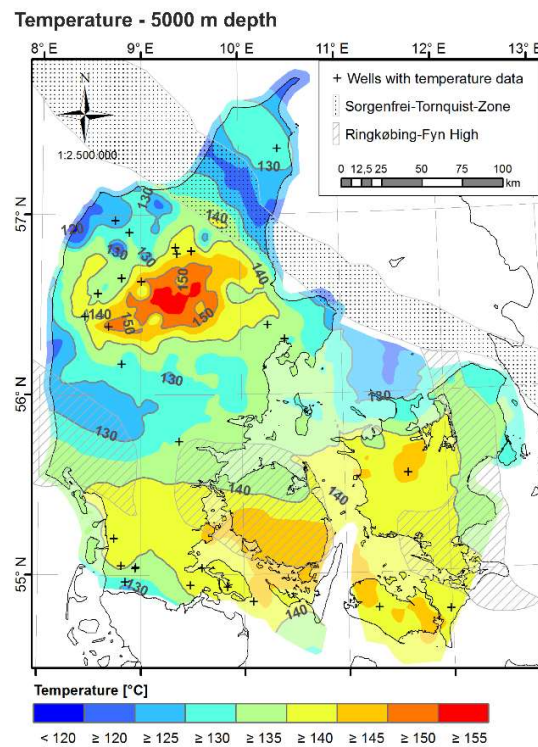
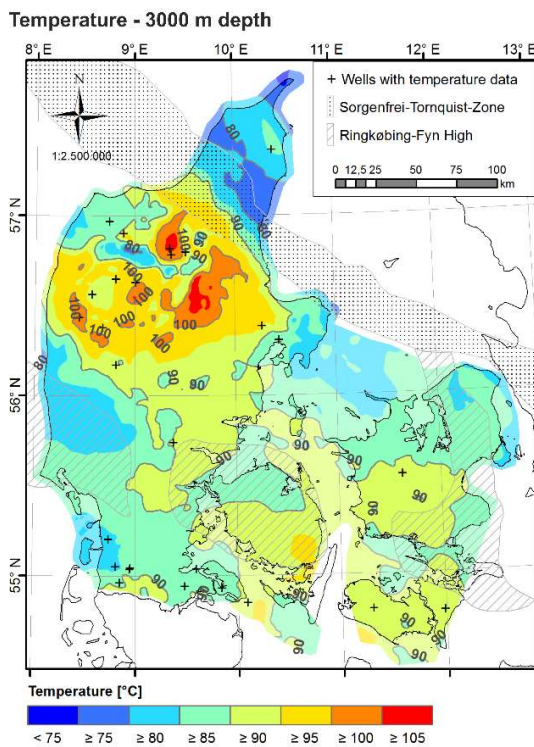
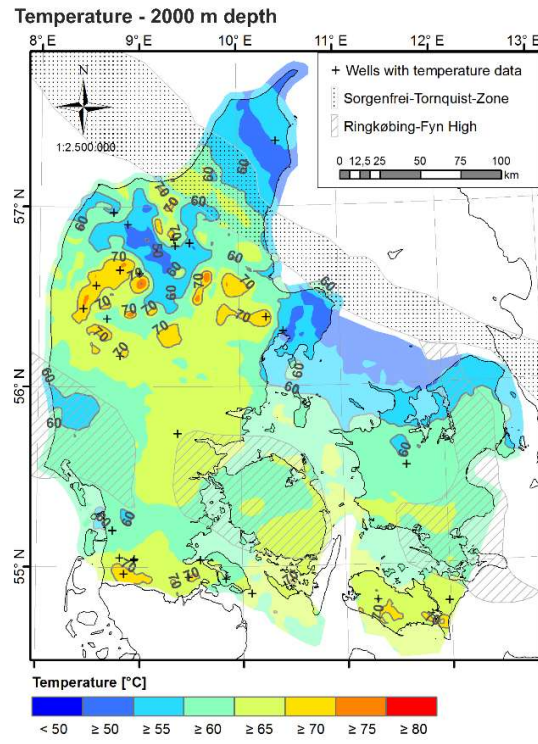
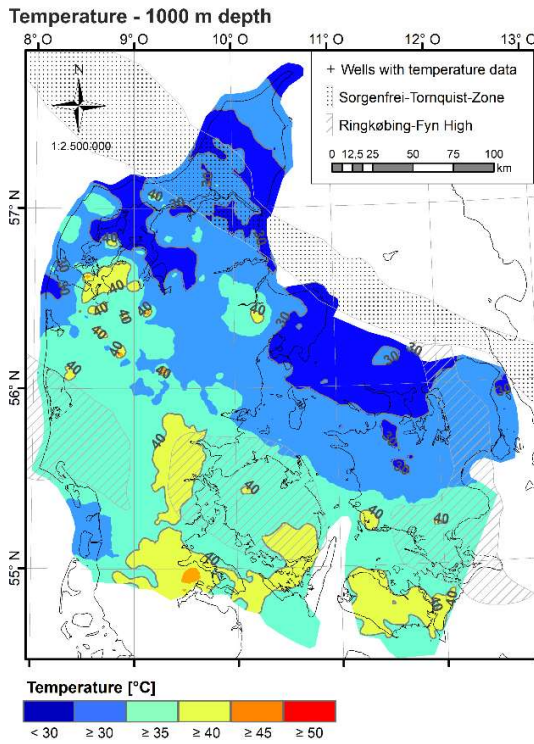


Figure 2.3. Modelled temperature distribution for selected constant depth levels as indicated. Reference depth is sea level – max. 171 m below ground level; average is 34 m. (Areas around Langeland are not included due to complex subsurface cf. Fig. 2.1).

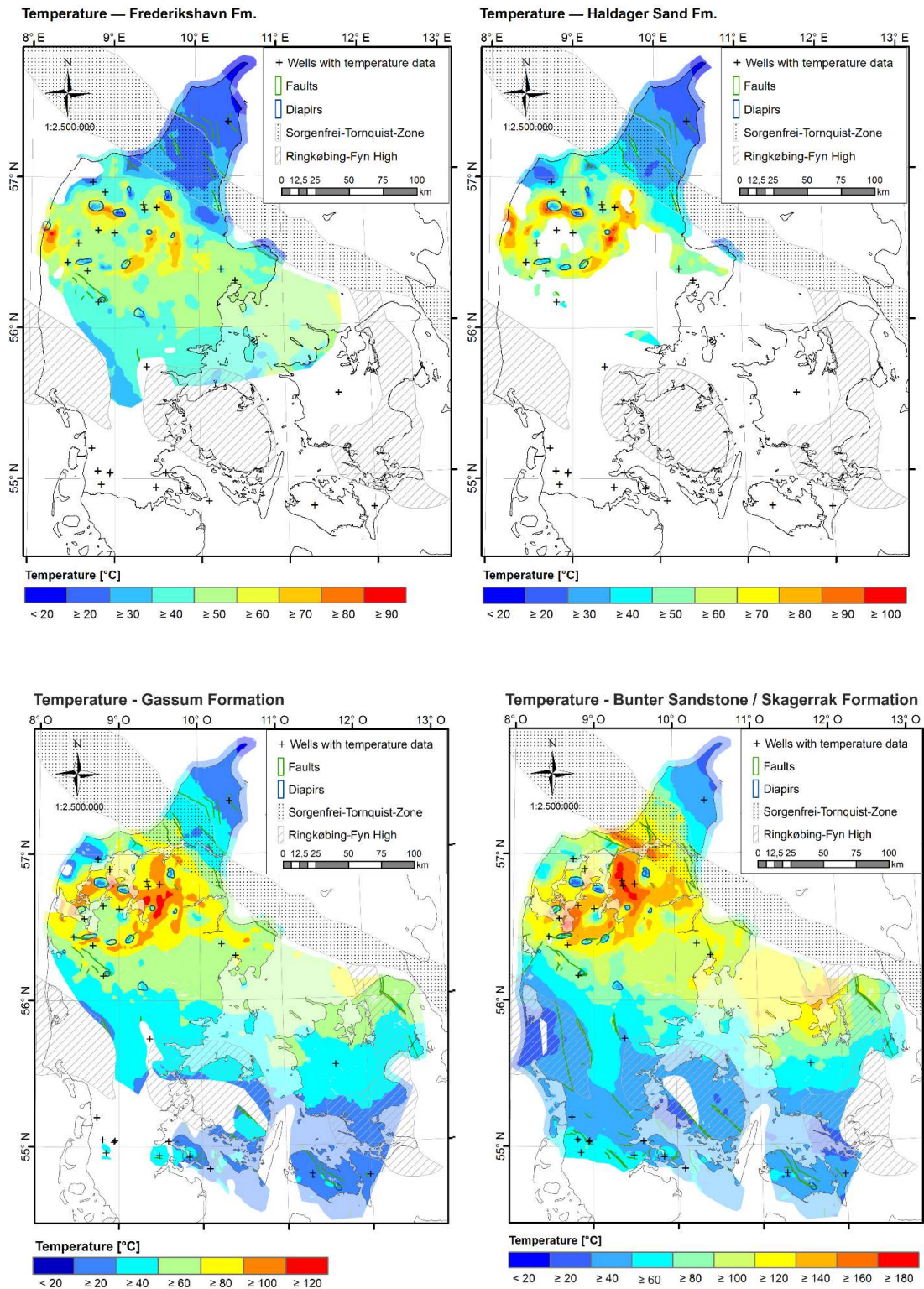


Fig. 2.4. Temperature distribution modelled at the top of main geothermal reservoir formations: Frederikshavn Fm, Haldager Sand Fm, Gassum Fm and Bunter Sandstone/Skagerrak Fm. (Areas around Langeland are not included due to complex subsurface cf. Fig. 2.1).

These results clearly demonstrates that temperature gradients are by no means constant but vary significantly both regionally across the country and locally. For depths of 2000–3000 m, we observe mean temperature gradients within the approximate range of 20–35 °C/km with a model mean value of 27 °C/km. The modelled temperature variations (consistent with observations in deep boreholes) are found to be caused by complex geological structures in terms of thickness variations of sedimentary formations, salt structures etc. and the associated variations of rock thermal conductivity related to lithological differences as well as by lateral variations in background heat flow.

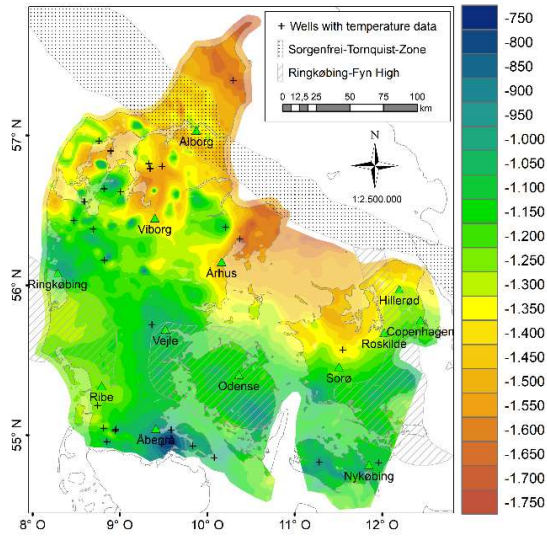
The isothermal maps for main geothermal reservoirs (Fig. 2.4) show a very large span of temperatures as well as large areas of reservoirs with temperatures suitable for geothermal exploration. The reservoirs of main interest are the Gassum Formation (Upper Triassic–Lower Jurassic) and the Bunter Sandstone/Skagerrak Formation (Lower–Upper Triassic) currently being exploited for geothermal energy (cf. Chapter 3). For the Gassum Fm, we model temperatures within the range of 25–130 °C and 25–190 °C for the Bunter Sandstone/Skagerrak Formation which extends to depths of more than 5 km in the deeper parts of the Danish Basin (central/northern Jutland).

For the generally more shallow geothermal reservoirs of more restricted areal extent, the Haldager Fm (Middle Jurassic) and the Frederikshavn Fm (Upper Jurassic–Lower Cretaceous), we find temperatures within the ranges of 20–90 °C and 20–80 °C, respectively. For larger areas in the central and northwestern parts of Jutland these formations have temperatures of around 50–75 °C (cf. Fig 2.4). Fuchs et al. (2020) provide additional isothermal maps for several lithological units.

As a guide for geothermal exploration, model depths of the 45 °C and 130 °C isotherms are shown in Fig. 2.5. These temperatures are often referred as approximate reference levels for the geothermal energy exploitation for heat and electricity production, respectively (e.g. Huenges, 2010). The isothermal level of 45 °C varies significantly with a depth range between 750 and 1750 m. The shallowest level is found locally in the southernmost Jutland (around Aabenraa), rather close to the heating plant at Sønderborg. In the southern part of Denmark, the level of 45 °C can be drilled at depth between 750 and 1250 m, whereas in the northern part, depths up to about 1700 m need to be penetrated. These differences will have a significant impact on drilling costs. For the 130 °C isotherm our model shows a depth range of 3.6–5.6 km.

These results, demonstrate the existence of large regions of geothermal reservoirs with temperatures within the approximate range of 45–80 °C and at depths of estimated sufficient reservoir quality for geothermal production (cf. Olivarius *et al.*, 2015; Kristensen *et al.*, 2016) and thus of special interest for heating purposes. Reservoir temperatures above 130 °C, of interest for the production of electricity, are observed for some local areas, however, likely, too deep for non-stimulated sufficient reservoir quality (cf. Blöcher et al., 2016). When the above temperature information is combined with the results of resources estimation, presented in the following chapter, the areas of special interest are revealed.

Depth [m] at 45 °C isotherm



Depth [m] at 130 °C isotherm

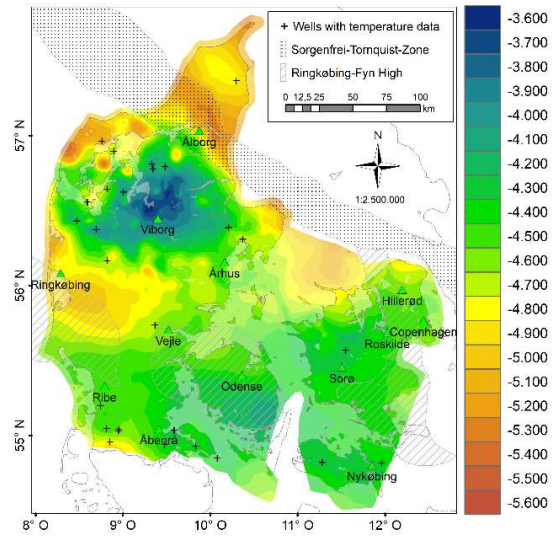


Figure 2.5. Model depth to the isotherm levels of 45 °C (potential direct heating) and 130 °C (potential electricity production).

3. Geothermal resources

The currently available geothermal resource estimates are preliminary first order maps for the four main reservoirs (WebGIS portal for deep geothermal energy: dybgeotermi.geus.dk). Resources were calculated as 'Heat in Place' (see below) from a regional temperature model with constant temperature gradient from surface to the reservoirs. The methodology followed the classical calculation by Muffler and Cataldi (1978). With the availability of the new 3D geothermal model described above, and based on the results of reservoir simulations (Chapter 5), new fully updated resource calculations were made for the main reservoirs, where also some contributions from the layers above and below the reservoir units are included.

3.1 Method

A classic method for estimation geothermal resources is by calculating the so called 'Heat in Place', which represents the maximum theoretically extractable heat in an aquifer (Muffler and Cataldi, 1978). There are several recent published methods and models for calculating geothermal resources, but most are site specific (e.g. Kastner et al., 2015), and not easily comparable and extended to general applications.

Thus, as a starting point, we follow the classic procedure for calculating 'Heat in Place' (H₀), represented as energy per unit area as:

$$H_0 = c_v (T - T_0) h,$$

where c_v is the weighted volumetric heat capacity of rock and pore fluid, $(T - T_0)$ is the temperature difference between reservoir (T) and mean surface temperature (T_0), and h is the cumulative thickness of effective sandstone layers in the reservoir. For porosity, we apply a depth dependent and spatial variable model, with porosities derived from petrophysical well-log analysis combining shale content, sonic porosity, neutron porosity and density porosity. For the layer thickness h , we include only the 'Potential Reservoir Sand' (i.e. PRS or net sand thickness), here defined as the part of sandstone layers having 'good sandstone properties' (i.e. $V_{\text{shale}} < 30\%$; porosity $> 15\%$) and with a further requirement of a total thickness exceeding 15 m, evaluated from seismic and well data as well as according to local geological distribution. The reservoir temperatures (T) are taken from the middle of the reservoir formations and based on the new temperature model (Chapter 2).

Based on reservoir simulation results (Chapter 5), we extend the classic method to include an additional amount of heat, which may be extracted from the layers above and below the reservoir. We include additional heat from up to a distance of 100 m above and below the reservoir boundaries and assume a linear decrease of contribution away from the boundary (cf. temperature profiles in Fig. 5.6). For our case, this additional heat is equivalent to a full contribution from two 50 m thick layers, one above and one below the reservoir. These confining layers are assumed to be claystone-dominated with parameters defined as a mixture of sand- and claystone. Thus, our new Heat in Place, H_0 values are calculated as the sum of two elements, the classical Heat in Place from the reservoir, as described above, and the contribution from the confining layers. The effect by including

heat from the confining layers adds up to 20 to 30 % compared to the traditional method of only including heat from the cumulative thickness of effective sandstone layers in the reservoir.

In cases where, within a geothermal reservoir unit, good quality reservoir sections may be separated by relatively thin clay-rich, low-permeable sections, which quite often occur, our procedure also serve as an approximate model for including contribution from such non-permeable layers. This is justified from our model simulations, as well as from those of Poulsen *et al.* (2015), which show a rapid thermal depletion of an aquitard.

The amount of heat, which in practise may be extracted from a specific reservoir, depends on several factors. Based upon Muffler and Cataldi (1978) and Lavigne (1978), and applied in the resource assessment in the 2002 European Geothermal Atlas (Hurter and Haenel, 2002), a recovery factor may be applied, which, for a geothermal doublet, was defined as 0.33. Introducing the temperature of the return injection water (T_r) together with the surface reference temperature (T_o), we arrive at a new resource assessment base level, H1 by the following relations:

$$H1 = R_o H0,$$

where

$$R_o = 0.33 (T - T_r)/(T - T_o)$$

These estimated values of H1 represents a first step into a simple but well-defined procedure for estimating the fraction of energy, which may be utilised. More detailed estimates will be highly site specific and depends on many factors including the configuration of wells, production profile, time frame etc.

For the H1 estimations presented here, we apply a surface temperature, T_o of 8 °C and an injection temperature, T_r of 20 °C. The chosen injection temperature assumes the use of heat pumps, such as the absorption heat pumps applied in the Danish geothermal plants. Lower injections temperatures of about 5 °C may be achieved by using electrical compression heat pumps. For areas with reservoir temperatures of less than 20 °C, R_o will be negative and the H1 estimate is defined as zero.

3.2 Reservoir thermal resources maps

With the above procedure and with a selection of both variable (thermal conductivity) and fixed rock thermal parameters (heat capacity and heat production) as applied for the temperature modelling (Chapter 2 and Fuchs *et al.*, 2020), resources maps were generated for H0 and H1 for each of the four main geothermal reservoirs: Frederikshavn, Haldager Sand, Gassum and Bunter/Skagerrak. Resources are displayed for reservoirs within the depth intervals of 800–3000 m and having ‘potential reservoir thickness’ that exceeds 15 m, currently assumed to be of prime interest (Figs 3.1–3.4). The energy resource is indicated as heat per unit area ($\text{GJ/m}^2 = 10^9 \text{ J/m}^2$).

It is important to note, that in evaluating the potential resources in specific areas, a comparison with the above maps of reservoir temperatures (Fig. 2.4) is important. Notable, relatively large resources may be present in areas with thick reservoirs of large extend, but of relatively low temperatures. Furthermore, the detailed quality of the reservoir in terms of hydraulic transmissivity (i.e. permeability and thickness of reservoir) is of prime importance.

From Figs. 3.1–3.4 it is apparent that large amounts of geothermal resources are available across most of the Danish onshore areas. Especially in the northern part of Jutland, resources are present in more than one reservoir. The modelled resources reveals large lateral variability, mainly associated with variations in temperatures and thickness and properties (i.e. porosity) of the reservoirs. Temperature variations, as discussed above, may originate from thickness variations of sedimentary formations, presence of salt structures etc. and the associated variation of rock thermal conductivity between and within geological formations of different lithology.

We observe a typical range of 3–10 GJ/m² for ‘usable energy’ (H1) for individual reservoirs. Values of 5–15 GJ/m² are seen in the central parts of the Danish Basin, locally up to 15–18 GJ/m² for the Gassum Formation (Fig. 3.3) and 1–15 GJ/m² in the southern parts of Denmark (south of the Ringkøbing-Fyn High) for the Bunter Sandstone/Skagerrak Formation (Fig. 3.4). For the shallower Frederikshavn and Haldager Sand Formations (Figs. 3.1 and 3.2), the larger resources are found mainly in the deepest central parts of the Danish Basin and in northern Jutland.

Important input parameters for the resource estimation like effective porosity, temperature, and cumulative reservoir thickness varies depending on the location. The actual areal extend for potential utilization of a specific reservoir, needed to calculate the total amounts of energy, depends on the distance to and density and magnitude of faults (i.e., reservoir continuity). For the resource estimates presented here (as heat energy per unit area), such detailed areal considerations are not included. Still, the regional distribution of reservoirs are apparent from the maps. For an upscale to large areas, we note that a resource of 1 GJ/m² yields 10⁶ GJ/km² (10¹⁵ J/km² = 1 PJ/km²) of heat energy. This is 24,000 tonnes of oil equivalent (toe) for each square kilometre. Thus, several reservoir units have heat energy equivalent to about 100,000–200,000 toe per square kilometre. When compared with the temperature maps in Fig. 2.4, we see that vast amounts of resources exist in areas of reservoir temperatures within the approximate range of 45–80 °C, suitable for utilization for heating purposes.

We emphasise that this is a general, regional resource assessment, where details of reservoir properties (e.g. permeability variations related to diagenetic processes and facies changes) and local geological complexities (impact of salt structures, faults etc.) are not specifically included. However, the combined information from the resources maps and the above temperature maps, demonstrates that vast amounts of geothermal resources are present in the Danish sedimentary reservoirs, indicating that geothermal energy has the potential for supplying district heating networks with sustainable energy for hundreds of years into the future. A closer inspection of the maps will show that large amounts of geothermal energy are available also in areas of several of the larger cities, representing a significant heating demand, such as the Copenhagen and adjacent areas, Aalborg and Aarhus.

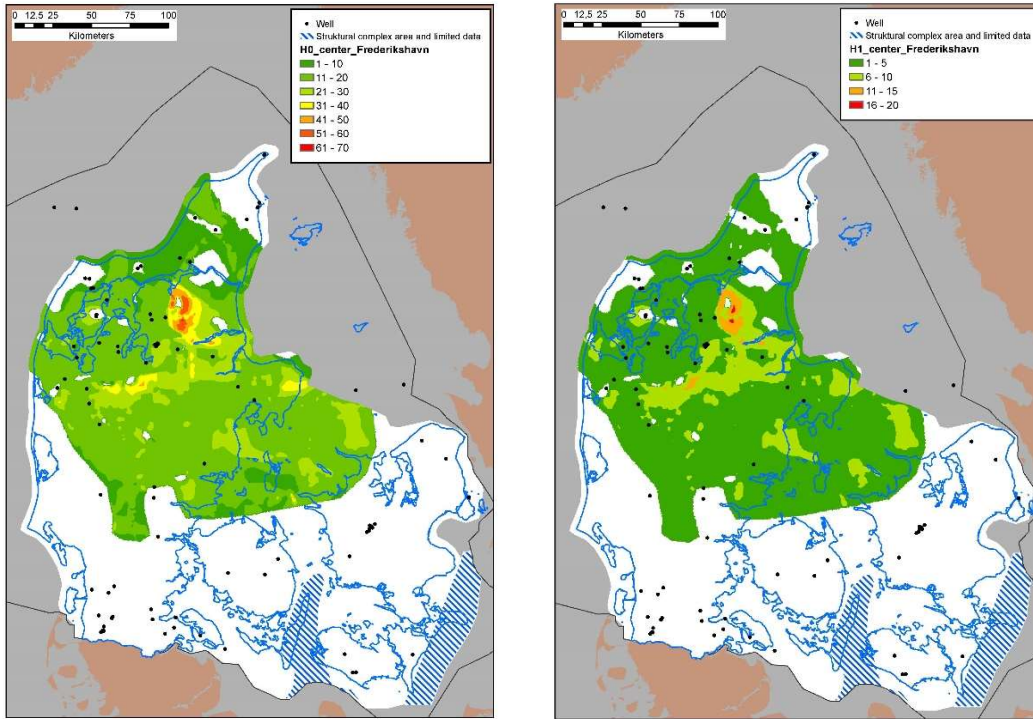


Figure 3.1. Resource estimation, H0 and H1 (GJ/m²) for the Frederikshavn geothermal reservoir.

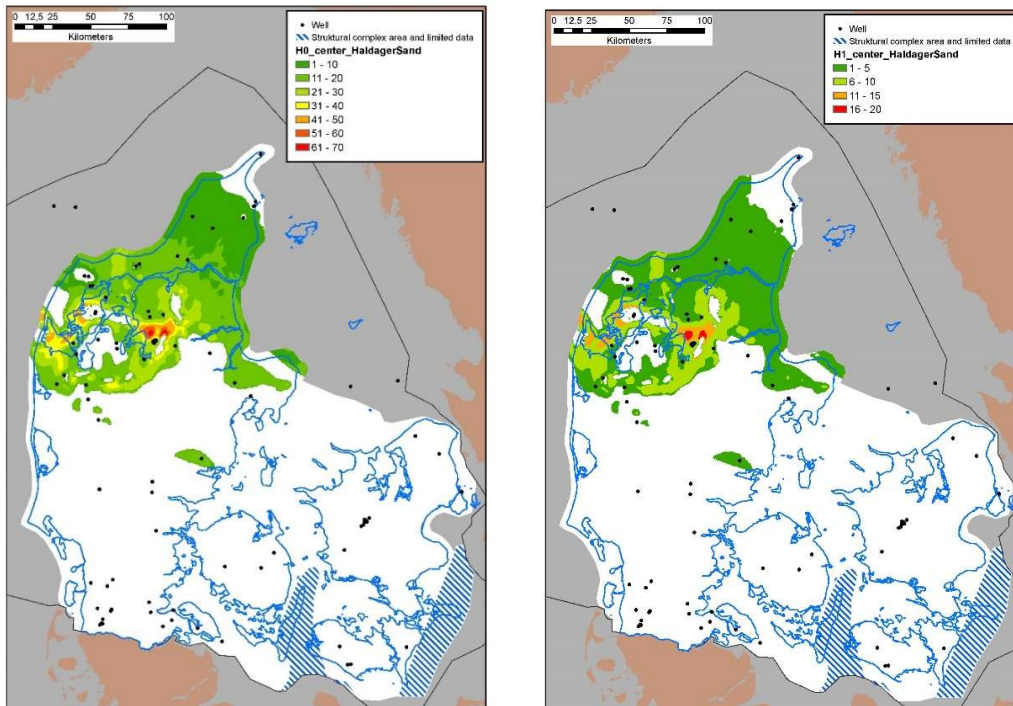


Figure 3.2. Resource estimation, H0 and H1 (GJ/m²) for the Haldager geothermal reservoir.

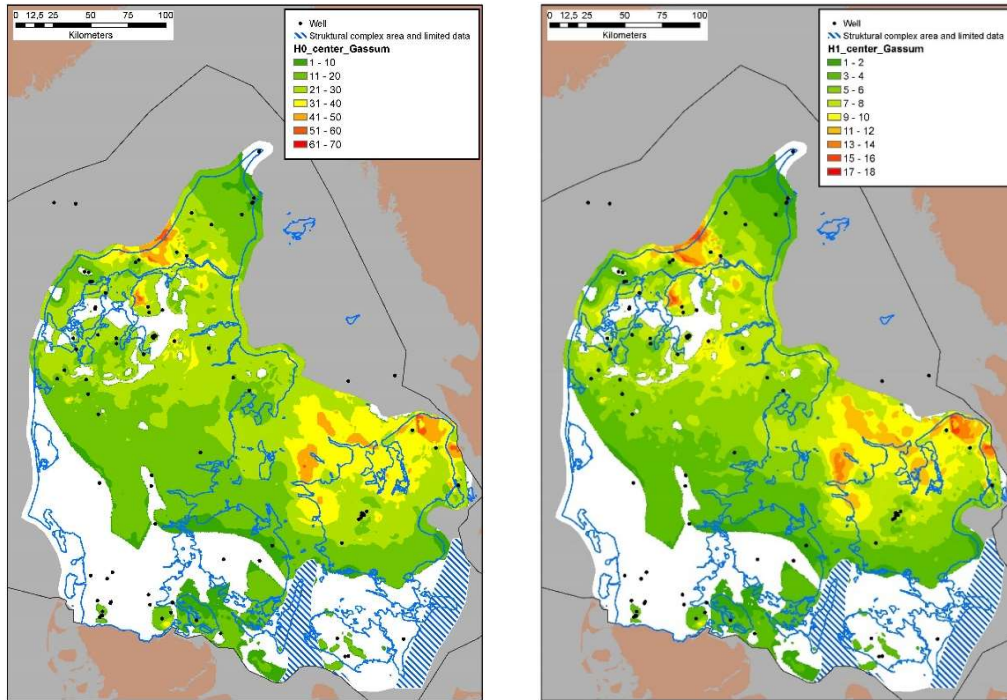


Figure 3.3. Resource estimation, H0 and H1 (GJ/m²) for the Gassum geothermal reservoir.

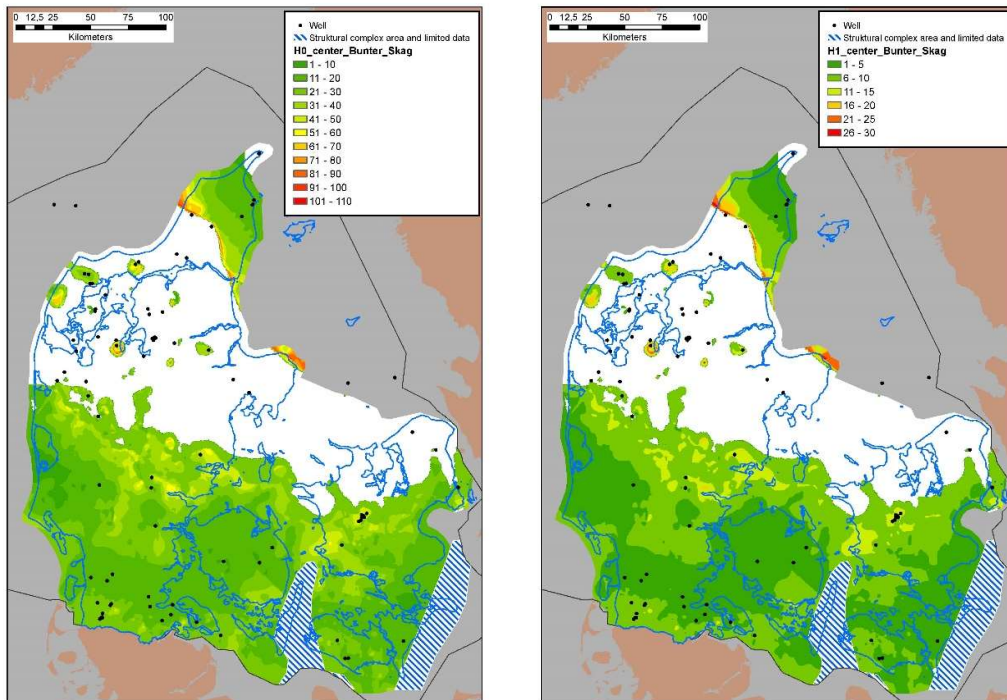


Figure 3.4. Resource estimation, H0 and H1 (GJ/m²) for the Bunter/Skagerrak geothermal reservoirs.

4. Rock thermal properties

GEO THERM Interim report M4.3 (Fuchs and Förster, 2019) describes the results of laboratory measurements carried out at GFZ, Potsdam on rock thermal properties. It comprises petrophysical measurements on a suite of 42 drill core samples from the Danish Basin. Thermal conductivity and thermal diffusivity were measured under ambient conditions on samples from the Gassum Fm., Fjerritslev Fm., Haldager Sand Fm., Flyvbjerg Fm. (all Lower Jurassic/Upper Triassic), Frederikshavn Fm. and Vedsted Fm. (both Cretaceous). For a subset of samples, temperature-dependent specific heat capacity was measured under dry conditions for temperatures up to 400 °C. The data form an extension of input data for numerical temperature models developed for the assessment of geothermal production and reinjection cycles.

Some main elements and results are summarized below.

4.1 Sample preparation and laboratory measurements

The sample collection consists of cylindrical core sections between 6 and 12 cm in diameter, most of them cut in half along the major axis (Fig. 4.1a). The length of each sample is in the approximate range of 5-20 cm. From 20 of the original samples, subsamples of 4 cm in diameter and 3 cm in height were cored for the planned autoclave experiments (Fig. 4.1b). These plugs were also prepared for transient divided bar measurements at Aarhus University. For further five samples, the preparation of plugs (water driven drilling and polishing) failed mostly due to clay swelling effects and sample disintegration or poor compaction. The remaining pieces of core samples were sawed for the optical scanning measurements. The plugging and sawing were performed in the GFZ laboratories. For a subset of 10 samples, cylinders of 4.9 mm (D) x 16 mm (L) and powders were prepared for specific heat capacity measurements.

Measurements of the following parameters were conducted: Effective porosity, density (density of the matrix and bulk density in saturated and dry conditions), thermal conductivity at dry (air) and saturated (water-filled pores) conditions, thermal diffusivity at dry and saturated conditions and specific heat capacity at elevated temperatures under dry conditions.

The Thermal Conductivity Scanner (TCS, produced by Lippmann and Rauen GbR) based on the optical scanning (OS) technology was used for the measurements of thermal conductivity (TC) and thermal diffusivity (TD). This is a transient-state, non-destructive method that works at ambient laboratory conditions (20–25 °C; 1atm) and permits the measurement of any consolidated rock type under variable saturated conditions (air, water, etc.). The OS is based on the determination of the maximum temperature rise (ca. 3–4 °C increase) induced on the surface of a sample by a known heat source in comparison to the temperature rise of standards of known thermal properties. Details of the method are given by Popov *et al.* (1985, 2016). Accuracy of the method is estimated at 3% for TC and 5% for the combined TC/TD mode applied in this study.

The isobaric heat capacity of the clastic and carbonate samples was measured in the temperature range of 60 to 400 °C using a DSC HTC (Differential Scanning Calorimetry/High Temperature Calorimeter), produced by Setaram and equipped with a thermal analysis. A constant heating rate

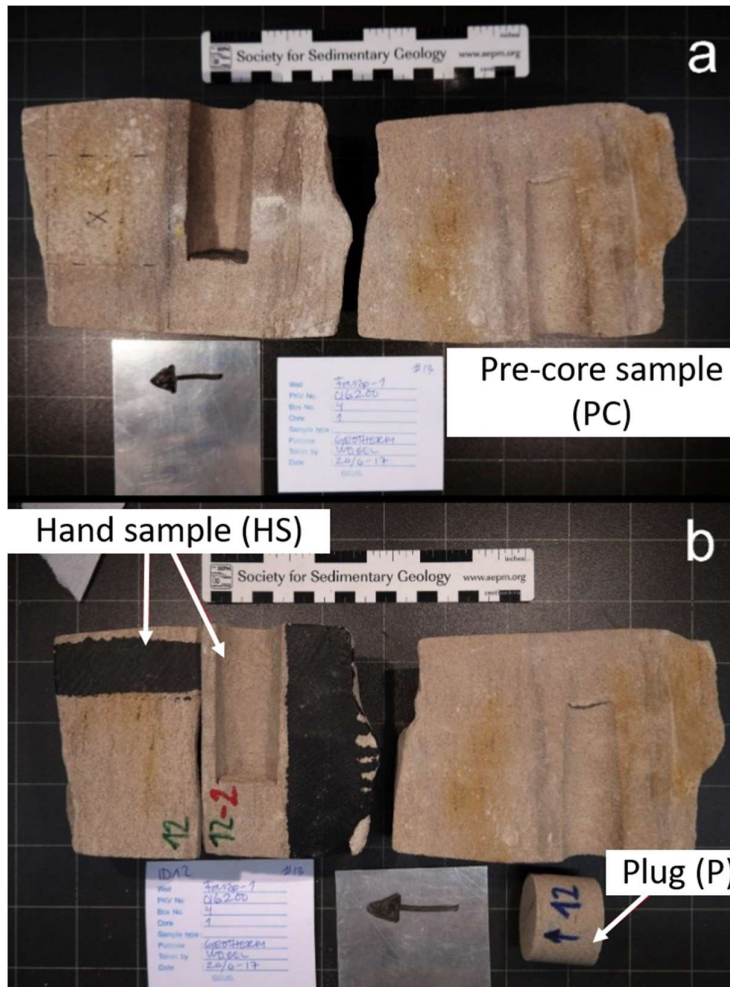


Figure 4.1. Sample preparation, exemplified on sample no. 12. a) Pre-coring sample, as it was received from GEUS. b) Samples after the treatment: two hand samples (left) and a plug (bottom-right). The black paint on the hand samples is required for optical scanning.

of 3 K/min was applied. DSC analysis was carried out to determine the thermal behaviour of the sample from the thermograms. An Al_2O_3 powder was used as reference standard.

4.2 Measuring results

The bulk thermal conductivities (BTC) and diffusivities (BTD), measured with the TCS, are shown in Fig. 4.2. These graphs show all measurements at surface of samples, per lithological class. Here, no distinction between parallel and perpendicular values was done. For clay-rich lithologies, the iso-octane-saturated measurements were converted to pure water saturated equivalents by the geometric mean formula.

For both BTC and BTD, water-saturated values are higher than those measured at dry conditions. The range for BTC under dry conditions ('dry TC') is from 1.08 W/(m K) for limestones to a

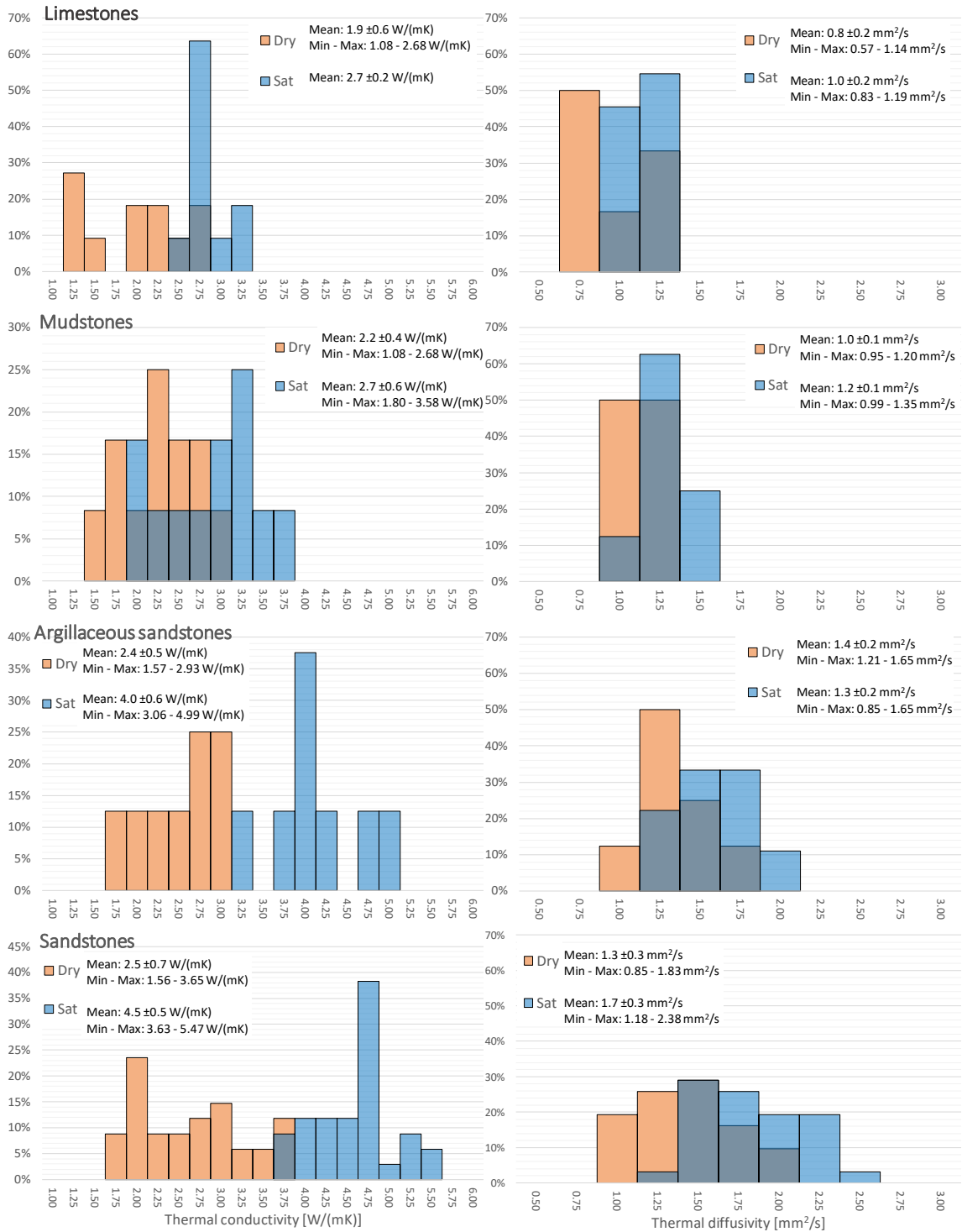


Figure 4.2. Frequency distribution of TC (left) and TD (right) for dry (orange bars) and saturated (blue-transparent bars) samples; overlaying distributions in dark blue. Number of measurements (TC/TD): Limestone: 11/12; Mudstone: 12/8; Sandy mudstone: 19/13; Argillaceous sandstone: 8/8; Sandstone: 34/31.

maximum of 3.65 W/(m K) for sandstones. For saturated conditions ('sat TC'), measurements range between 1.80 W/(m K) for mudstones and 5.47 W/(m K) for sandstone samples.

For BTC, the distributions in dry and saturated conditions are generally similar in shape, except for the limestones, which plot around 2.75 W/(m K) for saturated conditions contrarily to the wider distribution in dry conditions. Moreover, mudstones and sandy mudstones show a smaller difference between the distributions in dry and saturated conditions, relatively to the sandy classes. In fact, the mean difference between saturated and dry TC is about 0.6 W/(m K) for both muddy rock types, while it is highest (1.6 W/(m K) and almost 2 W/(m K)) for sandstones and argillaceous sandstones, respectively.

The BTD measured under dry conditions ('dry TD') ranges between 0.57 mm²/s (limestones) and 1.83 mm²/s (sandstones). Limestones and sandstones represent also the minimum and the maximum values for saturated conditions ('sat TD'), respectively: 0.83 mm²/s and 2.38 mm²/s. The BTD distributions are constrained to smaller ranges of values than BTC and delineate very small differences between dry and saturated conditions. Nonetheless, a larger difference between the two conditions is evident for sandy samples, compared to the muddy ones.

For both TC and TD, values generally increase from muddy to sandy samples when measured under saturated conditions. For dry measurements, the increase of values is smaller.

Data were analysed in terms of correlation between measured TC and TD and porosity as well as for anisotropy (Fuchs and Förster, 2019; Fuchs *et al.*, 2020 submitted).

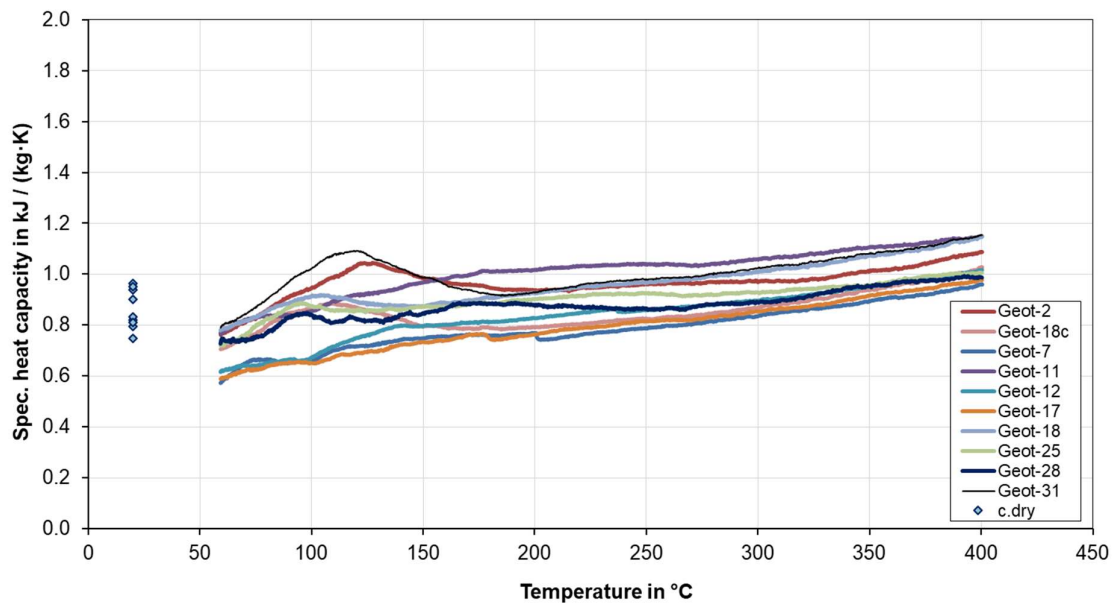


Figure 4.3. Temperature-dependent specific heat capacity of selected samples (dry conditions). Lines are DSC-measured data. Dots are calculated from the ratio of TC/(TD x density).

Specific heat capacity increases with increasing temperature. The range is between ca. 0.6 and 0.8 kJ/(kg K) at 60 °C, and between ca. 0.95 and 1.15 kJ/(kg K) at 400°C. For sample depth of 1500 to 3000 m, the average increase is by 10 to 17%.

4.3 Summary

The presented new data on thermal conductivity and thermal diffusivity at ambient conditions and specific heat capacity at *in situ* temperature conditions of sedimentary rocks from the Danish Basin extend previous data by Balling *et al.* (1981) and Balling *et al.* (1992). The majority of the analysed samples were taken from depths between 1500 and 3000 m. Data on thermal diffusivity and specific heat capacity were not measured before and are a valuable new source of data for reservoir models addressing thermal aspects (production, reinjection, etc.).

5. Reservoir simulation – conceptual models

State-of-the-art numerical software were applied to produce estimates for the temperature and pressure development in the reservoir during production and for the overall geothermal production performance.

Numerical modelling includes results from conceptual models where the importance of thermal recharge by flow of heat from layers above and below reservoirs are evaluated as well as sensitivity of long-term production profile to thickness of reservoir and distance between production and reinjection wells.

With modern renewable energy supply systems, over time, surplus of energy in terms of heat is produced with a significant need for long-term seasonal energy storage. Numerical simulation on conceptual models is extended to include examples of combined geothermal production and seasonal heat storage with evaluation of the amount of heat recovered and associated increased performance.

These studies are followed by modelling on selected Danish cases, including the existing geothermal plants at Thisted and Sønderborg.

5.1 Method and theory

We are dealing with combined groundwater flow and heat flow, which involve three sets of equations. The standard flow equation for a confined aquifer with a groundwater source is of the form:

$$Q = S_s \frac{\partial h}{\partial t} + \nabla \mathbf{q} \quad (1)$$

where Q is the volumetric source rate per unit volume, S_s is the specific storage, h is the hydraulic head, and \mathbf{q} is the Darcy velocity. Since both viscosity and density are temperature dependent parameters, and the Darcy velocity (\mathbf{q}) is dependent on them, the formulation of the Darcy equation becomes:

$$\mathbf{q} = -\mathbf{K} f_\mu \left(\nabla h + \frac{\rho_f - \rho_0}{\rho_0} \mathbf{e} \right) \quad (2)$$

where \mathbf{K} is the hydraulic conductivity tensor, f_μ is the ratio of reference viscosity to dynamic viscosity, h (as above) is the hydraulic head, ρ_f and ρ_0 are the fluid and reference density respectively, and \mathbf{e} is the gravitational unit vector.

Finally, the density coupled heat equation, taking into account thermal dispersion, is:

$$(\rho c)_b \frac{\partial T}{\partial t} = \nabla \cdot [(\lambda_b \mathbf{I} + (\rho c)_b \mathbf{D}) \cdot \nabla T] - (\rho c)_f \mathbf{q} \cdot \nabla T + H \quad (3)$$

where $(\rho c)_b$ and $(\rho c)_f$ is the bulk and fluid volumetric heat capacity, respectively, λ_b is the bulk thermal conductivity, \mathbf{I} is the unit tensor, \mathbf{D} is the tensor of mechanical dispersion, and H is the bulk

heat sink/source. For further explanation on above equations and parameters included, we may refer to Diersch (2014).

For the reservoir simulations presented in the following sections, two different software systems were applied, FEFLOW (Diersch, 2014) and Eclipse 100 (ECLIPSE, 2017). Both are robust and well-proven numerical codes for solving the above equations for combined water and heat flow. In FEFLOW the equations are solved by the finite element method. As the name suggests, model areas are divided into finite number of elements with certain geometry (triangular, quadratic, etc.). Eclipse 100 applies the finite difference method for solving the equations. It is widely used in the oil industry for reservoir simulations and has a built-in temperature option for integrating the heat equation and simulating temperature distribution.

In the present project, the FEFLOW software (applied by the Department of Geoscience, Aarhus University) and the Eclipse software (applied by GEUS) were compared in terms of modelling results on well-characterised conceptual geothermal cases, with combined geothermal production and injection, similar to those discussed in the following sections. The two systems were found to produce realistic and equivalent results with only very small long-term temperature differences (Nielsen and Major, 2018).

5.2 Heat extraction by geothermal doublets

The importance of thermal recharge by flow of heat from layers above and below reservoirs are evaluated as well as sensitivity of long-term production profile to thickness of reservoir and distance between production and reinjection wells. Present results build upon previous comprehensive parameter sensitivity studies by Poulsen *et al.*, (2015) and results obtained by Major (2016), some of which are included in the results presented below.

Model set up, parameters and boundary conditions

The subsurface model extends 10 km x 10 km horizontally and 1050 m in the vertical direction (Fig. 5.1) with the reservoir represented by a 50 m thick permeable layer bounded by two 500 m thick impermeable confining beds. The top of the model was set to 2050 m depth resulting in the reservoir extending from 2550 to 2600 m depth. Distance between production and injection at reservoir level is 1200 m. Reservoir depth and well separation are similar to those of the Margrethholm geothermal plant (Copenhagen area) exploiting the Bunter Sandstone reservoir (Røgen *et al.*, 2015; Poulsen *et al.*, 2015).

The finite element mesh was generated using FEFLOW's automatic mesh generator with triangular elements. Vertical discretization of both the reservoir and the confining beds was implemented by subdividing into multiple layers. Minimum layer thickness is 0.5 m and gradually increased away from the layer boundary to 140 m in the confining beds and 5 m in the reservoir. After refinement the base model consists of 37 slices and 36 layers respectively and has more than 900 thousand nodes and 1.75 million elements.

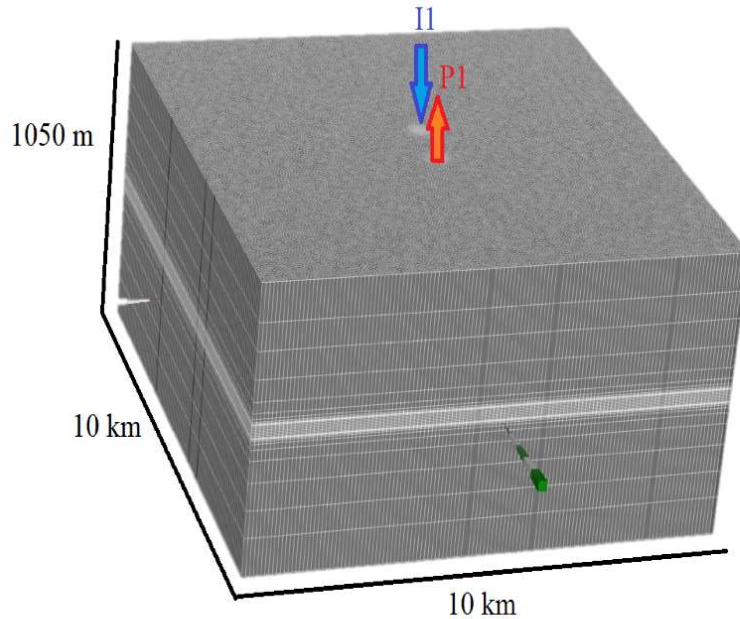


Figure 5.1. Model domain with spatial discretization and refinements. P1 denotes the production well and I1 the injection well.

This base model, both in terms of model set up and the model parameters (Table 5.1) is similar to that of Poulsen *et al.* (2015). Fluid density is 1170 kg/m^3 corresponding to a 20 w% NaCl brine at $20 \text{ }^\circ\text{C}$, and both density and viscosity are dependent on temperature. The hydraulic conductivity of the reservoir of $4 \times 10^{-6} \text{ m}^{-1}$ corresponds to 0.5 darcy in permeability.

Homogeneity is assumed for both the reservoir and the confining beds, and the boreholes are treated as ‘perfectly insulated’, thus, with no heat exchange between the boreholes and the confining beds. In Chapter 6, we model reservoirs representing specific geological situations with reservoirs having lateral as well as vertical variability.

The upper model boundary is represented by a constant temperature and hydraulic head of 0 m, and horizontally, the model ends in thermal and hydraulic no-flow boundaries. With an upper boundary temperature of $55 \text{ }^\circ\text{C}$ and a lower boundary background heat flow of 65 mW/m^2 an average reservoir temperature of $75 \text{ }^\circ\text{C}$ is obtained for the steady-state initial conditions. Flow rates of the wells are modelled constant at $150 \text{ m}^3/\text{h}$ ($3600 \text{ m}^3/\text{day}$) and injection temperature is set to $20 \text{ }^\circ\text{C}$.

Modelling results, long-term heat extraction

The effect of reheating of the cold injection water, referred to as thermal recharge (cf. Poulsen *et al.*, 2015) is modelled by comparing the modelled temperatures of the production well with the equivalent, but hypothetical, situation of ‘no flow of heat and mass’ across the boundaries to the confining beds. The two models (Fig. 5.2) show similar characteristics at early stages with

Table 5.1 Model thermal and hydraulic parameters

Parameter	Reservoir	Confining bed
Thickness (m)	50	500
Hydraulic conductivity (m/s)	4×10^{-6}	10^{-11}
Specific storage (1/m)	2×10^{-6}	2×10^{-6}
Thermal conductivity of matrix (W/m/K)	6.0	2.0
Thermal conductivity of fluid (W/m/K)	0.62	0.62
Volumetric heat capacity of matrix (MJ/m ³ /K)	2.3	2.3
Volumetric heat capacity of fluid (MJ/m ³ /K)	4.0	4.0
Longitudinal dispersivity (m)	10	10
Transverse dispersivity (m)	1	1
Porosity (%)	25	25

temperature breakthrough (defined when temperature declines by 0.1 °C) around 26 years in the no-flow model and about 32 years in the base model. Then, over time, the curves show increasing separation. After 50 years, the base model temperature has declined only by 1 °C, whereas the no-flow model shows a decline by 5 °C. After 100 years the values are 5.5 °C and 16 °C, respectively and after 300 years, the base model temperature decline is 13 °C (production temperature about 62 °C) and 27.5 °C in the no-flow model (production temperature 47.5 °C). Thermal recharge plays a significant role in keeping production temperatures at a high level and making the lifetime of the reservoir substantially longer. Present model results compare well with those of Poulsen *et al.* (2015), showing only small differences, about 1-2 °C, in long-term production temperatures, thus, confirming the very long lifetime of geothermal reservoirs.

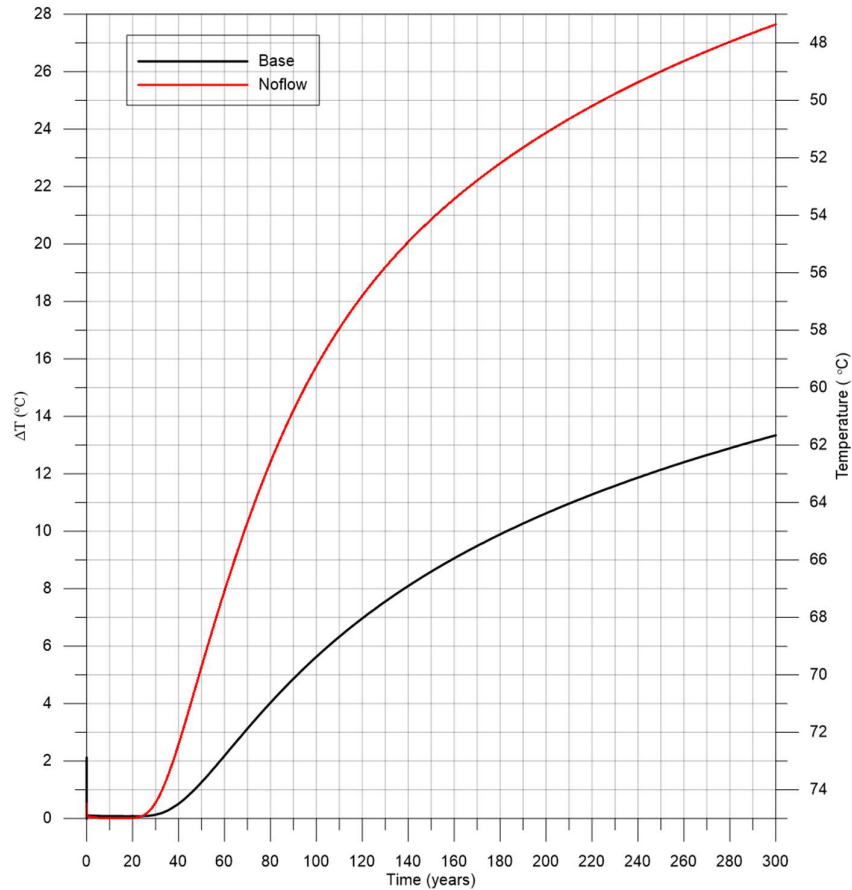


Figure 5.2. Production temperatures (right) and temperature decline (left) during 300 years of simulation. Base model (black) compared with no heat-flow from the confining beds (red).

The difference in energy production between the two models, normalized to the base model, is shown in Fig. 5.3. Until the production temperature starts to decline in the no-flow model, at about 26 years, production temperatures are the same, thus no difference. Then, the curves separate with 7.5% additional energy in the base model at 50 years increasing to 20% and 30% at 100 and 200 years, respectively. Thus, the difference is modest in the first phases of production but becomes substantial for long-term production.

The distribution of the cold water around the injection well at selected times is shown in Fig. 5.4. The cold plume develops almost radially around the well with a slightly elongated feature towards the production well. The front of water of reduced temperature reaches close to the production well after about 30 years (Fig. 5.4b; 74.8 °C isoline in red); after 50 years, the 70 °C isoline is close to the well and after 100 years, the 60 °C isoline. However, due to the extraction of warm water from all directions around the production well, the colder injection water is only marginally affecting the

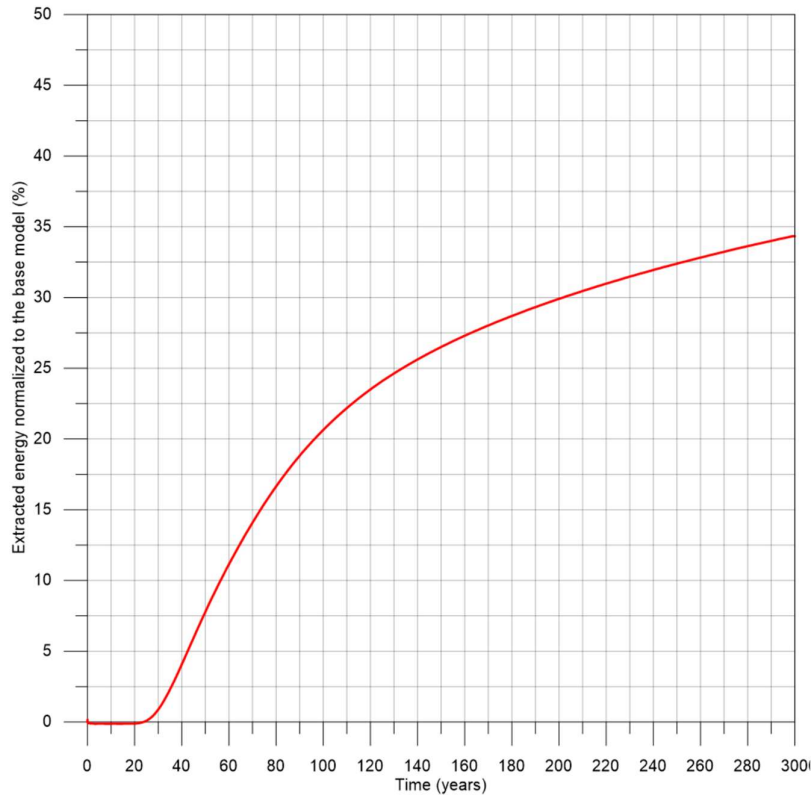


Figure 5.3. Difference in energy production between base and no-flow models in terms of total extracted energy normalized to the base model energy production.

production temperatures cf. Fig. 5.2. In terms of energy production and energy resources, the basemodel yields 7.5×10^{16} J during the modelled 300 years, which is 10% of the total energy stored in the model part of the reservoir. In comparison, the case with no contributions from the confining beds produces 5.8×10^{16} J.

Well distance

Long-term production temperatures and energy extraction are sensitive to the distance between production and injection wells. This is demonstrated by Fig. 5.5 showing simulations with well distances of 600 m, 1200 m (base model), and 2400 m. A significant difference is apparent in the time in which the temperature front of the injection water reaches the production well. This is around 7 years in the 600 m-distance model, a quarter of the time in the base model. Doubling the distance to 2400 m results in almost no temperature drop, by mere 1 °C to 74 °C after 300 years of continuous production. After 50 years production, temperatures in the 600 m-doublet has declined by 16 °C compared with 1 °C in the 1200 m-doublet.

It is obvious, that the distance between wells may have a significant impact on production temperature. Here, the bigger doublet maintains its production temperature for a very long time. This advantage is to be balanced against disadvantages such as potential reservoir discontinuities

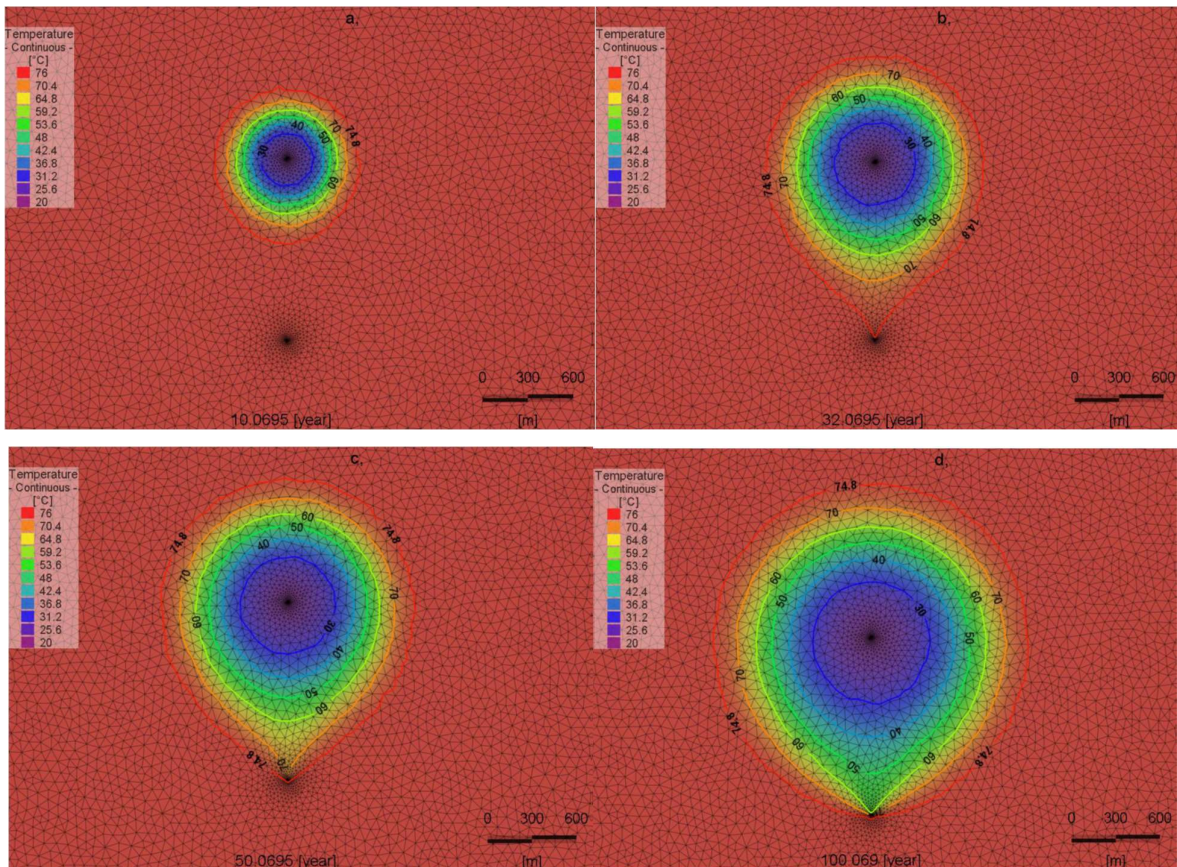


Figure 5.4: Evolution of the cold-water plume during production. a-d show the temperature distribution at mid reservoir after 10, 32, 50, 100 years, respectively.

causing connectivity problems and logistic issues regarding the longer distances in building the required surface installations, especially in densely populated areas.

The effect of thermal recharge upon production temperatures is also highly dependent on well distance. This is illustrated by Fig. 5.6 showing the modelled temperature-depth profiles at the production well after 300 years of production. Both for the 600 m and 1200 m distance cases, temperature reduction is significant at up to more than 150 m above and below the aquifer. For the 2400 m case, this effect is very small. In Fig 5.6, we note small temperature jumps (about 1 °C or less) in the model curves at the aquifer boundaries. These variations are likely due to minor numerical errors associated with boundaries of abrupt parameter changes. Temperatures above and below the aquifer should not be lower than that of the aquifer.

Aquifer thickness

Thicknesses of geothermal reservoirs may vary significantly; main potential geothermal reservoirs in Denmark ranging from about 15-20 m to more than 100 m in thickness (see Chapter 2). Simulation

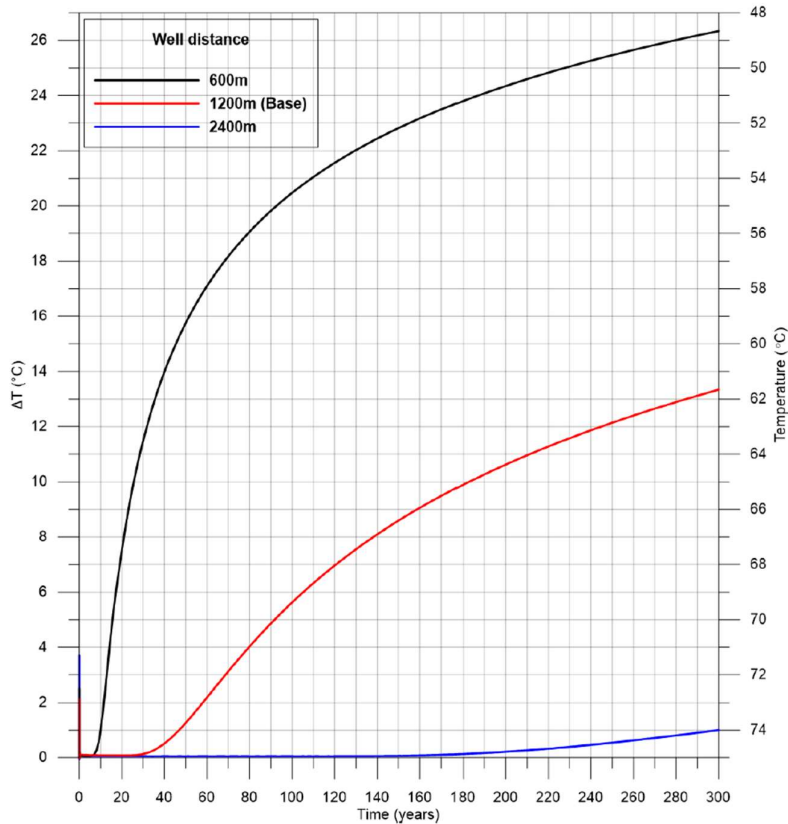


Figure 5.5. Results of the simulated production temperatures with different well distances: 600 m (black), 1200 m (red) and 2400 m (blue). Continuous constant production rate at 150 m³/h.

results for the evolution of production temperatures with aquifers of differing thicknesses (5, 10, 25, 50, and 100 m) are shown in Fig. 5.7. Here, aquifer temperatures have slightly different steady-state starting positions and these small differences were corrected to more easily compare temperature drop values.

For the early phases of production, large relative differences are observed. Temperature breakthrough time decreases with decreasing aquifer thickness as expected. About 5, 9, 15, 32, and 50 years for thicknesses of 5, 10, 25, 50 and 100 meters, respectively are modelled. However, the rate of temperature decline after the breakthrough is much less affected resulting in thin aquifers also showing modest long-term temperature decline. After 50 years, the base model (50 m thick aquifer) shows a temperature decline of about 3.5 °C and the 5 and 10 m thick aquifers show modest 5–6 °C. The same figures after 100 years of production are about 5.5 °C and 9 °C, respectively. A comparison of the temperature decline for 25 m thickness and 5–10 m thickness show surprisingly small differences, generally around 1–2 °C.

For very long-term production relative differences become even smaller. After 300 years, for the 5 m thick aquifer, production temperature declines to about 60 °C which is only 2 °C less than in the base model and merely 0.2 °C less than for a 10 m thick aquifer. With 25 m, half the thickness of the base model, temperature difference is only around 1°C. Doubling the thickness (to 100 m)

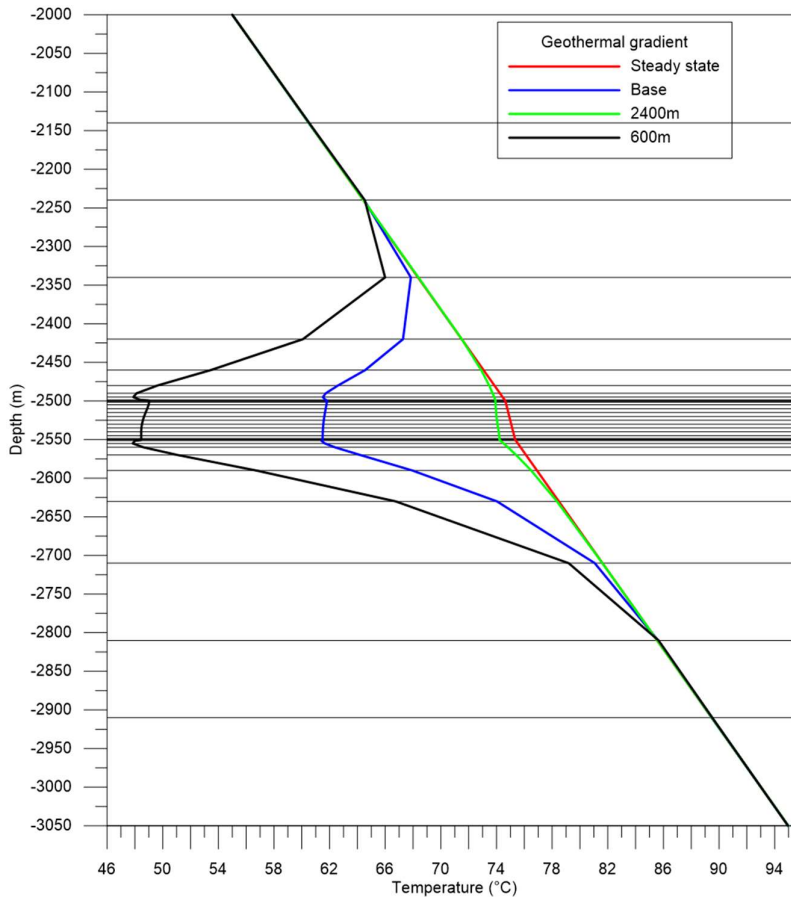


Figure 5.6. Influence of well distance on the temperature-depth profiles in the production well. From right to left: steady state (red), 2400 m (green), 1200 m (blue) and 600 m (black) respectively.

results in temperatures of about 64 °C, about 2 °C increase compared to the base model. These results, showing surprisingly little sensitivity to layer thicknesses, are consistent with those obtained by Poulsen *et al.* (2015).

Small differences are also apparent when comparing the long-term total amount of extracted energy. With only 5 m in thickness, total extracted energy amounts to 7×10^{16} J, which is 93% of the energy extracted from the 10 times thicker base model at 50 m. The 25 m thick reservoir yields 7.2×10^{16} J, corresponding to 96% of the base model. For the reservoir double the thickness of the base model at 100 m, only increases energy production by 5% at 7.9×10^{16} J.

The reason for those small differences is that thermal recharge from the confining units is capable of compensating for the absence of reservoir volume and keeping the relatively high production temperatures. A thinner reservoir is more easily re-heated during depletion. These results suggest, that even very thin reservoirs could be worth exploiting, if horizontal continuity may be ensured.

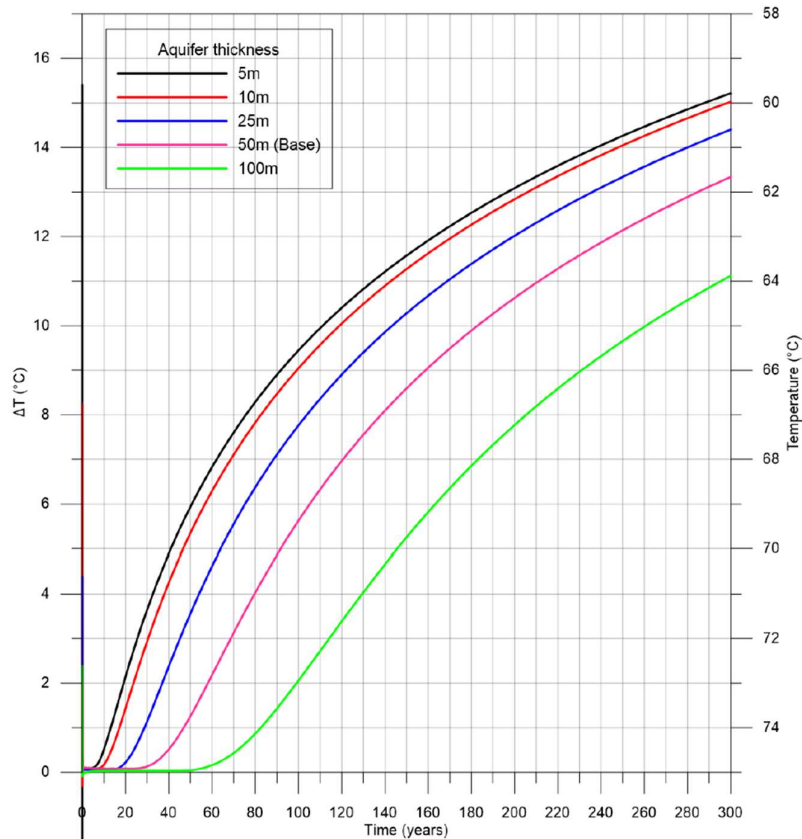


Figure 5.7. Decline of production temperature for aquifers of differing thicknesses of 5, 10, 25, 50 and 100 m as indicated.

Conclusions

The simulations show that in long-term exploitation, significant amounts of heat energy are obtained from the layers above and below the reservoir. This flow of heat into the reservoir holds part of the explanation for the observed very small drop in production temperatures observed over several decades. This applies to the distances of 1000–1500 m between production and injection, which are typically found in geothermal plants. At significantly smaller distances (600 m in example), an early, and over time, significant decrease in production temperature is modelled. Thus, distance between wells is important. In contrast, reservoir thickness, in terms of thermal evolution, means significantly less than one would expect. Small thicknesses, down to about 10-20 m or less, are largely compensated by a higher degree of reheating from the surrounding layers.

5.3 Combined heat extraction and heat storage

Sedimentary reservoirs may be applied for thermal energy storage, a concept that is gaining attention as the share of renewable energy use is increasing. Production of solar and wind energy is generally not aligned with demands. There may also be large amounts of excess heat from waste incineration and industrial processes such as cement production. In many countries like Denmark, heating demand vary significantly over the year with lower demands during summer period and

high demand in winter. Seasonal storage of heat from summer to autumn and winter months is becoming increasingly important.

Reservoirs at different depths have been tested and modelled (Molz *et al.*, 1978; Drijver *et al.*, 2012; Sommer *et al.*, 2014; Welsch *et al.*, 2015). Shallow aquifers are widely used for storing excess energy produced by solar panels for the winter months, as is with the German Parliament in Berlin, where an underground storage system has been operational since 2002 (Sanner *et al.*, 2005). These shallow systems are capable of aiding district heating systems, but sometimes strict regulations prohibit the injection of high temperature water, due to environmental concerns and potential contamination of drinking water. Storing higher temperatures in shallow depths is also less efficient because of higher energy loss, due to larger temperature gradients. For these reasons, it makes sense to investigate the possibility of storing high temperature water at medium and even high depths.

ATES basic concept

This type of subsurface energy storage is referred to as "Aquifer Thermal Energy Storage" (ATES). The basic principle is illustrated in Fig. 5.8 with a system consisting of two wells into the aquifer. The principle is essentially the same regardless of whether the aquifer is shallow or at greater depth. As is the case for geothermal production, a geological unit of good reservoir quality is needed, which means sufficient thickness, porosity and permeability. In general, reservoirs bounded by confining units of low permeability are preferred.

Regarding the deeper reservoirs, main interest is on long-term storage such as seasonal storage. Here warm water is injected into the reservoir during the period of heat surplus (the summer season) to be recovered during the period of high heat demand in autumn and winter. During heat storage, relatively cold water from the reservoir is produced from the 'cold well' to be heated from the heat source of surplus energy and injected, by the 'storage well' or 'warm well', into the aquifer as warm water.

When the heat is recovered during periods of heat demand, the system is reversed and warm water is produced from the reservoir and heat is extracted (by heat exchangers and/or heat pumps) and the resulting cold water is reinjected back to the aquifer by the 'cold well' (Fig. 5.8). During this last phase of heat recovery, the system is working like a traditional geothermal plant with production and reinjection. The number of wells, distances between wells etc. will depend on local conditions. Like in our case, such systems may be integrated with a traditional geothermal plant, where excess heat may be stored in the reservoir in summer season. If a geothermal plant contains a number of wells, part of the system may be designed for this option.

While several studies are available for shallow reservoir applications, much less work has been done on deep sedimentary reservoirs, especially combining storage and production. We investigate, by numerical models, storage capabilities of such a deep sedimentary reservoir representing characteristic deep geothermal conditions. We are using a single doublet system with combined production and reinjection, where excess heat, at temperatures above that of the aquifer, is stored via reversed flow during the summer months. When production is resumed production temperatures will initially be at those higher temperature levels and then decline towards the original ambient reservoir temperature.

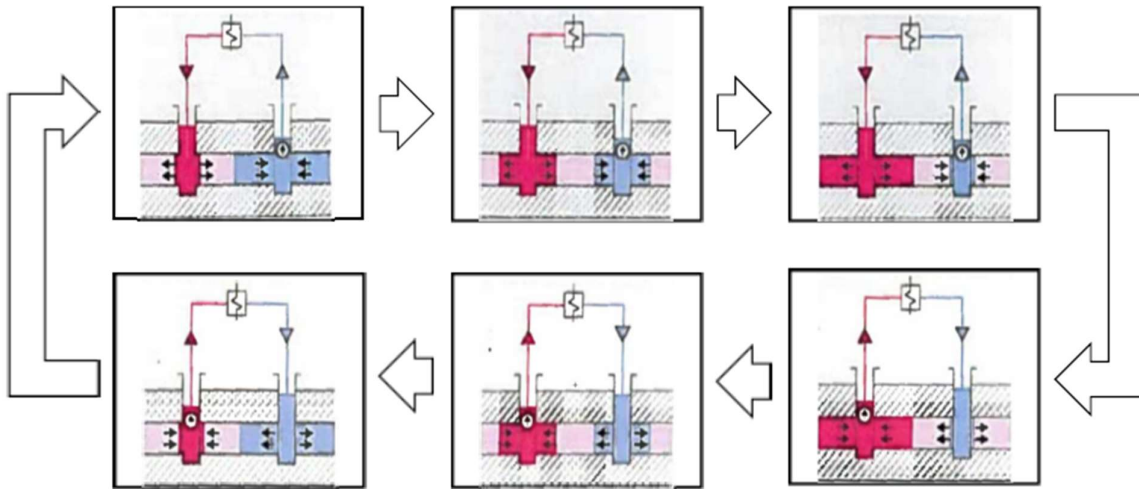


Figure 5.8. Basic principles of subsurface seasonal heat stores by the 'Aquifer Thermal Energy Storage (ATES)' concept, illustrated with two wells. During the summer season, heat is stored by injecting warm water into the aquifer (storage recharge, upper panels) and during the winter season the system is reversed and heat is recovered (storage discharge, lower panels). (Modified from Köhler *et al.*, 2013).

This system is very well suited for numerical reservoir modelling, and we apply the same procedures as above for geothermal production. Model set up in terms of model parameters, depth and temperatures are the same as for that of the base model (section 5.2), and, again, the FEFLOW modelling software was applied.

Model examples and results

Model examples and results summarised here are from project results published in Major *et al.* (2018).

Heat at 90 °C is stored, which is 15 °C above the ambient reservoir temperature at 75 °C, and injection temperature is set to 20 °C. Aquifer thickness is 50 m and flow rates of the wells are constant at 150 m³/h (3600 m³/day). In order to apply the same model set up as in the conceptual models above, a relatively deep reservoir and associated high reservoir temperature is applied, resulting in a rather small temperature difference between reservoir and storage temperature.

The main goal is to evaluate the recovery efficiency of the stored energy by calculating recovery factors. Our definition of the recovery is the ratio of recovered energy to the stored energy with respect to ambient reservoir temperature and with equal volume of water stored and produced. This definition of the recovery is similar to that of previous studies (e.g. Molz *et al.* 1978; Drijver *et al.* 2012; Sommer *et al.* 2014). Other methods of calculating recovery, efficiency and extracted heat may be applied as discussed below.

The effect of the length of the storage time is investigated by modelling injection times of 1, 2, 3 and 4 months, corresponding to June, June - July, June - August and June - September in terms of time of year. Obviously, longer injection time results in more surplus energy stored and higher production temperatures for the winter months. Total simulation and running time was 1.4 years in all cases.

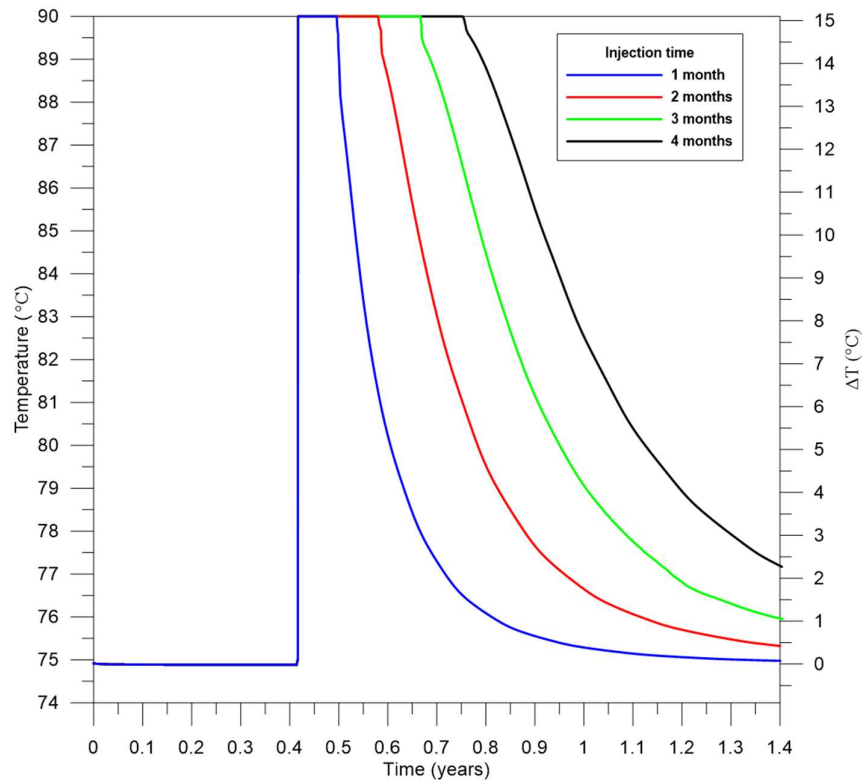


Figure 5.9. Production temperatures during a full storage cycle (1.4 years) with varying storage times of 1 month, 2, 3 and 4 months as indicated. Flow rates are 150 m³/h in all cases.

Results are presented in Fig. 5.9. Significant difference in temperature decline is apparent between the models. After 1.4 years the production temperature only increases about 0.1 °C in the case of June injection, whereas injection throughout September generates about 2.3 °C warmer temperatures than before the storage phase. This difference corresponds to a 9.2 MWh increase in daily energy production at the end of the storage cycle.

Figure 5.10 shows how much of the stored energy is recovered during the pumping period. Recovery factors are calculated with respect to equal volume, as mentioned before. Since flow rates are the same, this means the 1-month storage phase is evaluated through 30 days of production and the 4-month storage period evaluated during a 123-day interval. Shorter storage time results in faster energy recovery as seen from the steepness of the curves. Recovery factors obtained after 30, 61, 92, and 123 days of production are surprisingly constant at 66%, 67%, 67%, and 67%, respectively.

Since the curves are normalized to the surplus stored energy during each time interval, this will not reflect the total produced energy, which, of course, is more after a 4-month storage period than in the other cases. Total surplus energy production during each recovery phase in these four cases are 2389 MWh, 4167 MWh, 5500 MWh, and 6667 MWh respectively. This is a 174%, 230%, and 279% increase in energy production for 2, 3, and 4 months of storage compared to 1 month.

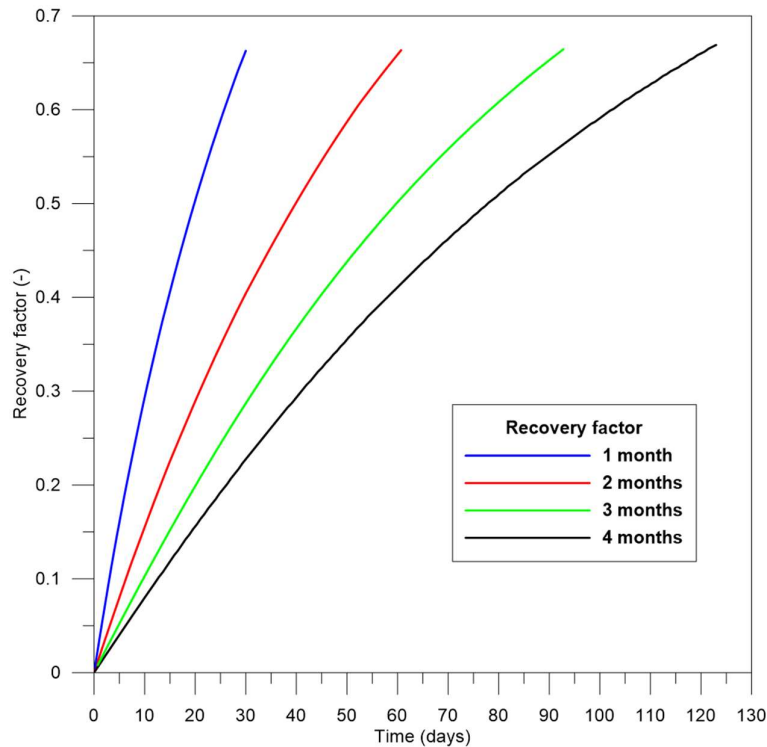


Figure 5.10. Recovery factors for varying storage phases of 1 month, 2, 3 and 4 months as indicated. Values are normalized to total surplus of energy stored during storage phase.

The distribution of the stored warm water in the reservoir is illustrated in Fig. 5.11. After 4 months of storage, temperatures above 85°C are seen to extend radially out to a distance of about 50 m from the production well applied for storage.

The long-term effect is evaluated by modelling 10 cycles, where storage time was set to 3 months, injection temperature 90 °C and flow rate 150 m³/h as before (i.e. 3 months of storage and 9 months production repeated 10 times). Results are shown in Figure 5.12. The early phases of production benefit from the higher temperatures and, at the end of each storage cycle, temperatures return almost back to the reservoir base level of 75 °C. After 3 cycles it settles around 76.4 °C, 1.5 °C higher than the starting production temperature. This temperature is then maintained throughout the simulation until the end of the 10th cycle. Recovery factor stays almost constant at the above 67%. Thus, this model produces only about 1% more energy in the tenth year of operation than in the first year.

Discussion and conclusions

This result of an almost constant recovery factor is different from that of Drijver *et al.* (2012), who obtained an improvement of close to 20% after several years of operation. The explanation for this difference is most likely the smaller temperature gradient in our setup, due to high ambient reservoir temperatures at large depths. Drijver *et al.* ran their model for an aquifer at medium depth (700 m) with a temperature difference of 42 °C between injected and reservoir temperature, which is significantly larger than the 15 °C difference used in our models. Furthermore, when applying a

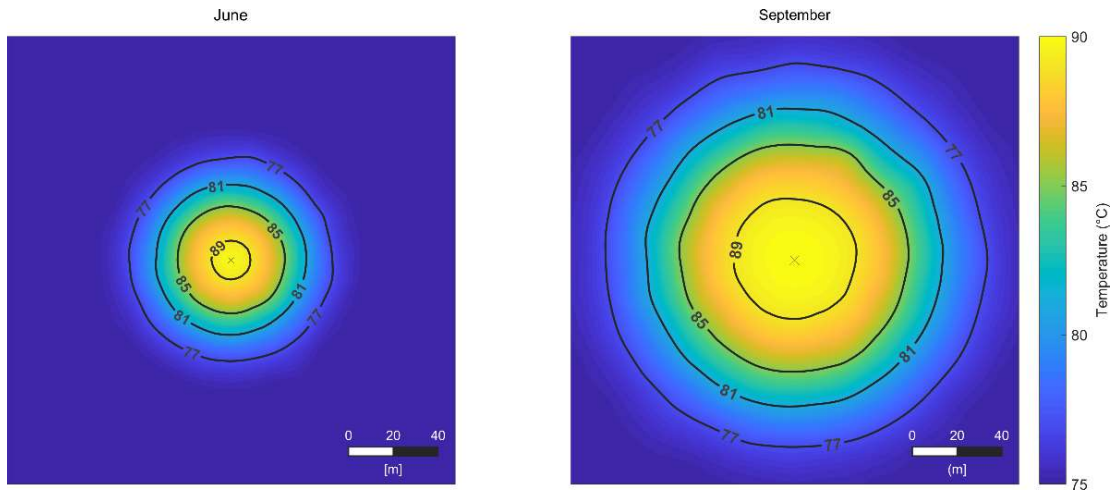


Figure 5.11. Temperature distribution at mid-reservoir level as affected by 90 °C injection after a 1 month storage period (June) and a 4-month storage period (September).

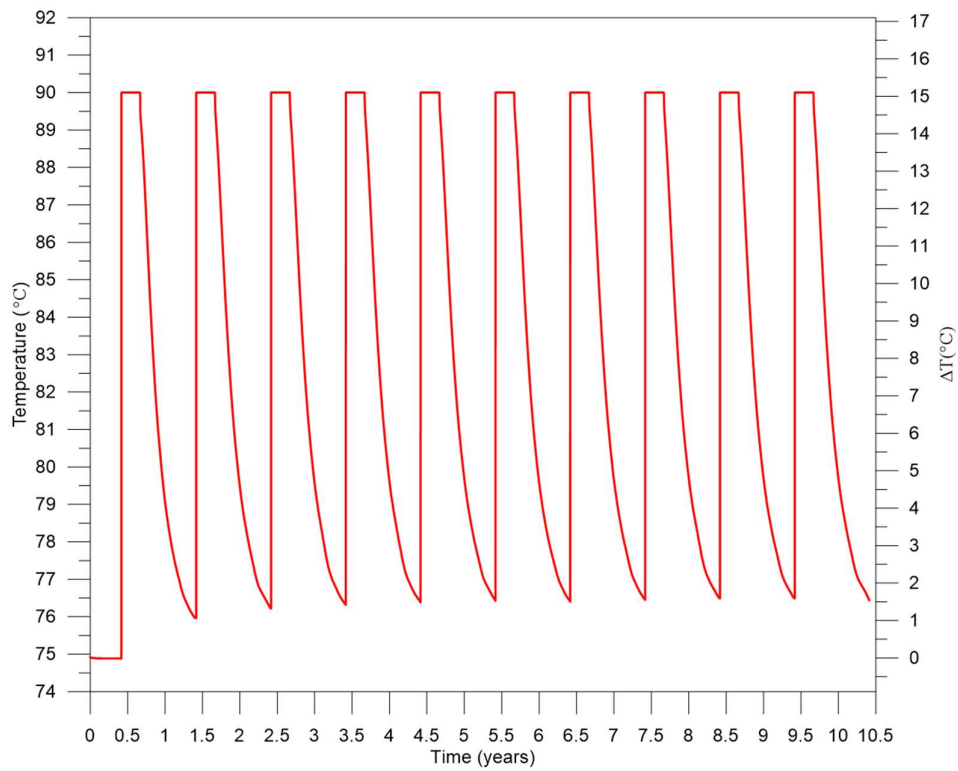


Figure 5.12. Modelled temperature history at the production well with 10 cycles of storage and annual storage phase of 3 months.

relatively short time interval for storage of 3 months compared with the production phase of 9 months, production temperatures settle very close to the ambient reservoir temperatures and new boundary conditions then similar to starting conditions. Recovering about two-thirds of the stored energy is in accordance with findings of earlier studies (Molz *et al.*, 1978; Drijver *et al.*, 2012; Sommer *et al.*, 2014).

There may be other options for calculating efficiency and recovery, which may be of interest when applied to specific cases such as those applied in Guldager *et al.* (2018). Our reasoning behind using the definition described above (recovery as the ratio of recovered energy to the stored energy, with respect to ambient reservoir temperature and with equal volume of water stored and produced), besides allowing us to compare results to previous studies, is the better understanding of heat loss processes. Calculating recovery with respect to cold well temperature was considered and eventually carried out for some of our simulations.

In these scenarios, water temperature increases when pumped up during storage phases, due in part to high ambient temperatures in the reservoir. This means that stored energy would be compared to higher temperatures than the extracted energy, which would result in positive bias towards recovery estimation. In some cases, we get recoveries as high as 115%. Values this high obviously do not reflect the subsurface physical processes and do not allow us to see the amount of losses occurred during the storage cycle. Furthermore, these values are highly dependent on the thermal history of the reservoir including the initially available cold-water volume.

Recovering about two-thirds of the stored energy as modelled here, and found in other studies, will depend on several factors including differences between ambient reservoir temperature and storage temperature.

This study shows that a combination of geothermal production and heat storage may be a valuable option. This is especially true for geothermal plants operating under conditions where the heat demand is not sufficiently large to produce all year round and may allow for high-temperature heat storage during the summer period. When energy production is resumed, production temperatures will start at these higher levels and more energy being produced.

We note, that technical questions, such as depth and placings of production pumps in wells in relation to size of wells etc., which are site specific, as well as any reservoir geochemical issues are not treated in this modelling study.

6. Reservoir simulation – geothermal plants

This chapter summarises main results obtained by modelling conditions at existing geothermal plants with realistic and complex lithology. (Most results, with some further local details provided in GEOTHERM interim report M4.4: Major *et al.*, 2019). Three geothermal plants are operating in Denmark, at Thisted, Copenhagen (Margretheholm) and Sønderborg, with production since 1984, 2005 and 2013, respectively (Mahler *et al.*, 2013; Røgen *et al.*, 2015). The Margretheholm and Sønderborg plants are with two boreholes of the doublet type, and Thisted, as well, until recently when extended with a new injection well. For all three plants, the produced energy is used for district heating. The reservoirs utilized are all sandstones of Late Triassic-Early Jurassic and Early Triassic age, at depths between 1.1 and 2.6 km, respectively, and with temperatures between 44 and 74 °C.

Throughout its 35-year production history (as of 2019), Thisted has had a stable production and without many problems. However, a steady increase in required injection pressure was observed, which prompted the expansion of the plant with a new injection well. This well is now functioning as the primary injection well. Reasons for the increasing injection pressure are unknown. One of the suggestions put forth is the higher viscosity of the cold water, which is making it difficult to inject more water. In this report, we investigate this hypothesis as well as the long-term thermal behaviour of the reservoir.

At Sønderborg, the production is challenged by decreasing injectivity during the project life. Two explanations have been put forward: near well bore blocking, either in the well bore completions or in the near well bore reservoir area owing to insufficient cleaning of well bore prior to completion, or the decreasing injectivity could be due to flow barriers in the reservoir at some distance to the wells. The first explanation seems the most obvious seen in the light of similar issues at other plants and this is evaluated in several ongoing studies. The second explanation can be evaluated with the use of reservoir simulation, and this is included in the scope of the present study case for Sønderborg.

For Margretheholm, for consistency and for a comparison with results from Thisted and Sønderborg, we summarise main modelling results obtained by Poulsen *et al.* (2015).

If historical production data exist, the simulated and real production data can be matched, ensuring a robust simulation model for predicting future production performance and reservoir management. Proper reservoir management is central both for securing a day-to-day production, potential future re-development and for regulatory purposes with respect to resource utilization. Such data are available for Thisted and Sønderborg.

6.1 The Thisted plant

The geothermal plant in Thisted has been in operation since 1984 and was the first of its kind in Denmark. It was operated as a pilot plant until the demonstration plant was commissioned in 1988. It produces 43 °C warm water from the Upper Triassic–Lower Jurassic Gassum Formation at about 1250 m depth. It contributes to satisfying heating demands in the late autumn and winter months. To this day, it is the best functioning plant in Denmark with good injectivity and high productivity at

up to 200 m³/h. However, over the years, injection pressure has steadily increased by about 30 bars (personal communication, Asger Goth, Thisted Varmeforsyning); therefore a new injection borehole was drilled in 2017 and was put into service in January 2019.

The plant has maximum capacity of 7 MW and utilizes two absorption heat pumps to cool the warm water to a minimum of 10–11 °C before reinjecting. The production and injection wells are located 1500 m apart, and the new injection well, TH5 lies approx. 600 m NNE of the TH3 injection well, about 1600 m from the production site (Fig. 6.1).

A modelling study has already been done on this site by GEUS in 2013 to determine the optimal location of the new borehole, TH5. These suggestions, however, were not realized mostly because of problems acquiring suitable property in the area (Asger Goth, personal communication). That study was taken as a basic reference point to present model, mainly in using data from well logs and core samples, as well as the interpreted horizons from the seismic surveys to define the reservoir boundaries.

In our new model, we use the state-of-the-art finite element simulation software FEFLOW, and aim to answer some remaining questions regarding the reservoir quality and geology of the area. Furthermore, we try to make accurate predictions for future evolution of the cold-water plume around the injection well.



Figure 6.1. Map of the Thisted-area with the model domain indicated by the red rectangle and boreholes indicated by yellow pin marks. TH2 is the production well and TH3 and TH5 are injection wells. TH1 and TH4 are older hydrocarbon exploration wells.

The reservoir

The formation used for geothermal extraction is the Gassum Sandstone reservoir, which lies between 1100 and 1250 m depth in the area of TH2 and TH3 (Fig. 6.2). Core measurements and well logs both indicate very good quality sandstones, with permeability in the order of 10 darcy.

Our geological model is set up based on well-log correlation and interpreted seismic horizons in the area, and the model honours the well logs exactly at the well locations and introduces lateral variation based on different statistical distributions. By using a high correlation length in statistical models, the continuity of the sand bodies is satisfied.

Based on the porosity-permeability measurements made on core samples, a double porosity trend seems apparent, meaning the reservoir can be split into a higher and lower permeability group. Most of the screened interval falls into the high permeability group in this instance. However, in present models, we use the regional-trend relationship for calculating permeability values from porosity.

Model set up and modelling procedure

Our model covers an 11 km x 13.5 km area around the city of Thisted and extends about 1200 m in the vertical direction. It includes two closed oil exploration boreholes TH1 and TH4 along with the boreholes used for the geothermal plant TH2, TH3 and TH5 (Figs. 6.1 and 6.3). The mesh is refined around the boreholes to ensure numerical stability. Minimum elemental diameter is set to 1.22 m around the boreholes and is increased gradually away from the wells up to around 120 m in the horizontal direction. Average diameter is around 73.5 m. The model is discretized into 2 m thick layers in the reservoir section. Overall, we have 81 layers and up to 5.5 million elements in the model.

Interpreted logs (from GEUS) are available in TH1, TH2, and TH3 (TH2 and TH3 shown in Fig. 6.2) which form the basis of discretization in the reservoir unit. Permeability of each section is calculated from the porosity logs using relationships set up from core samples. Permeability values are then converted into hydraulic conductivity for direct input into FEFLOW. The values are averaged to 2 m sections to match the reservoir discretization used in the model domain.

Statistical reservoir models

Geostatistical Gaussian simulation methods are used to setup a number of different statistical models of the 3D porosity distribution in the Gassum Formation. Specifically, the direct sequential simulation method (Soares, 2001) is used, which can honour any known 1D porosity distribution. This 1D porosity distribution is found from a histogram of all porosity values in the TH1, TH2, and TH3 wells. The minimum porosity is 0.04 and the maximum is 0.4.

Three different types of geostatistical models are considered, that represent different structural variability:

Nugget: No spatial correlation is assumed at all. This means that two neighboring pixels are assumed independent.

Gaussian: A Gaussian covariance model with a horizontal range of 4000 m and vertical range of 10 m is assumed. This provides a smoothly varying porosity field along the horizontal plane.

Spherical: This model is similar to the Gaussain model, except that more small scale variability will be evident. When testing the effect of different horizontal ranges, we elected to use this type of model. Ranges vary from 200 m to 8000 m throughout all simulations.

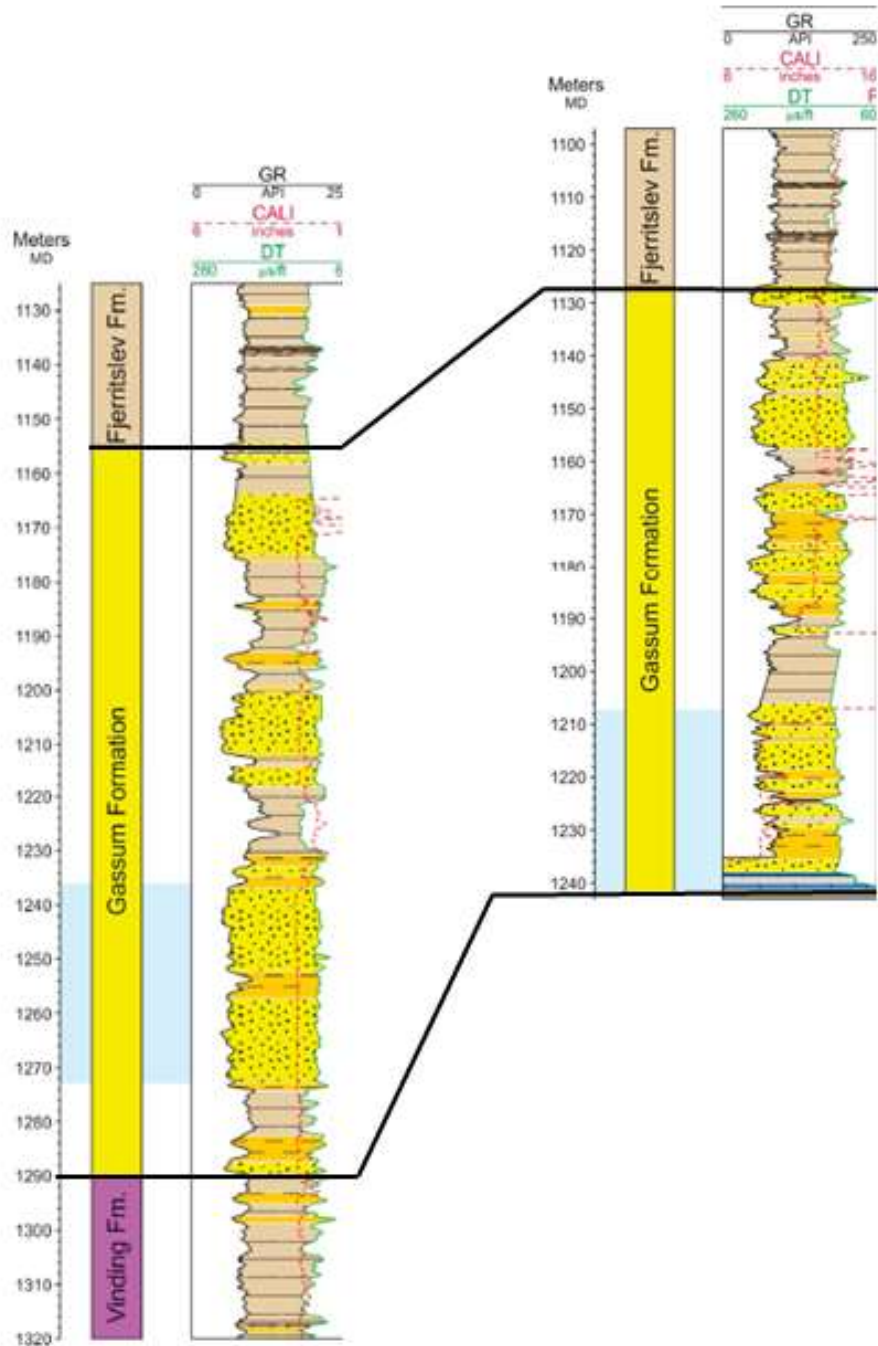


Figure 6.2. Interpreted logs from the production well, TH2 (left) and injection well, TH3 (right).

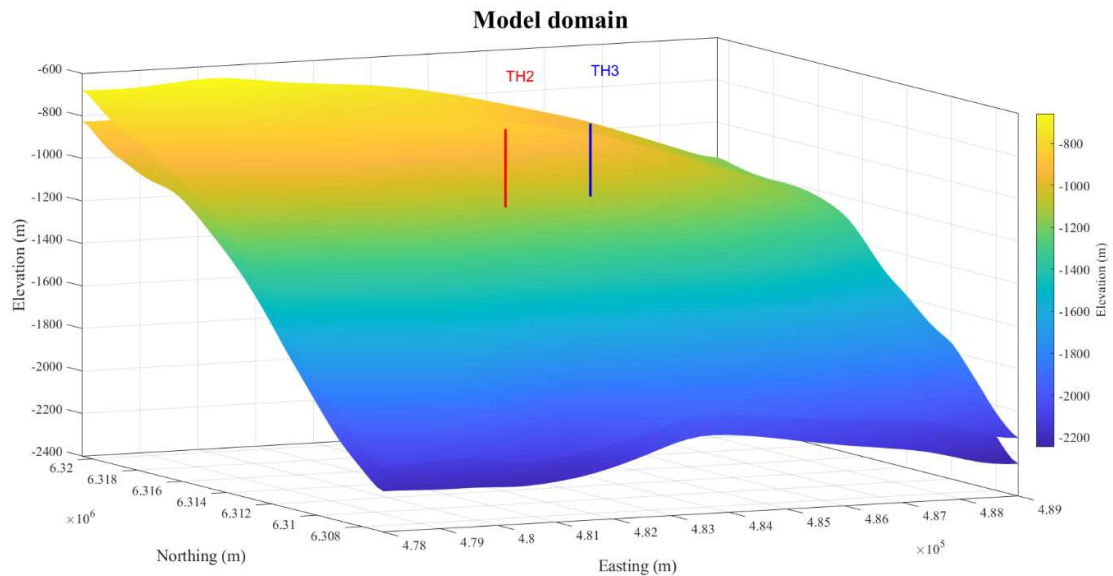


Figure 6.3. Top and bottom horizon of the Gassum Formation as interpreted from the seismic survey. Positions of boreholes TH2 and TH3 are indicated.

Layering is expected to follow the top and base of the reservoir. Therefore the 3D porosity realizations are first generated in a regular 3D grid. Once a realization has been generated, it is mapped into the reservoir with horizontal correlations following the structure of the reservoir. All realizations are generated such that they match the porosity data from TH2 and TH3 at the borehole locations.

Initial and boundary conditions

Initial thermal conditions for the transient model are achieved using a paleotemperature model where surface temperature is varied according to the glaciation history of the past 150,000 years and a constant background heat flow of 77 mW/m^2 is applied (Balling, 1992). Thermal conductivity and volumetric heat capacity values are taken from Bording (2010). This model is purely conductive and is verified by fitting reservoir temperatures to the undisturbed values measured in Thisted 3 before operation (Balling *et al.*, 1994). From this initial simulation, we arrive at an average reservoir temperature of around $43.5 \text{ }^\circ\text{C}$.

Based on this temperature-depth model we have a constant temperature boundary condition at the top of the model and the hydraulic head is set to 0 m. The lower boundary again has a constant background heat flow of 77 mW/m^2 and no fluid-flow across. Flow rate is held continuous at $150 \text{ m}^3/\text{h}$ in both boreholes, except for the seasonal model where pumping rates are controlled with a time-series and are calculated to monthly averages based on daily flow rate data received from Thisted Varmeforsyning. Injection temperature is controlled through a time-series boundary condition in TH3 and changes from $22 \text{ }^\circ\text{C}$ to $11 \text{ }^\circ\text{C}$ after 16 years of operation in all cases.

The setup described above was used to run the following scenarios:

1. Layer-cake models, where vertical porosity and hydraulic conductivity distribution comes from either the production (TH2) or the injection (TH3) well (two simulations). These are simulated with constant production and reinjection for 150 years with a pumping rate of 150 m³/h. A cross section view of this model setup is shown in Fig. 6.4.
2. Statistical models, where both porosity and hydraulic conductivity are varied laterally and realizations are created with three different geostatistical models: Gaussian, spherical or nugget (40 simulations). These scenarios are again run continuously for 150 years with 150 m³/h. A cross section view of a laterally varying model setup is shown in Fig. 6.5.
3. Layer-cake model with porosity and hydraulic conductivity values based on production well (TH2) data and production rate is matched to historical data received from Thisted Varmeforsyning. Rates are calculated to monthly averages in this case and the model is run for 34 years (one simulation).

All together, we have run 43 different scenarios for the Thisted case. Injection into the new well, TH5, is not included in the simulations presented here, but subject to ongoing modelling.

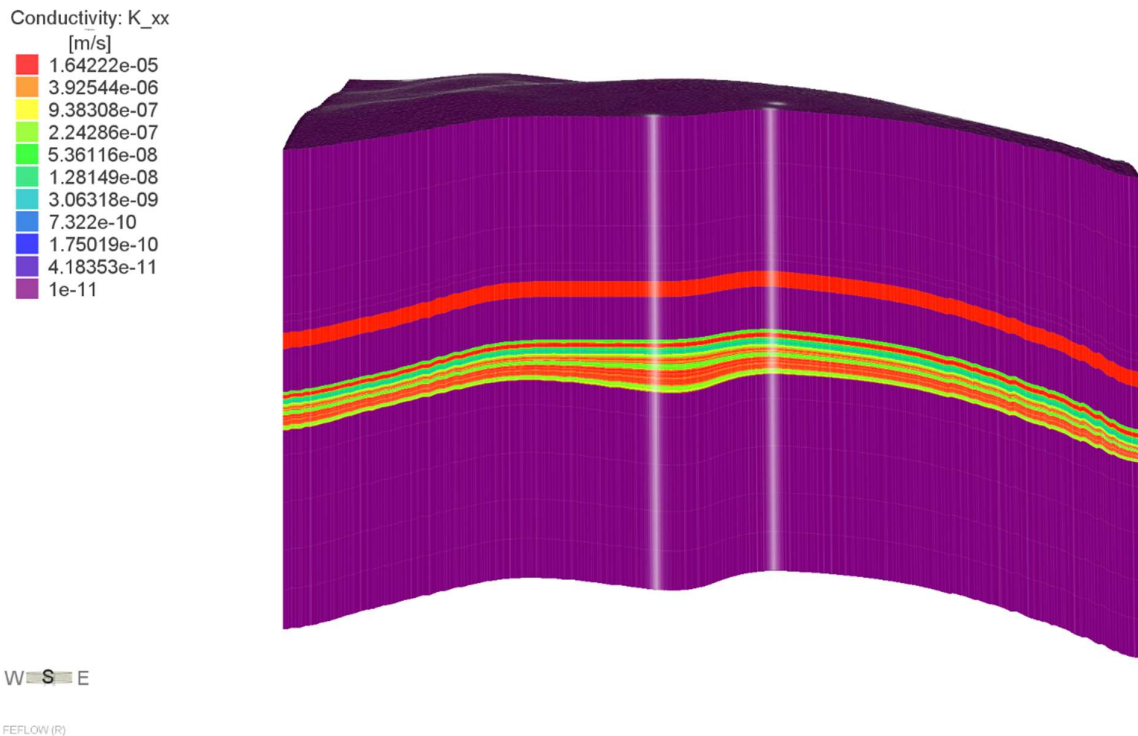


Figure 6.4. Cross section view of the layer-cake model where vertical white lines indicate borehole locations. The uppermost high-conductivity unit is the Haldager Formation, which is included into the model domain.

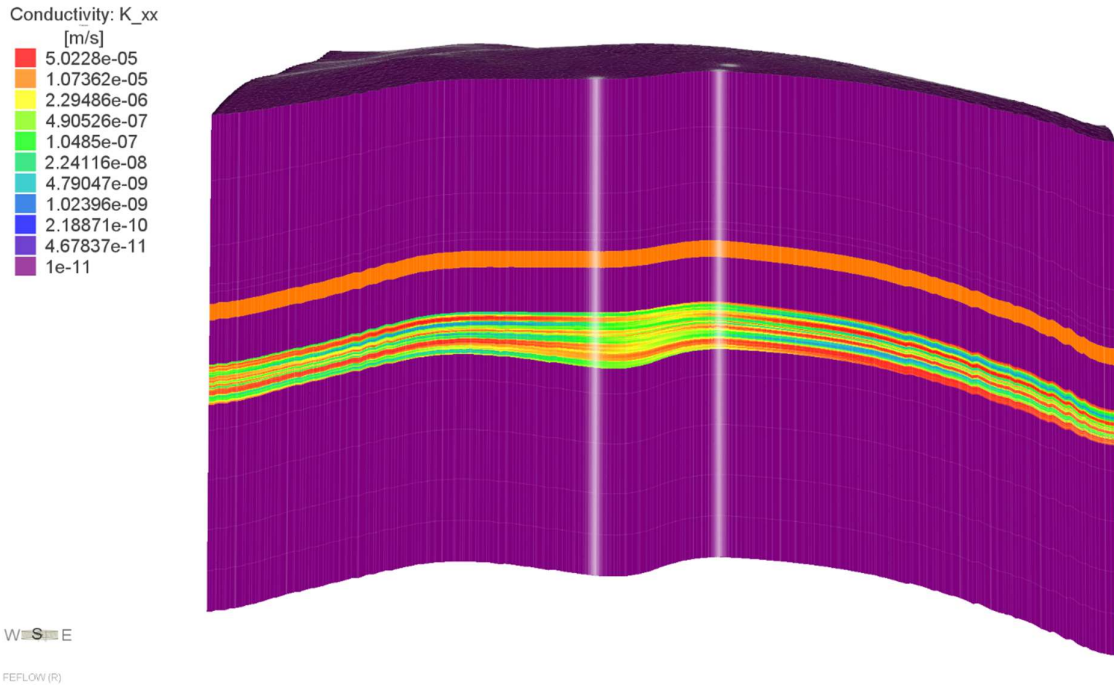


Figure 6.5. Cross section view of laterally variable reservoir model. A high correlation length of 4000 m was chosen to reflect the small variability.

Results and discussion

Figure 6.6 shows the comparative results from the layer-cake and statistical simulations, respectively. Production temperature with time is shown for all the different simulations. We can see production temperature curves when porosity and hydraulic conductivity are based on TH2 and TH3, respectively, and both production and injection is in the highly permeable lower section of the reservoir. No drastic difference is noticeable as both curves show the same trend. Production temperature declines about 2.7 °C after 150 years in both cases.

The reason for very small declines is most likely related to the orientation of the boreholes compared to the dip of the reservoir and the draw in of warmer water, even after breakthrough, from regions away from the cold front. This feature is clearly visible in the contour plots of Fig. 6.8. This interpretation is supported by the modelling results from the conceptual models (Chapter 5) and the model results from the Margrethholm plant, where more than twice the temperature decrease (ca. 6 °C) is found for similar production rate and time span (see below).

It is not obvious when breakthrough starts because of an initial decline in temperature, which is apparent in all the curves. This is due to the fact that temperatures are calculated as averages of the whole production interval at the bottom of the well. This means the different temperature water from adjacent layers is mixed to give an average temperature. Additionally, here, initially, the production borehole TH2 is drawing in more water from the higher elevated, colder area on the northern side of the well (Fig. 6.3). Based on the curves and 2D view of the cold plumes, we estimate breakthrough to occur after between 60 and about 100 years in all simulations, but quite a big spread is observed (Fig. 6.7).

Figure 6.7 shows a number of models with different vertical ranges where directional anisotropy was considered to simulate direction of deposition. In these models, range was set 5 times higher in the direction of supposed sediment deposition, and this direction was assumed to be 30 degrees from north. These results show a bigger difference between production temperatures and breakthrough times also vary, as mentioned above. Reason for these differences is the different flow paths the water has to take in order to reach the pumping well. Equivalent effects have been studied in Shetty *et al.* (2018), who investigated the effect of well placement to breakthrough time. In our case, wells are unchanged, but the formation is changing leading to similar effect. Figure 6.8e shows an example of the plume shape from one of these scenarios.

Figure 6.6b shows the comparison of a layer-cake model to a Gaussian model where lateral variability is included. Now the two curves look somewhat different. After an initially higher decline the Gaussian scenario shows 0.6 °C higher production temperature at the end of 150 years. This is a 22% difference relative to an overall temperature loss of 2.7 °C. All other laterally varied models show the slightly higher production temperatures after 150 years. Still, for any practical purpose, and considering other sources of uncertainty, modelled temperature differences between different reservoir models are very small. These small differences seem related to the presence of a high permeability reservoir unit and an indication of large lateral continuity of reservoir properties. This may not apply to geothermal reservoirs in general, and more studies are needed on this issue.

Figure 6.6c shows the comparison between simulations ran with different statistical distributions, Gaussian, spherical and nugget. All statistical model runs give roughly the same temperature decline after 150 years. This makes sense when all realizations are conditioned at the boreholes and correlation lengths much higher than the borehole distance are used. Differences in initial decline can be attributed to different layers having higher permeability in each realizations and therefore contributing more or less water of lower temperatures, to production.

The evolution of the cold-water front for each of these simulations is shown in Figs. 6.8a-d. The extent of the plume after 150 years changes, depending on the models used. However, the shape is consistently symmetrical in all cases. This can again be due to the high correlation lengths used. The Gaussian and spherical models produce roughly the same contours, where the 40 °C contour is just about reaching the production well (Figs. 6.8b and c).

Additional two examples are showing cases where the shape of the plume is no longer symmetric (Figs. 6.8e and f). These are selected examples of the models investigating the effect of depositional direction and long vertical correlations, respectively.

According to observations in Thisted, the injection pressure elevated 30 bars during the past 34 years with respect to the same injection rate (personal communication, Asger Goth). In our models, there is no evidence of such a drastic increase in pressure when continuous 150 m³/h rate is used. During 150 years of constant operation, the pressure increase is insignificant (1–2 bars), aside from the jump in pressure when injection temperature is lowered from 22 °C to 11 °C. This effect is due to the viscosity increase of the cold water and contributes about 10 bars. However, based on our current models, we cannot explain the remaining 20 bars. A suggestion could be near wellbore

effects from fines migration or related to chemical reactions. Investigations are ongoing, where potential geochemical reactions related to the injection of cold water are modelled.

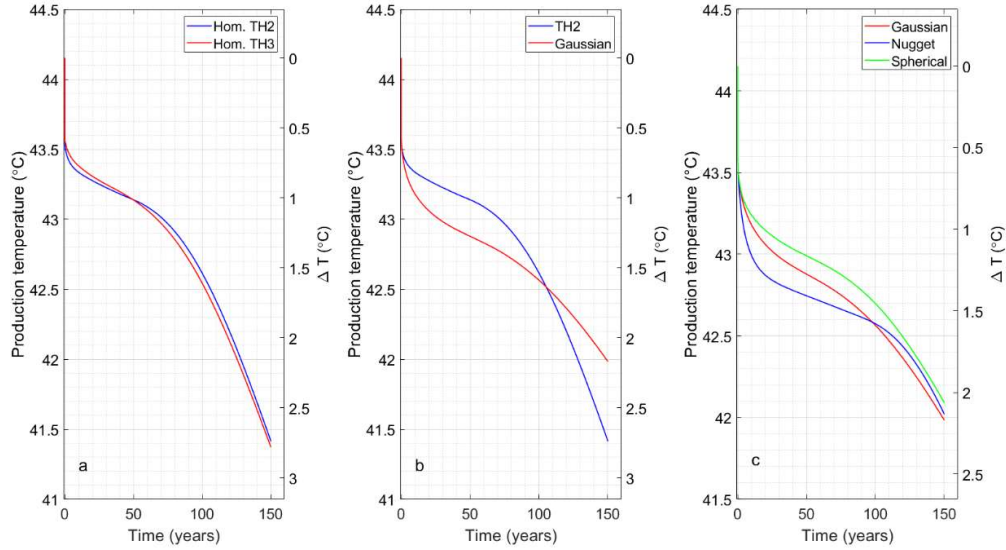


Figure 6.6. Production temperature with time. a, ‘Layer-cake’ models with porosity values from TH2 (in blue) and TH3 (in red); b, ‘Layer-cake’ model based on TH2 (in blue) vs. Gaussian simulated porosity values (in red); c, models with simulated porosity distributions using different methods, Gaussian (blue), nugget (red) and spherical (green).

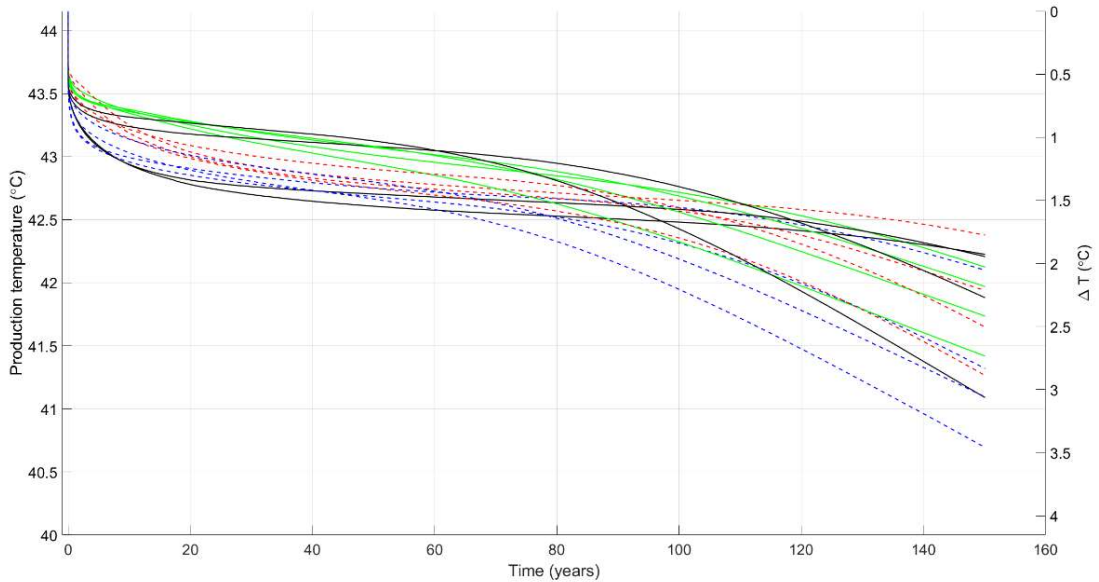


Figure 6.7. Subset of results where directional anisotropy was included to represent depositional direction. Angle was chosen to 30 degrees from north.

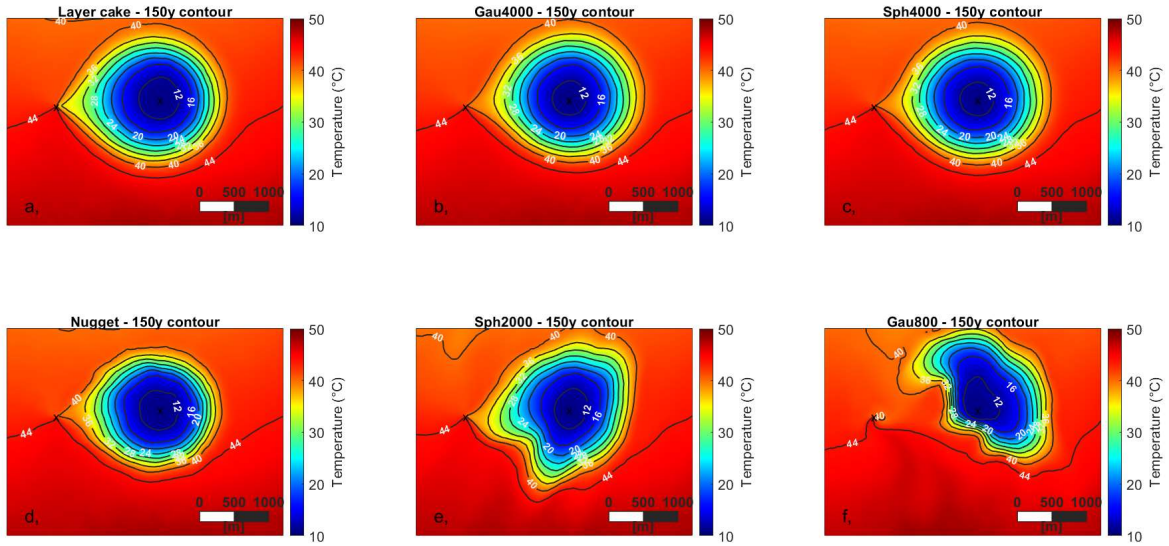


Figure 6.8. Contour plot of the extent of the cold-water plume after a 150-year simulation; continuous production rate of 150 m³/h. a, ‘Layer-cake’ model with porosity based on TH2 data; b, porosity from a Gaussian simulation; c, porosity from a spherical simulation; d, porosity from purely random simulation; e, porosity from spherical simulation including directional anisotropy; f, porosity from Gaussian simulation with high vertical ranges

The remaining scenario is implementing the seasonal production and true production rates in terms of monthly averages. This simulation was run on a layer-cake model (using TH2) for 34 years to match the history of the actual plant (1984–2018). Fig. 6.9 shows the production temperature and rate series during the 34-year simulation. It is obvious that the temperatures do not decline within this time, which is in line with observations at the site. Also noticeable the slight increase in temperature during idle summer periods where the subsurface has some time to recover. With no production, there may be absence of water of slightly lower temperatures coming from the upper layers of the reservoir.

The extent of the cold-water plume is shown on Fig. 6.10. The area affected extends out to 500–600 m from the injection well, which is only about one-third the distance to the production well. However, it is clear that the cold water may have reached the location of the new well, TH5 by now and could have contributed by about 1°C decline in the reservoir temperature. Daily average production temperatures were measured in January 2018 to be around 39.4 °C when this well, for some time, was used for production (personal communication, Asger Goth). This indicates reservoir temperatures to be close to 40 °C, which is 3–4 °C lower than the reservoir temperature at TH2. This seems explained by the combination of a somewhat shallower reservoir position (about 80 m) and the above effect from the injection well, which fits very well with the temperature indicated by our models (Fig. 6.10).

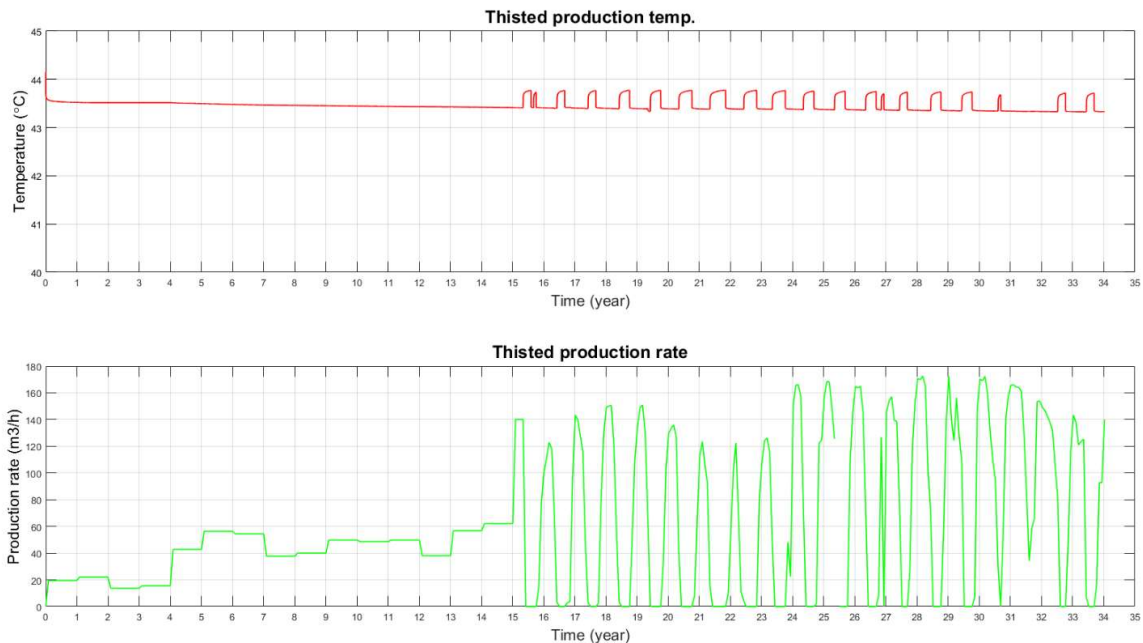


Figure 6.9. Production temperature and production rate over the 34-year simulation period (1984–2018). The slight temperature increase in idle periods is due to the reheating of the reservoir and the absence of colder water coming from the upper layers.

Conclusions

The Thisted model retains relatively warm temperatures even after 150 years of continuous production and reinjection. We see overall temperature decline of about 2.7 °C. This is less than half the amount expected for horizontal layering and is interpreted as due to the orientation of the boreholes compared to the dip of the reservoir and the very good quality of the Gassum Formation in the area. The orientation of the boreholes is important in the draw-in of warmer water away from the cold front, which keeps temperatures at a relatively high level.

History matching shows no sign of temperature decline in the past 34 years, as expected. The frontal part of the cold-water plume extends only to about one-third of the way between the two boreholes, but it does seem to reach the position of the new injection well, TH5. The modelled temperature here is in line with observations at the borehole site. In terms of thermal structure, these models indicate the current utilization scheme to be sustainable, in terms of temperatures, for decades to come.

Statistical models show that representing lateral variation in the fluid flow properties has some impact on production temperature over long periods. Based on our results, using layer-cake models may lead to some overestimation of the long-term temperature decline.

Pressure increase at the injection site is not explained by the increased viscosity of the colder water as this effect only contributes about 10 bars in extra pressure. The remaining 20 bars could perhaps be due to near wellbore effects or chemical alterations related to the injection of cold water.

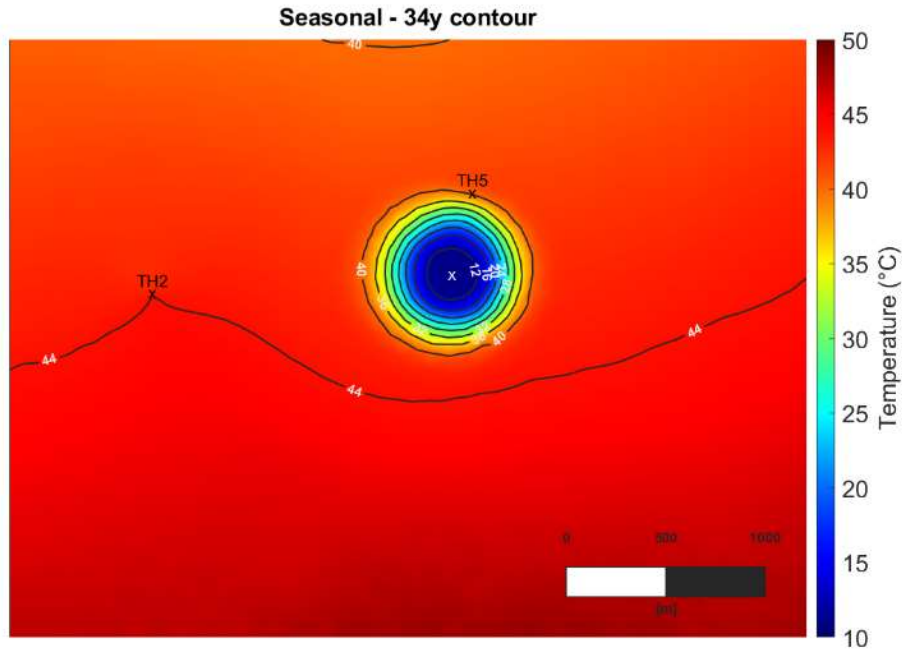


Figure 6.10. Extent of the cold-water plume after a 34-year simulation (1984–2018) with history matched production rates.

6.2 The Søndersborg plant

Geothermal production from the Søndersborg plant commenced in 2013, and the plant has been producing in a seasonal operation scheme displayed in Fig. 6.11. It has been challenging to obtain a steady production/injection rate during the season and difficult to reach the planned production target.

The plant is constructed as a classical doublet system; one production and one injection well and run at full voidage replacement, even though a small volume was directed to the Augustenborg fjord in the beginning of the production. This volume is neglected in the following reservoir simulation study.

Both Søndersborg wells are deviated and drilled from the same spud location. The Søndersborg-1 well is the injector well and Søndersborg-2 the producing well. The production temperature is around 48 °C and the target reservoir is the sandstone of the Gassum Formation in a depth of approximately 1150 m. A small depth shift of about 30–40 m between the two wells are inferred from well logs and seismic surveys, and this could indicate reduced flow communication between the production and injection wells. The impact of any flow barriers in the reservoir around the wells is examined.

The reservoir

Similar to that of the Thisted plant, the target geothermal reservoir at Søndersborg is the Gassum Formation. The sandstone reservoir is of very good to excellent reservoir quality; well tests interpreted a transmissibility of about 130 Dm (uncertain).

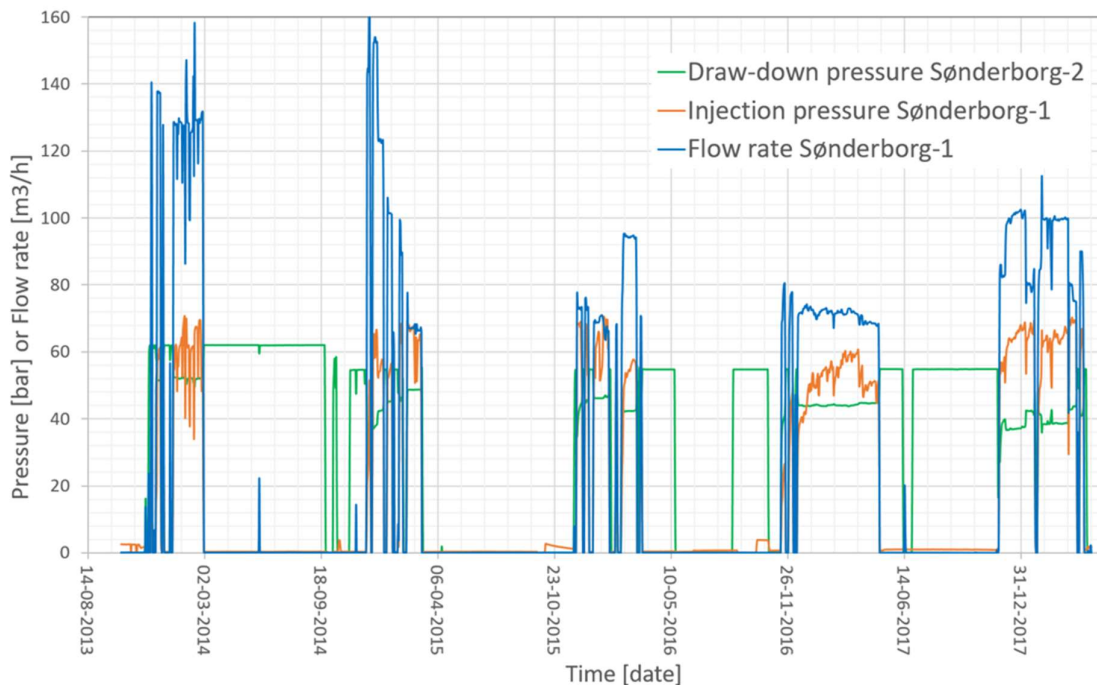


Figure 6.11. Production data provided by Sønderborg Fjernvarme. Five flow periods. In green the drawdown pressure in Sønderborg-2 (bottom-hole pressure for production), in orange the injection pressure for Sønderborg-1 and in blue the flow rate measured in the injection well.

A geological model is constructed based on the geological knowledge and available geophysical and petrophysical data of the Sønderborg area (Vosgerau *et al.*, 2015). A 3D reservoir simulation (or dynamic) model is defined based on the geological model. Reservoir performance is evaluated through the dynamic modelling. Focus is on the reservoir connectivity and the impact on the injectivity and production performance.

Model set up and modelling procedure

The Petrel software (Petrel, 2015) is used for the static model construction and the Eclipse 100 software (ECLIPSE, 2017) is used for the dynamic modelling part. This section describes the input data used for setting up the 3D static- and dynamic reservoir models and the assumptions and constraints behind the choice of input data.

The top Gassum surface is imported into the Petrel software from the regional seismic interpretation of the top Gassum Formation for 'the Sønderborg locality' in Vosgerau *et al.* (2015). This surface has been QC with respect to the area around Sønderborg in order to check the gridding/contouring of the surface. In the above project, the top Gassum horizon is seismically picked on a regional scale, whereas for the local Sønderborg model, it is of importance to get a detailed description of the surface.

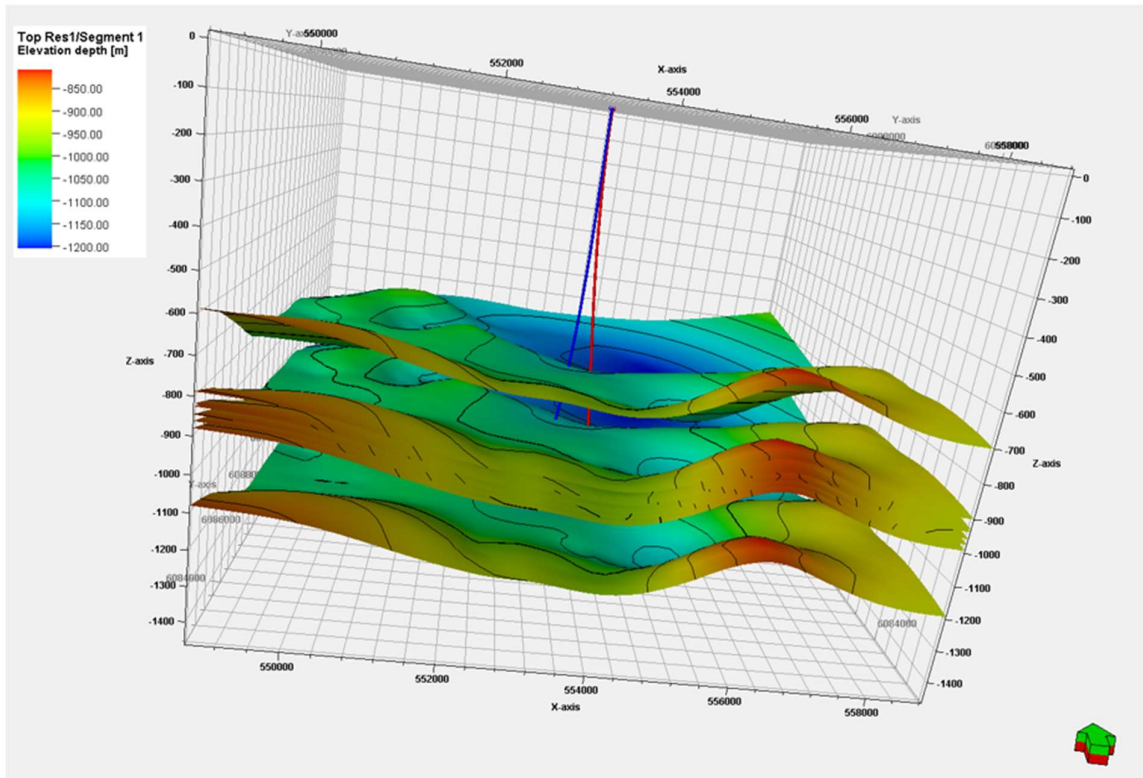


Figure 6.12. Model surfaces from top to bottom: top Fjerritslev, top Gassum (seismically interpreted), top Res1, top Res12, base Res12, top Res3, base Gassum and base Vinding. For both the Fjerritslev and Vinding Formations, only 200 m were included, even though the formations are thicker. These formations do not contribute to flow but are only included to ensure proper boundary conditions for the pressure and temperature modelling.

Due to the short distance between the two Søndersborg wells at reservoir level, approx. 800 m, and the relative poor quality of the seismic data, it was decided to use the interpreted top Gassum surface as a proxy for the additional surfaces in the model. Seven additional surfaces were added to the model based on the individual depths interpreted from the Søndersborg wells. The stacked surfaces encompassing the 3D model are shown in Fig. 6.12. The formations above and below the Gassum reservoir are included to secure proper vertical boundary conditions for the pressure and temperature calculations. The general geophysical interpretation of the seismic data and the time/depth conversion is described in detail in Vosgerau *et al.* (2015).

An area of interest (AOI) is defined around the Søndersborg wells. The AOI is 10 km x 10 km, which is sufficient to model the geothermal operation and securing proper boundary conditions in the lateral direction. The geological model is constructed for the AOI with the two Søndersborg wells in the centre of the area (Fig. 6.12).

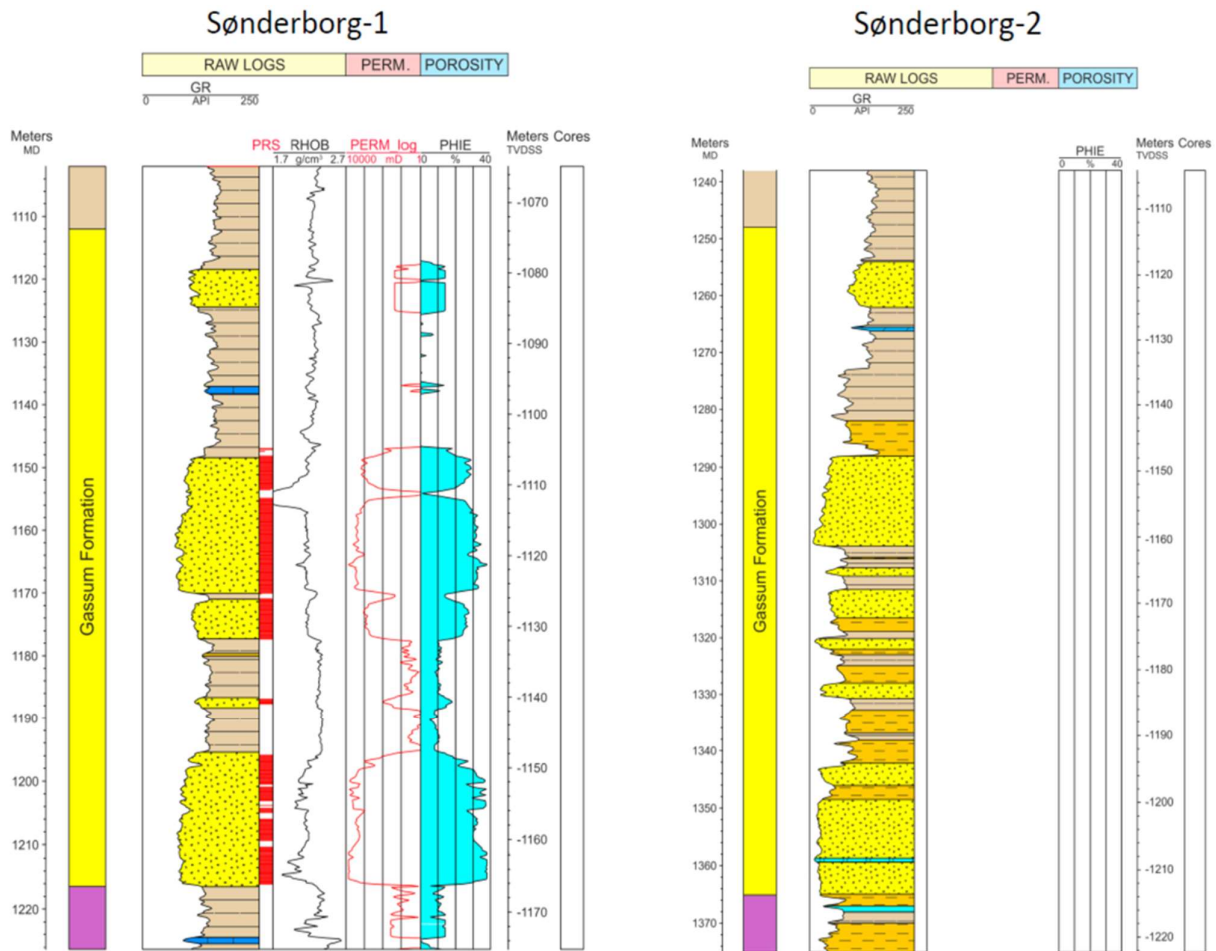


Figure 6.13. Well panel for the two Søndersborg wells. A porosity log is interpreted in Søndersborg-1. The well panel shows a 25 m depth offset between the wells.

The interpreted porosity log for the Søndersborg-1 well is imported in Petrel as a function of depth. The “true vertical depth” (TVD) is used to compensate for the well deviation from vertical. The deviation track for both wells are taken from the Final Well report (DONG Energy, 2010a; 2010b) and imported in Petrel. Only a lithology log exists for the Søndersborg-2 well. The well data are used to populate the 3D geological model with porosity values. A well panel for the two wells is shown in Fig. 6.13.

A 3D corner point grid is constructed from the imported and adjusted surfaces. A total of 54 layers in the depth direction are used with a vertical resolution of 2 m in the reservoir interval and up to 20 m in the over- and underburden layers.

Grid resolution in the lateral direction is 200 m x 200 m for the AOI, resulting in a total grid size of the AOI of 50 x 50 x 54 (=135000) grid cells. In order to avoid numerical dispersion in the solutions from the reservoir simulations a local grid refinement is imposed around the two wells. The

refinement has increasingly higher resolution toward the wells with a grid cell size of 10 m x 10 m in the near well area. The grid refinement process adds an additional 907200 grid cells to the model.

To populate the grid with reservoir properties, *i.e.* porosity and permeability values, the Søndersborg-1 porosity well log is used (Fig. 6.13). The model is constructed as a 'layer-cake' model, *i.e.* no lateral variation in reservoir properties, only vertical variation. The seismic resolution is too low to incorporate a more detailed lateral variation in reservoir parameters.

The geological understanding of the area supports this approach, as the geology is interpreted as being relatively unruffled. Also, the narrow well distance supports a layer-cake model. Still, the seismic interpretation could to some extent indicate a small discontinuity in the layers in the reservoir interval, but this is difficult to verify.

To populate the model with permeability values, a porosity-permeability relation is used. This relationship between porosity and permeability is established from laboratory flooding experiments on core samples. A general porosity-permeability relationship for the Gassum Formation is discussed in Vosgerau *et al.* (2015). For the present study, this relationship has been refined to focus mainly on core samples that are assessed to be representative for the Søndersborg area. From this relationship, permeability values are calculated for each of the grid cells in the model (Fig. 6.14). The over- and underburden are assigned a constant value for both porosity and permeability (0.05 porosity fraction and 1 mD).

A factor of 1.25 is multiplied on the permeability values to account for the upscaling process from core analysis data measured in the laboratory to field scale values and to convert from gas permeability to water permeability. Also based on core analysis a ratio between the vertical and horizontal permeability of 0.3 is used. Grid and grid properties as described above are exported from the static Petrel model into the Eclipse software for the dynamic modelling.

Model parameters and boundary conditions

Thermal conductivity for the geological layers is assumed to be 2.5 W/(m K) together with volumetric heat capacity of 2.2 MJ/(m³ K) and 4.0 MJ/(m³ K) for the geological layers and the formation water, respectively. For the present flow modelling no distinction between clay and sandstone was made.

A temperature profile for the Søndersborg area is discussed in Vosgerau *et al.* (2015) and the values taken from Balling and Bording (2013). Temperature gradients vary with depth between different lithologies, but for the present purpose, the constant temperature gradient of 34 °C /km and a mean annual surface temperature of 8 °C are used in the reservoir simulations.

The viscosity of the formation water is strongly dependent on temperature and a table of viscosity as function of temperature must be entered as input in the simulation model. Table of temperature and viscosity is created from CREWES (2007) assuming a salinity of 157000 ppm (T. Laier, personal communication).

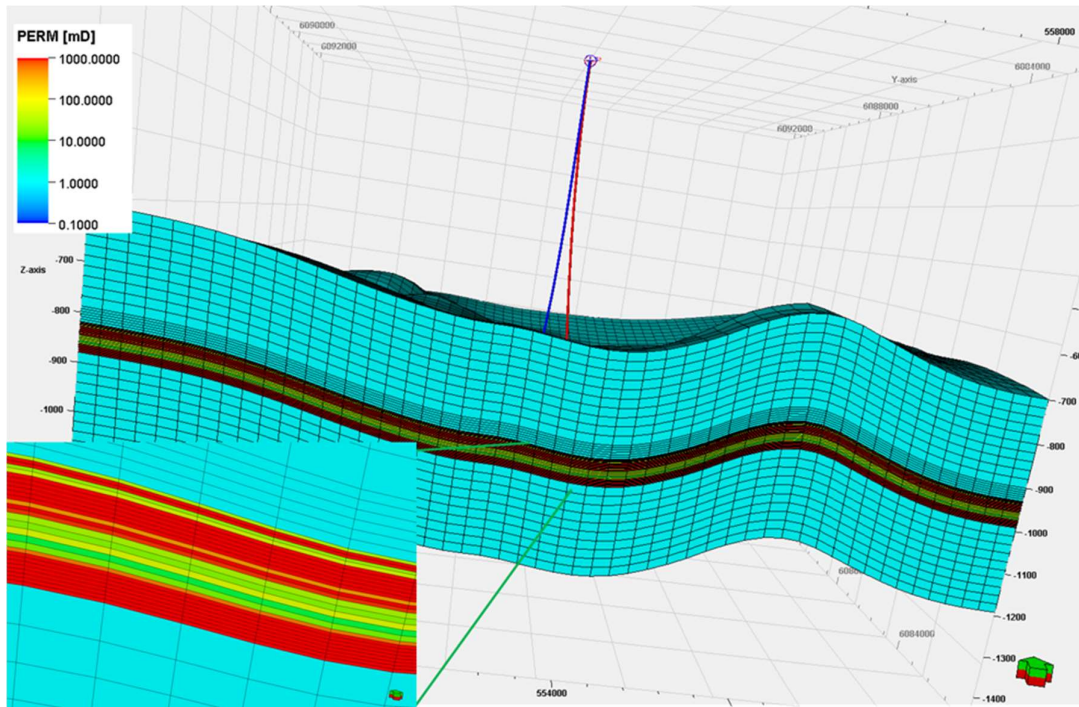


Figure 6.14. 3D model populated with permeability values. The reservoir interval at high vertical resolution in the middle of the model.

Proper boundary conditions must be applied for the simulation model. Even though the simulation of a geothermal plant operation involves production and injection of equal volumes of water (full voidage replacement), it must be secured that the simulated pressure and temperature development is not influenced by the model boundary. For this study, ‘pore volume multiplication’ is used as a boundary condition, *i.e.* the pore volumes of the outermost grid cells of the model have been multiplied by a high number to mimic that the model area is situated in an infinite aquifer. Further, as described above, the over- and underburden is included in the reservoir model to secure correct handling of the temperature and pressure vertical boundary conditions.

The wells are controlled by volume rate at surface conditions, *i.e.* a specific desired production and injection rate, specified by the historical production data provided by Sønderborg Fjernvarme, cf. Fig. 6.11. For each production period, the injection rate is averaged in the simulations. The volumes going to Augustenborg fjord are neglected. The Eclipse well option balances the rate from the wells to the reservoir for the individual grid cells by a ‘connection transmissibility factor’.

One production well and one injection well are placed in the model with the well tracks taken from the deviation files (DONG Energy, 2010a; 2010b). The wells are modelled as being open in the two main reservoir intervals, *i.e.* each well has access to the entire thickness of the two intervals. The well diameter is arbitrarily set to 0.245 m with an initial guess on the skin factor taken from the well test results, 20/54 for the upper/lower interval in Sønderborg-1 and 7/54 for Sønderborg-2. These values were tuned during the simulations in order to match the historical production data. The

present study did not have access to the original well test data, making the determination of the skin factors uncertain.

In the reservoir model, the water phase is given properties to mimic the saline formation water in the Sønderborg area, *i.e.* a density of 1097 kg/m³. The initial pressure of the formation water is calculated as hydrostatic (hydrostatic equilibrium) for each grid cell from the density and the depth of the respective grid cell. Density is assumed to vary linearly with depth.

Model temperature is calculated for each grid cell from the temperature-depth relation given above (34 °C/1000 m and a surface temperature of 8 °C). Thus, it is assumed that the entire reservoir model is in thermal equilibrium and the temperature-depth relation is approximated by a constant temperature gradient.

Three sets of simulation cases were run:

1. The first set of simulations were run to history match the simulation model to the historical production data. The simulations are run in a constant rate mode and the simulated flowing bottom hole pressure for the production well is matched to the actual production drawdown pressure. The matching parameters are the permeability of the individual reservoir intervals and the well skin factor.
2. A second set of simulation cases were run to evaluate the reservoir connectivity. As stated in the introduction paragraph, there are indications that a potential flow barrier (flow restrictions) may exist in the reservoir. Figure 6.15 illustrates how the flow restrictions are modelled; one model with a flow barrier to the west of the two Sønderborg wells, one model with the flow barrier between the wells and one model with the barrier to the east of the wells. The flow barriers are modelled as vertical zones with low permeability, varying from 90% of the original reservoir permeability down to zero permeability.
3. A third set of simulations were run to evaluate the project lifetime for the Sønderborg geothermal plant with the existing well configuration and production profile. Simulations were run for a total of 30 years, the first five years were simulated as the actual historical production profiles, and the next 25 years were run as 5 replicas of the historical profile. Additional simulations were run for 60 and 150 years to assess long-time effects on the temperature profile.

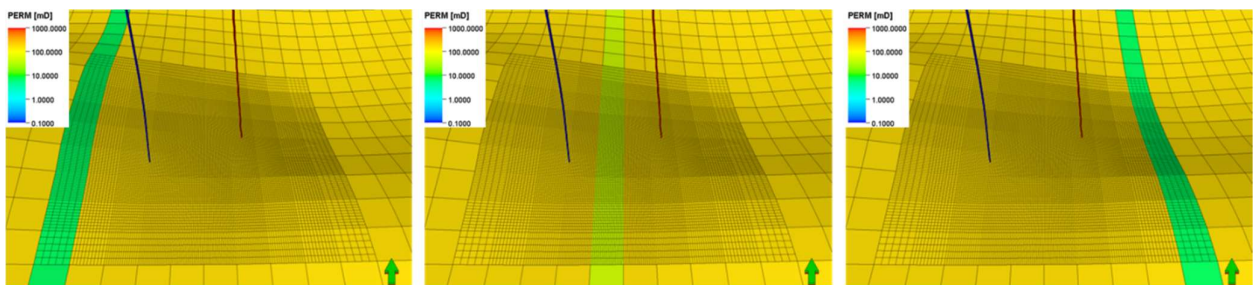


Figure 6.15. Simulation case configuration to evaluate potential flow restriction in the reservoir. Three extreme cases.

Results and discussion

The results from the simulations must be evaluated with respect to the assumptions, limitations and uncertainties described in the previous sections; *i.e.* the simple 'layer-cake' modelling approach and the determination/selection of reservoir properties.

Simulations show that it is possible to get a reasonable match between the simulated bottom hole pressure for the model production well and the actual drawdown pressure in the Sønderborg-2 well (production well), cf. Fig. 6.16. The second flow (production) period was difficult to match. The reason could be the very unstable start-up of the production period and the fact that the production pump (ESP, Electrical Submersible Pump) apparently was moved to a shallower depth in the wellbore (some 80 m) during that period. In the late part of the period, the drawdown shifts to a more stable level but with a lower injectivity.

The best match for the drawdown pressure was obtained with a split in transmissibility between the two reservoir intervals of 46 Dm for the upper interval and 68 Dm for the lower interval and skin factors of 14 and 44 for the upper and lower intervals. The results are in some contradictions to the results obtained from the wells tests, where a split in transmissibility of 19 Dm and 110 Dm were interpreted. As stated in the well test documentation (DONG Energy 2010a; 2010b), the well results are subject to uncertainty.

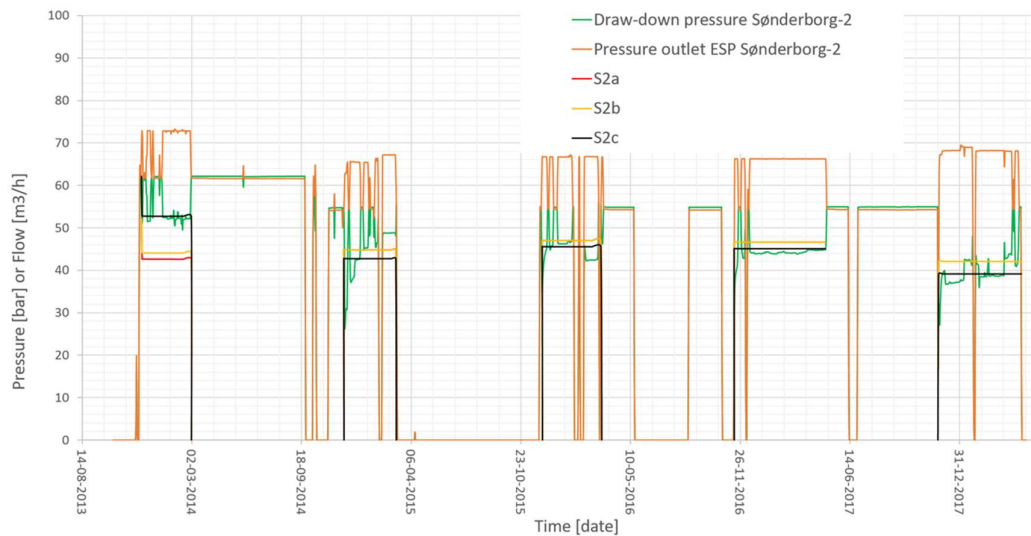


Figure 6.16. Matching the simulated bottom-hole pressure (black curve) with the production pressure (drawdown in the production well, green curve)).

The uncertainty or non-uniqueness of the results also holds for the reservoir simulation results. Both reservoir intervals were tested simultaneously, *i.e.* no packing off one interval and testing the other. The reservoir simulations were run in the same configuration. However, examining the log interpretation for the Sønderborg-1 well there seems to be support for a more uniform split in transmissivity for the two reservoir intervals.

Figure 6.17 shows simulation results for the pressure and temperature development for the configuration with the potential flow restriction between the two Søndersborg wells. The flow barrier has some influence on the water potential (water potential = water pressure at a fixed datum, i.e. pressures can be compared without gravitational effects), but no effect on the temperature development.

Figure 6.18 shows the development in productivity and injectivity index for the Søndersborg wells. The injectivity index is defined as the ratio between the flow rate and the pressure difference induced to produce the flow. This figure compares the results for a simulation case with a closed flow barrier between the wells and a case with no flow barrier. There are no influences on the well performance from the closed barrier. This is interpreted as, even if there exist a flow barrier in the reservoir, the reservoir transmissibility is so high that flow barriers will not influence the well performance significantly. This also indicates that the actual decreasing performance of the Søndersborg wells is not subject to the influence of barriers in the reservoir, but most likely attributed to obstacles in the wellbore or near wellbore area. These obstacles are presumably related to scaling and corrosion in the wellbore of Søndersborg-1. Precipitation of iron-rich minerals are observed in filter extracts. Scaling production caused by geochemical reactions between water and casing material are observed in the injection well.

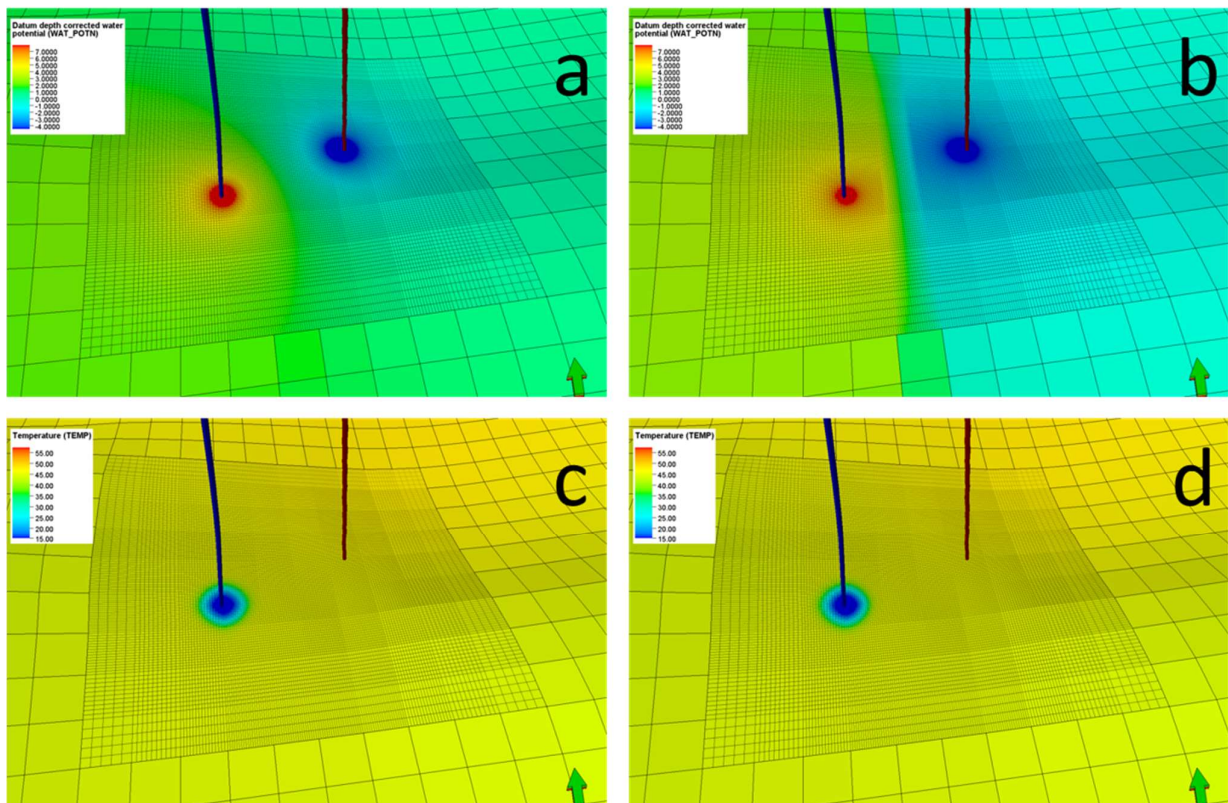


Figure 6.17. Development in water potential and temperature after the first 5 production periods. a) Water potential with no flow restriction, b) water potential with closed flow barrier between the wells, c) temperature development with no flow barrier, d) temperature with flow barrier between the wells.

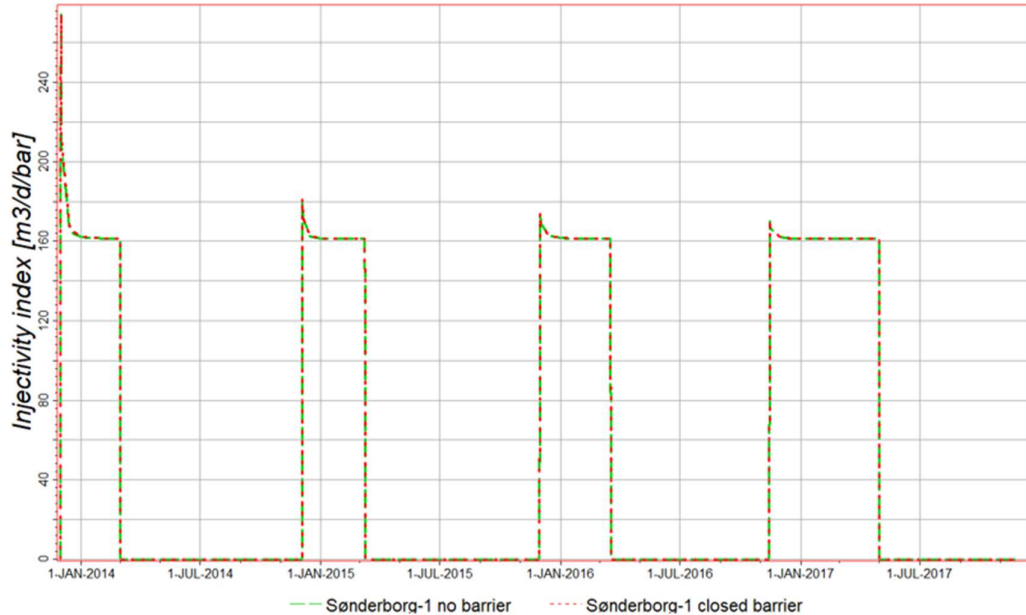


Figure 6.18. Development in injectivity index for the Søndersborg-1 well for the simulation case with an almost closed flow barrier between the two wells. There are no observed influences on the well performance from the almost closed barrier.

The above findings for the simulated development in productivity and injectivity also applies for the flow barrier configurations with barrier located west and east of the two wells, respectively.

The last set of simulations were run to test the long-term temperature evolution with the existing well configuration. Figure 6.19 (top panel) shows the temperature development for a 30-year production period. Simulations were run with and without flow barriers in the reservoir. The barrier configurations were as illustrated in Fig. 6.15, i.e. flow barrier to the west, east or between the wells. The temperature differences after a 30-year long production period were below 0.2 °C for the different configurations.

Each simulation shows an insignificantly small drop in production temperature during the 30-year production. Actually, the production temperature increases a little in the beginning, which is due to the fact that the Gassum reservoir is dipping towards the production well. The dipping is not fully symmetrical around the well, so relative more of the produced water comes from a deeper part of the reservoir around the production well, where the formation water is slightly warmer. For the case with the closed barrier between the wells the effect of the incoming cold injection water is almost screened off.

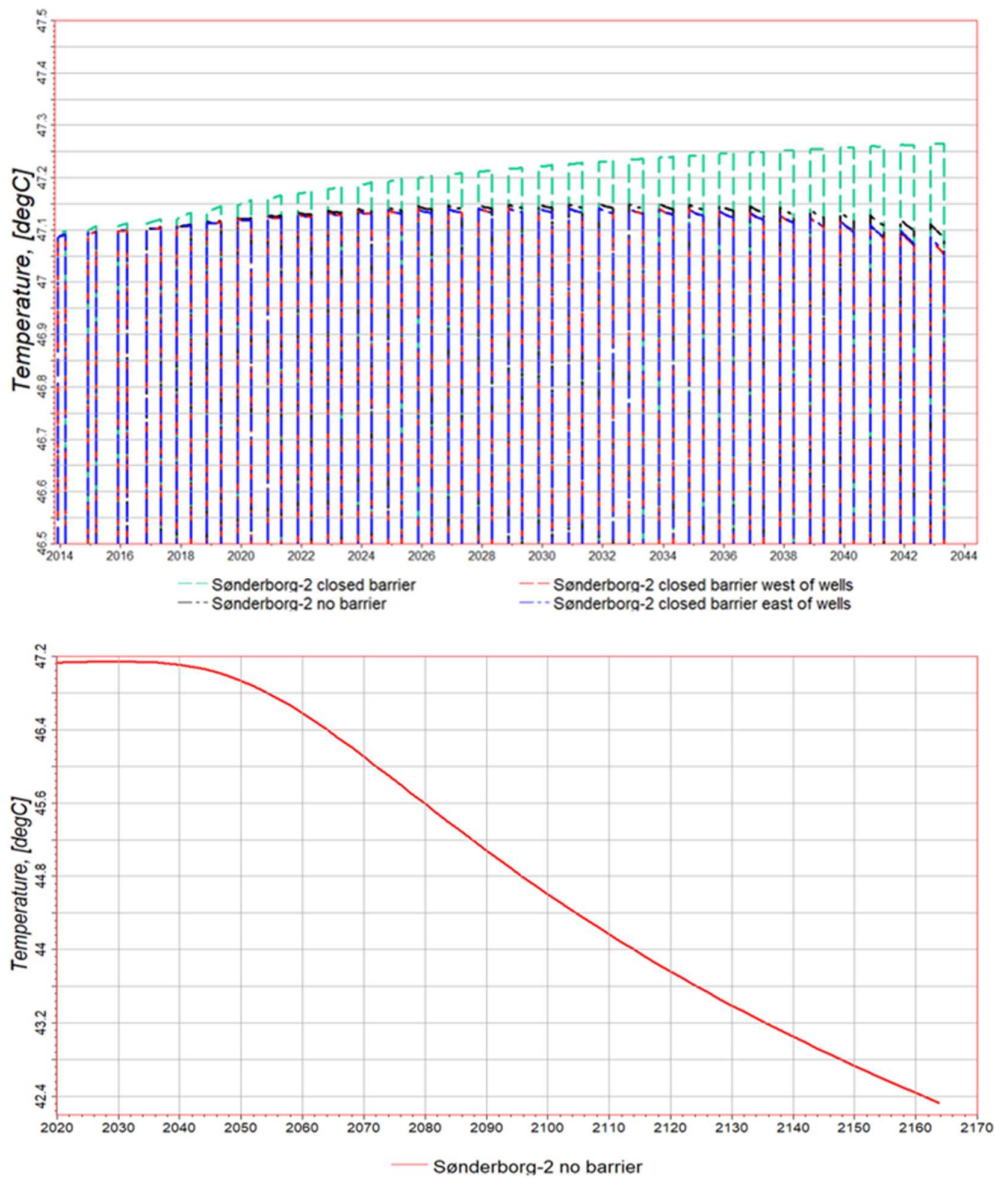


Figure 6.19. Top: temperature development for a 30-years production period. Simulations were run with and without flow barriers in the reservoir. The barrier configurations were as illustrated in Figure 6.15, i.e. flow barrier to the west, east or between the wells. Bottom: temperature development for a 150-years production period and no flow barriers.

The case with the flow barrier between the wells was the most optimal case with respect to the production temperature; i.e. the flow barrier prevents the cold injection waterfront from reaching the production well.

Simulations run for an extended production period of 150 years, showed a drop in production temperature of about 5 °C (Fig. 6.19, bottom panel). Despite a short distance (about 800 m) between production and reinjection, we observe relatively small long-term drop in production temperature.

Compared with the Thisted case (previous section), we note a somewhat higher temperature decline and for a significantly lower flow rates (cf. Fig. 6.11). Flow rates are also significantly lower than that applied in the conceptual models (section 5.2) and, furthermore, the Sønderborg plant is modelled with the seasonal mode of operation compared with continuous production in the conceptual models. Still, for the short well distance, the long-term temperature decline is low, and the dipping reservoir may have an effect with in-take of somewhat warmer water from deeper levels.

Conclusions

A history matched reservoir simulation model was constructed in the Petrel and Eclipse software. The model was used to assess the production performance of the geothermal plant in Sønderborg, specifically to assess if the decreasing injectivity could be attributed to flow barriers in the reservoir interval.

Simulations show no indications of flow barriers in the reservoir interval, when the model is matched to the historical production; i.e. injectivity issues originate from wellbore or near wellbore obstacles.

Even if flow barriers are present in the reservoir interval, these barriers will have only infinitesimal effect on the performance of the plant in a 30 year production period, due to excellent reservoir properties of the Gassum Formation in the Sønderborg area.

Simulations run for an extended production period of 150 years (in seasonal mode), show a relatively small decline in production temperature (about 5 °C), despite a rather short distance between production and injection well. This is to be seen in relation to the applied low flow rates and, likely, also related to a dipping reservoir and draw-in of water from slightly deeper reservoir levels of higher temperatures.

Such reservoir models can be used for predicting future production performance and assessing potential future re-developments.

6.3 The Margrethholm plant

The Margrethholm geothermal plant in the Copenhagen area started production in 2005. Similar to the plants at Thisted (until recently) and Sønderborg, it consists of two wells for production and reinjection. Production is from a significantly greater depth, about 2560 m, from the Lower Triassic Bunter Sandstone Formation, and the higher temperature of 74 °C. It supplies heat to the district heating network and was designed for a thermal output of 14 MW for a production rate of about 200 m³/h and injection temperature of about 18 °C. A recent description of the Margrethholm geothermal plant, including technical details of its surface systems, is found in Røgen *et al.* (2015).

At the site of this plant, the Bunter Sandstone Formation, with a thickness of 270–300 m is a sequence of claystones, siltstones and sandstones. It contains a reservoir unit, referred to as the Bunter Sandstone Reservoir, with good reservoir properties situated at a depth of around 2500–2575 m. A detailed lithological profile is shown in Fig. 6.20. This reservoir is applied for production and reinjection separated in the reservoir at a distance of ca. 1200 m.

The Margretheholm geothermal plant was included as an actual case in the conceptual parametric reservoir modelling study by Poulsen *et al.* (2015). For consistency, and for a comparison with the above results from Sønderborg and Thisted, we summarize main results from that study.

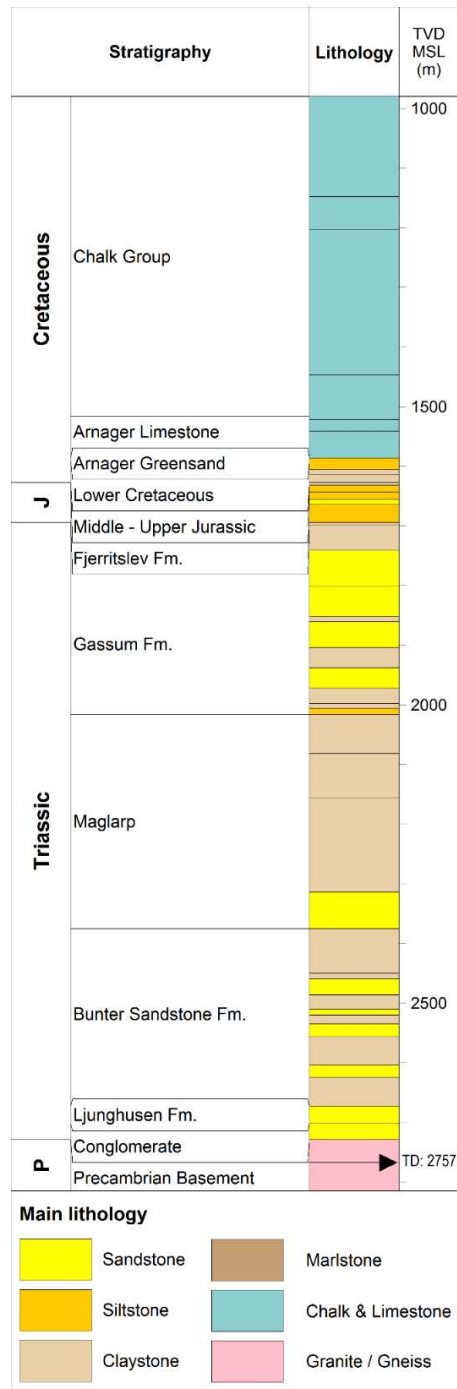


Figure 6.20. Lithological profile for the deeper part of the Margretheholm-2 well.

Model reservoir properties were determined based on information available from well testing. A flow log showed that 28 m of the 75 m of total perforated section contribute significantly to the flow into the well, and the transmissivity of this permeable section was estimated at 11.7 Dm. This yields a permeability of 418 mD. In the reservoir simulation, the transmissivity was distributed equally over the 75 m model reservoir with a permeability of 156 mD and a corresponding hydraulic conductivity of 3×10^{-6} m/s. As for the Thisted case above, the FEFLOW modelling software was applied. For further details regarding model set up and model parameters, we refer to Poulsen *et al.* (2015).

Main results

Figure 6.21 shows model results in terms of production temperature, given as temperature decline relative to current production at 74 °C and for long-term continuous production at three different constant flow rates of 100, 150 and 200 m³/h. The temperature break-through (entering of the front of cold injection water) occurs after 79, 55 and 34 years, respectively. For the intermediate flow rate of 150 m³/h, a temperature decline of 5 °C is seen after about 130 years and a decline of 10 °C after about 250 years of production.

When compared with model results from Thisted and Sønderborg, we see similar temperature declines as in Sønderborg and larger declines than in Thisted. It is important to note, that Thisted and Sønderborg are with seasonal operation and Margretheholm with continuous operation. The shorter distance between production and injection in Sønderborg and with significantly lower flow rates, results in a temperature decline similar to that of a continuous production and higher flow rates at Margretheholm.

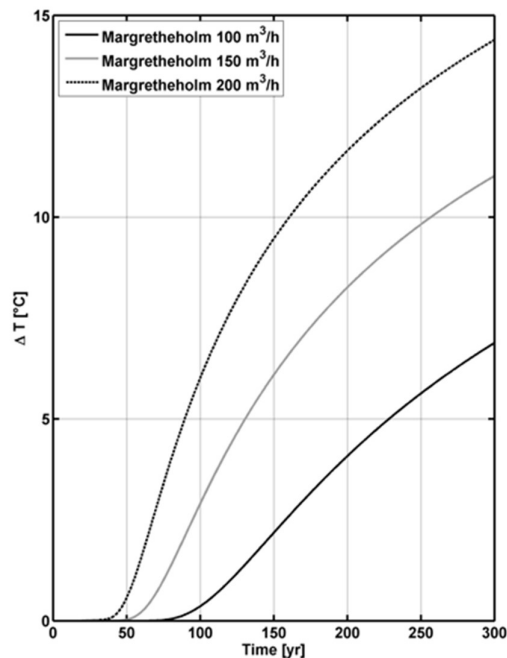


Figure 6.21. Modelled long-term decline in production temperature for continuous production at the constant flow rates of 100, 150 and 200 m³/h as indicated (From Poulsen *et al.*, 2015).

Conclusions

With equivalent constant flow rates, as in the conceptual models (section 5.2), we observe similar temperature evolution as for those models, again demonstrate the thermal longevity of geothermal reservoirs and long-term slow decline in production temperature after thermal break-through. Injectivity issues, recently observed, are not considered in models presented here.

6.4 General conclusions

Our modelling studies demonstrate that numerical reservoir models are a powerful tool for predicting thermal production performance of geothermal plants. Common to all models is the demonstration of longevity of geothermal reservoirs. This applies to sites with different geological reservoir conditions and variable distances between production and injection. Production may continue for decades with no or very little decrease in production temperature.

History matching at Thisted shows no sign of temperature decline, consistent with observations. The model cold-water plume, after 34 years of production, extends only about one-third the way from the injection borehole to the production borehole, but its front seems to reach the position of the new injection well.

The increased viscosity of the colder water does not explain the increase in pressure at the injection site at Thisted. This effect only contributes a minor part. The remaining part may be due to near wellbore effects.

For the Søndersborg case, history-matching simulations show no effect from potential flow barriers in the reservoir interval, and injectivity issues seem to originate from wellbore or near wellbore obstacles.

For Søndersborg, as well as Thisted, inclined reservoirs seem to have an effect on production temperatures. Draw-in of warmer water from deeper reservoir levels yields reduced long-term temperature decline.

Preliminary modelling comparing results from traditional 'layer-cake' reservoir models and geostatistical models with lateral variability in reservoir properties for the Thisted case shows some, but small differences in production temperatures. These small differences may be due to the specific situation of high reservoir permeability and a high lateral continuity of the Gassum Formation.

Recently, the Margretheholm geothermal plant, as at Søndersborg, is challenged by decreasing injectivity. These injectivity issues are treated in separate parts of the GEOTHERM project and are not included in the long-term reservoir model simulations presented here.

References

- Balling, N., 1992. Denmark. In: Hurtig, E., Cermák, V., Hänel, R. and Zui, V. (eds.), *Geothermal Atlas of Europe, Explanatory Text*. Hermann Haack, Gotha, Germany, 25-28.
- Balling, N. and Bording, T. 2013. Temperatur, temperaturgradienter og varmeledningsevne i den geotermiske boring Sønderborg-1/1A. Forskningsrapport, Institut for Geoscience, Aarhus Universitet, 12 pp.
- Balling, N., Hvid, J.M., Mahler, A., Moller, J.J., Mathiesen, A., Bidstrup, T., Nielsen, L.H., 2002. Denmark. In: Hurter, S. and Haenel, R. (eds.), *Atlas of Geothermal Resources in Europe*. Publication No. EUR 17811. The European Commission, 27–28 and plates, pp. 15–16.
- Balling, N., Hvid, J.M. and Nielsen, S.B., 1994. Temperaturinformation fra dybe boringer i det danske område. Database/teknisk rapport, Geologisk Institut, Aarhus Universitet.
- Balling, N., Kristiansen, J.I., Breiner, N., Poulsen, K.D., Rasmusen, R. and Saxov, S., 1981. Geothermal measurements and subsurface temperature modelling in Denmark. *GeoSkrifter*, 16, Aarhus University, 172 pp.
- Balling, N., Nielsen, S.B., Christiansen, H.S., Christensen, L.D., Poulsen, S., 1992. The subsurface thermal regime and temperature of geothermal reservoirs in Denmark. Synthesis Report to Commission of the European Communities, Contract EN3G-0029-DK. Department of Geoscience, Aarhus University, 89 pp.
- Balling, N., Poulsen, S.E., Fuchs, S., Mathiesen, A., Bording, T.S., Nielsen, S.B. and Nielsen, L.H., 2016. Development of a numerical 3D geothermal model for Denmark. In: *Proceedings, European Geothermal Congress*. Strasbourg, France, 2016. 9 pp.
- Blöcher, G., Reinsch, T., Henniges, J., Milsch, H., Regenspurg, S., Kummerow, J., Francke, H., Kranz, S., Saadat, A., Zimmermann, G., Huenges, E., 2016. Hydraulic history and current state of the deep geothermal reservoir Gross Schoenebeck. *Geothermics*, 63, 27–43.
- Bording, T. 2010. En procedure til modellering af temperaturer for geotermiske reservoirer med anvendelse i det nordlige Jylland. Bachelor thesis, Aarhus University.
- CREWES, 2007. Fluid Property Calculator 2007. University of Calgary.
- Diersch, H.-J., 2014. *FEFLOW - Finite Element Modeling of Flow, Mass and Heat Transport in Porous and Fractured Media*. Springer.
- Drijver, B., Aarssen, M.V. and Zwart, B., 2012. High-temperature aquifer thermal energy storage (ATES): sustainable and multi-usable. Paper presented at Innostock, 2012.
- DONG Energy, 2010a. Sønderborg Geothermal Wells, Final Well Report – Sønderborg-1/1A.
- DONG Energy, 2010b. Sønderborg Geothermal Wells, Final Well Report – Sønderborg-2.
- ECLIPSE, 2017. Schlumberger Information Solutions.
- Fuchs, S., Balling, N. and Mathiesen, A., 2020. Deep basin temperature and heat-flow field in Denmark – new insights from borehole analysis and 3D geothermal modelling. *Geothermics*, 83, 101722.
- Fuchs, S. and Balling, N., 2016. Improving the temperature predictions of subsurface thermal models by using high-quality input data. Part 1: uncertainty analysis of the thermal-conductivity parameterization. *Geothermics*, 64, 42–54.
- Fuchs, S., Balling, N. and Förster, A., 2015. Calculation of thermal conductivity, thermal diffusivity and specific heat capacity of sedimentary rocks using petrophysical well logs. *Geophysical Journal International*, 203, 1977–2000.
- Fuchs, S. and Förster, A., 2019. Thermal transport properties of Mesozoic formations in the Danish Basin. *GEOTHERM Interim Report M4.3*, GFZ, Helmholtz Center, Potsdam, 22 pp.

- Guldager, C., Poulsen, S.E. and Balling, N., 2018. Numerisk modellering af varmelagring i dybe sedimentære reservoirer med særligt henblik på Aalborg-området. Forskningsrapport, EUDP, Institut for Geoscience, Aarhus Universitet, 37 pp.
- Hill, M.C. and Tiedeman, C.R., 2007. *Effective Groundwater Model Calibration*. John Wiley & Sons.
- Huenges, E. (ed.), 2010. *Geothermal Energy Systems: Exploration, Development and Utilization*. Wiley, 463 pp.
- Hurter, S. and Haenel, R. (eds.), 2002. *Atlas of Geothermal Resources in Europe*. Office for Official Publications of the European Communities, Luxemburg. Publication No. EUR 17811, 92 pp, 89 plates.
- Lavigne, J., 1978: Les ressources géothermiques françaises – possibilités de mise en valeur. *Ann. Des Mines*, avril, 16 pp.
- Kastner, O., Sippel, J. and Zimmermann, G., 2015. Regional-scale assessment of hydrothermal heat plant capacities fed from deep sedimentary aquifers in Berlin/Germany. *Geothermics*, 53, 353–367.
- Köhler S., Kabus, F. and Huenges, E., 2013. Seasonal storage of thermal energy - Heat on call, In: Wengenmayr, R. and Bührke, T. (eds.), *Renewable Energy – Sustainable Concepts for the Energy Change*, Wiley-VCH, 123–129.
- Kristensen, L., Hjuler, M.L., Frykman, P., Olivarius, M., Weibel, R., Nielsen, L.H. and Mathiesen, A., 2016. Pre-drilling assessments of average porosity and permeability in the geothermal reservoirs of the Danish area. *Geothermal Energy*, 4 (1), 6. <https://doi.org/10.1186/s40517-016-0048-6>.
- Mahler, A., Røgen, B., Ditlefsen, C., Nielsen, L.H. and Vangkilde-Pedersen, T., 2013. *Geothermal Energy Use, Country Update for Denmark*. Proceedings European Geothermal Congress 2013, Pisa, Italy.
- Major M., 2016. Numerical modelling of heat recovery and storage potential in deep geothermal reservoirs. Unpublished MSc thesis, Aarhus University.
- Major, M., Nielsen, C.M, Hansen, T.M. and Balling, N., 2019. Numerical reservoir simulation for Danish geothermal plants: Thisted, Sønderborg and Margrethholm. GEOTHERM Interim Report M4.4, Aarhus University and GEUS, 30 pp.
- Major, M., Poulsen, S.E. and Balling, N., 2018. A numerical investigation of combined heat storage and extraction in deep geothermal reservoirs. *Geothermal Energy*, 6:1, doi.org/10.1186/s40517-018-0089-0.
- Mathiesen, A., Nielsen, L.H. and Bidstrup, T., 2010. Identifying potential geothermal reservoirs in Denmark. *Geological Survey of Denmark and Greenland Bulletin*, 20, 19–22
- Muffler, P. and Cataldi, R., 1978. Methods for regional assessment of geothermal resources. *Geothermics* 7, 53–89.
- Molz, F.J., Warman, J.C. and Jones, T.E., 1978. Aquifer storage of heated water: part 1-a field experiment. *Groundwater*, 16, 234–241.
- Nielsen, L.H., 2003. Late Triassic – Jurassic development of the Danish Basin and the Fennoscandian Border Zone, southern Scandinavia. *Geological Survey of Denmark and Greenland Bulletin*, 1, 459–526.
- Nielsen, C.M. and Major, M., 2018. Conceptual numerical models – production and reinjection. GEOTHERM Interim Report M4.2/4.3, GEUS and Aarhus University, 14 pp.
- Olivarius, M., Weibel, R., Hjuler, M.L., Kristensen, L., Mathiesen, A., Nielsen, L.H., Kjoller, C., 2015. Diagenetic effects on porosity–permeability relationships in red beds of the Lower Triassic Bunter Sandstone Formation in the North German Basin. *Sedimentary Geology*, 321, 139–153.
- Petrel, 2015. Schlumberger Information Solutions.
- Popov Y., Beardsmore G., Clauser C. and Roy S., 2016. ISRM suggested methods for determining thermal properties of rocks from laboratory tests at atmospheric pressure. *Rock Mech. Rock. Eng.*, 49, 4179–4207.
- Popov Y.A., Berezin V.V., Semionov V.G. and Korosteliov V.M., 1985. Complex detailed investigations of the thermal properties of rocks on the basis of a moving point source. *Izv. Phys. Solid Earth*, 21, 64–70.

- Poulsen, S.E., Balling, N., Bording, T.S., Mathiesen, A. and Nielsen, S.B., 2017. Inverse geothermal modelling applied to Danish sedimentary basins. *Geophysical Journal International*, 211, 188–206.
- Poulsen, S.E., Balling, N. and Nielsen, S.B., 2015. A parametric study of the thermal recharge of low enthalpy geothermal reservoirs. *Geothermics*, 53, 464–478.
- Røgen, B., Ditlefsen, C., Vangkilde-Pedersen, T., Nielsen, L.H. and Mahler, A., 2015. Geothermal Energy Use, 2015 Country Update for Denmark. *Proceedings World Geothermal Congress 2015*, Melbourne, Australia.
- Sanner, B., Kabus, F., Seibt, P. and Bartels, J., 2005. Underground thermal energy storage for the German Parliament in Berlin, system concept and operational experiences. In: *Proceedings World Geothermal Congress 2005*, Antalya, Turkey.
- Shetty S., Voskov D. and Bruhn D., 2018. Numerical strategy for uncertainty quantification in low enthalpy geothermal projects. *Proceedings, 43rd Workshop on Geothermal Reservoir Engineering*, Stanford University, Stanford, California, 2018.
- Soares, A., 2001. Direct sequential simulation and cosimulation. *Mathematical Geology*, 33, 911–926.
- Sommer, W.T., Doornenbal, P.J., Drijver, B.C., van Gaans, P.F.M., Leusbrock, I., Grotenhuis, J.T.C. and Rijnaarts, H.H.M., 2014. Thermal performance and heat transport in aquifer thermal energy storage. *Hydrogeology Journal*, 22, 263–279.
- Vosgerau, H., Mathiesen, A., Andersen, M.S., Boldreel, L.O., Leth Hjuler, M., Kamla, E., Kristensen, L., Brogaard Pedersen, C., Pjetursson, B. and Nielsen, L.H., 2016. A WebGIS portal for exploration of deep geothermal energy based on geological and geophysical data. *Geological Survey of Denmark and Greenland Bulletin*, 35, 23–26.
- Vosgerau, H., Mathiesen, A., Kristensen, L., Andersen, M.S., Hjuler, M.L. and Laier, T., 2015. Det geotermiske screeningsprojekt, Sønderborg-lokaliteten. *Danmarks og Grønlands Geologiske Undersøgelse, rapport 2015/33*.
- Welsch, B., Rühaak, W., Schulte, D.O., Bär, K., Homuth, S. and Sass I., 2015. A comparative study of medium deep borehole thermal energy storage systems using numerical modelling. In: *Proceedings World Geothermal Congress 2015*, Melbourne, Australia, 19–25.